# UNIVERSITY OF NOVA GORICA
# GRADUATE SCHOOL

## BIOCHEMICAL CHARACTERISATION OF THE ROLE OF THE HUMAN RECQ1 HELICASE AT THE REPLICATION FORK

## DISSERTATION

## Shivasankari Gomathinayagam

Mentor: Dr. Alessandro Vindigni Ph.D.

Nova Gorica, 2013

# CONTENTS

# LIST OF FIGURES AND TABLES

**FIGURES:**

**TABLES:**

# ACKNOWLEDGMENT

I have realized lately that one of the joys in completion is looking at the journey I have taken to reach there and remembering fondly the people who helped me and supported me along this long, but fulfilling road towards my doctoral degree.

I am immensely pleased to have been a part of Dr. Alessandro Vindigni's group. The time spent with Dr. Alessandro has turned out to be enlightening both academically and personally. I cannot thank him enough for his guidance and support. I would also like to thank my tutor, Dr. Vittorio Venturi (ICGEB, Trieste). My thanks to ICGEB and University of Nova Gorica for my stint at St. Louis school of Medicine, St. Louis, thanks to which I could get a taste of the scientific atmosphere at ICGEB, Trieste and at St. Louis school of Medicine, St. Louis. I would like to thank my lab colleagues I have had the pleasure of working with - Ramiro, Bojana, Gianluca, Francesca and my current lab members Saravana, Matteo and Sasa for the all the sane discussions and insane fun we had together.

I am happy to acknowledge and profoundly thank the Arturo Falaschi Pre-Doctoral fellowship for providing financial assistance for my PhD. I thank Dr. Dave Wood for his valuable suggestions and advice with the biophysical experiments and Dr. Sergey Korolev (SLU) and Dr. Erik Feldmann (WashU) for helping me with the ultracentrifugation experiments. I would also like to extend my thanks to the members of ICGEB and SLU who have helped me during my PhD.

I extend my heartfelt thanks to our collaborator, Dr. Alessandro Costa, and his group (London Research Institute) for performing the cryo-EM experiments for us. I would also like to extend my thanks to Dr. Yuna Ayala for all the discussions we had and the inputs she gave. Special thanks to all my teachers and mentors who have guided and moulded me into what I am today. I would also like to thank my mom, dad, extended family and friends for all the amazing support they never failed to give me. This has been a fulfilling ride indeed, and I take with me brilliant experiences and memories for a lifetime to come. Thank you!

# ABSTRACT

RecQ DNA helicases are critical enzymes for the maintenance of genome integrity. Defects in three of the five human RecQ homologs give rise to distinct genetic disorders associated with genomic instability, cancer predisposition, and premature aging. Studies of RecQ helicases in model prokaryotic and eukaryotic systems have demonstrated their vital roles in DNA replication, recombination and repair. In particular, different members of RecQ family have been implicated in various mechanisms that act at the level of stalled or damaged replication forks to guarantee a faithful replication of our genome.

An emerging model of how stalled or damaged forks are processed is that replication forks can reverse to aid repair of the damage. In this thesis, I studied the role of the human RECQ1 helicase in replication fork reversal and restart using a combination of biochemical and biophysical approaches. I used series of model replication substrates that mimic either a functional replication fork or a reverse fork structure to show that RECQ1 specifically promotes the restart of reversed forks, but not the opposite reaction of fork reversal. I also provided novel insight into the role of the poly(ADP-ribosyl)ation activity of PARP in fork reversal by showing that PARylatedPARP1 inhibits the fork restoration activity of RECQ1.

Following these observations, I investigated the molecular mechanism by which RECQ1 promotes the branch migration of reversed replication forks. My data show that the functional form of RECQ1 that binds and branch migrates Holliday junctions is a tetramer *in vitro*. The formation of the tetramer is mediated by N-terminal coiled-coil region of RECQ1 involving two key leucine residues (Leu 18 and Leu 28). The point mutation of these leucines impairs the formation of tetramers, as well as the annealing and Holliday junction branch migration activities of RECQ1, while it does not affect the helicase activity.

These results together suggest that RECQ1 binds the regressed replication forks as a tetramer to re-establish a functional replication fork and that the interaction between RECQ1 and PARylatedPARP1 regulates this activity.

# TITLE AND ABSTRACT IN SLOVENE

## Biokemijska karakterizacija vloge človeške helikaze RecQ1 pri replikacijskih vilicah

Helikaze DNA iz družine RecQ so encimi, pomembni za vzdrževanje genomske celovitosti. Okvare treh izmed petih človeških homologov RecQ povzročajo različne genetske motnje, ki se kažejo kot genomska nestabilnost, povečana nagnjenost k razvoju raka in prezgodnje staranje. S preučevanjem helikaz RecQ v modelnih prokariontskih in evkariontskih sistemih je bila dokazana njihova ključna vloga pri podvojevanju DNA, rekombinaciji in popravljalnih mehanizmih. Predvsem so encimi iz te družine udeleženi pri različnih mehanizmih, ki delujejo na zaustavljenih ali poškodovanih replikacijskih vilicah in zagotavljajo zanesljivo podvojitev genoma.

Pred kratkim je bilo pokazano, da se replikacijske vilice pri okvari ali zaustavitvi lahko obrnejo in to pripomore k odpravi poškodbe DNA. V tej nalogi sem s kombinacijo biokemijskih in biofizikalnih metod preučevala vlogo človeške helikaze RecQ1 pri obrnitvi replikacijskih vilic ter pri ponovnem začetku podvajanja. Uporabila sem vrsto modelnih substratov, ki predstavljajo tako funkcionalne replikacijske vilice kot strukturo obrnjenih vilic in ugotovila, da encim RecQ1 specifično pospešuje ponoven zagon obrnjenih vilic, ne pa same reakcije obrnitve. Pridobila sem tudi nove informacije o vlogi poli(ADP-ribozil)acijske aktivnosti encima PARP pri obrnitvi vilic in sicer, da PARiliran PARP1 inhibira aktivnost encima RecQ1 pri obnovi replikacijskih vilic.

Da bi bolje razjasnili te ugotovitve, sem preučevala molekularni mehanizem s katerim RecQ1 pospešuje premik razvejitve DNA pri obrnjenih replikacijskih vilicah. Moji rezultati kažejo, da se funkcionalna oblika RecQ1 helikaze *in vitro* veže na razvejitev Hollidayeve strukture v obliki tetramera. Enote se povežejo v tetramer

preko N-končne obvite vijačnice, ključna pa sta aminokislinska ostanka Leu 18 in Leu 20. Točkovna mutacija teh dveh levcinov prepreči nastanek tetramera. Tak encim se ne more vezati na razvejitev Hollidayeve strukture in ne more premakniti razvejitve, med tem ko helikazna aktivnost encima ni okrnjena.

Skupaj ti rezultati kažejo, da se tetramer RecQ1 helikaze veže na obrnjene replikacijske vilice in sodeluje pri ponovni vzpostavitvi funkcionalnih replikacijskih vilic. Interakcija med proteinoma RecQ1 in PARiliranim PARP1 pa uravnava to aktivnost.

# 1. INTRODUCTION

## 1.1 Helicases

### 1.11 DNA helicases:

Around 1% of the open reading frames (ORF) in the human genome codes for a class of enzymes called helicases. Helicases use the energy derived from the hydrolysis of nucleotide triphosphate (NTP) to separate complementary strands of nucleic acid molecules [1]. The helicases can be broadly classified as DNA or RNA helicases, based on the substrates they act upon. DNA helicases catalyse the transient unwinding of duplex DNA in a NTP dependent manner and play important roles in all aspects of DNA metabolism. They play prominent roles in replication, repair and recombination and thereby contribute to the maintenance of genome stability of all living organisms. The importance of DNA helicases for the maintenance of genome integrity is underlined by the numerous human diseases associated with defects in the helicase genes [2-4].

### 1.12 Classification of helicases:

The two most popular methods to classify helicases are based on their direction of translocation or on presence of particular signature motifs [5]. *In vitro* experiments using partial DNA duplex substrates have shown that, helicases can translocate with either a 3' → 5' or 5' → 3' polarity along single stranded DNA. For example, helicases such us the minichromosome maintenance proteins (MCM) and the RecQ helicases translocate on the single-stranded DNA with a 3' → 5' polarity, while the bacterial DnaB and phage $T_7$ gp4 helicases translocate with a 5' → 3' polarity. However, this classification is only applicable to those helicases that bind a ssDNA terminus and then translocate along single-stranded before unwinding the duplex [1].

The second method of classification is based on the analysis of specific signature motifs. Using this approach, helicases have been classified into 6

superfamilies, SF1 through 6. The characteristic motifs of each family are shown in the figure 1.1 and the characteristics of each family are shown in table 1.1.
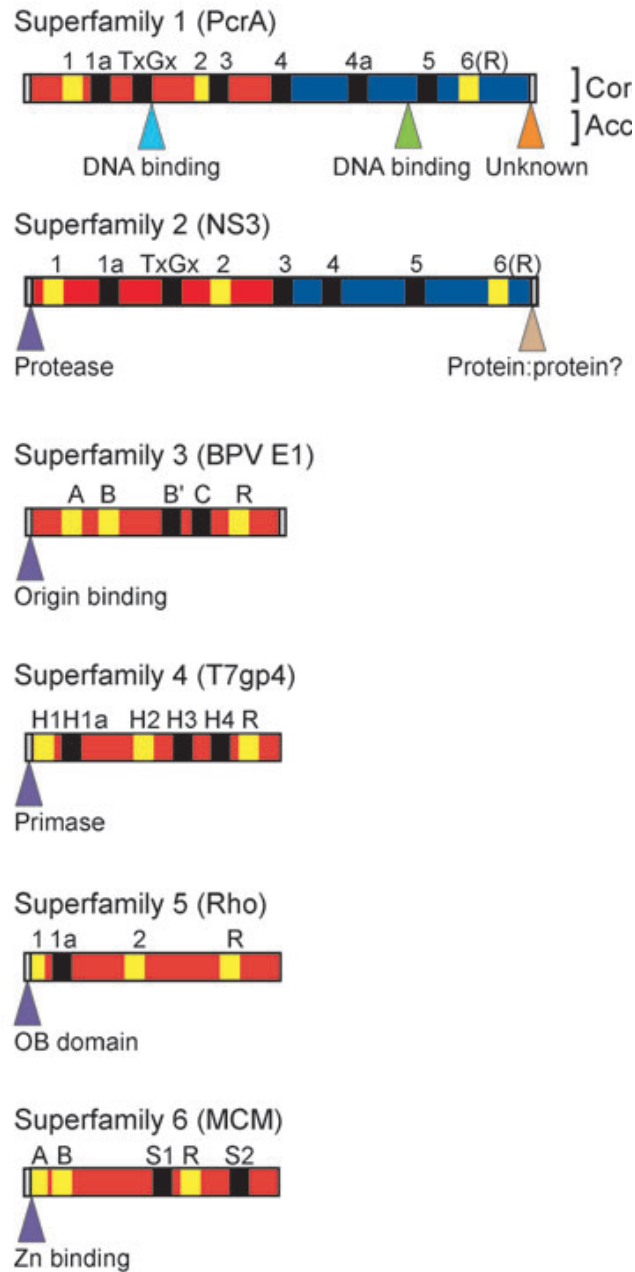


**Figure 1.1: Classification of DNA helicases based on conserved amino acid sequences.** The name of one representative member of each of the six superfamilies is given in parentheses. The domains and the positions of the signature motifs therein are shown for each class of helicase. Precise position of each motif is based on the example family member and is representative for the whole family. Motifs colored yellow represent universal structural elements in all helicases. The positions and functions of accessory domains in each example protein are also shown. Model adapted from [6].

Out of the 6 superfamilies, the SF1 and SF2 families contain only the non-ring forming helicases, while the SF3 and SF6 families include toroidal enzymes [6].

| Superfamily | Protein fold | Assembly state | Polarity | Functions | Example members |
|---|---|---|---|---|---|
| Superfamily 1 (SF1) | RecA (tandem pair) | Monomer (Dimer/multimer) | 3'-5' 5'-3' | DNA unwinding, repair and degradation | Bacterial PcrA, Rep, UvrD, RecBCD, Pif1, eukaryotic Rrm3 |
| Superfamily 2 (SF2) | RecA (tandem pair) | Monomer (Dimer/multimer) | 3'-5' 5'-3' | RNA-melting, RNA-binding protein displacement, NA unwinding and translocation, melting and migrating of Holliday junctions or branched substrates | Prp2, ski2, NS3 of hepatitis C, Rad54, bacterial RecQ, UvrB |
| Superfamily 3 (SF3) | AAA+ | Hexamer | 3'-5' | DNA unwinding/replication | Papilloma virus E1, Simian virus 40 large T-antigen, Adeno-associated virus Rep 40 |
| Superfamily 4 (SF4) | RecA | Hexamer | 5'-3' | DNA unwinding/replication, ssRNA packaging | Bacterial DnaB, Phage T7 gp4, T4 gp41 |
| Superfamily 5 (SF5) | RecA | Hexamer | 5'-3' | RNA translocation, RNA/DNA heteroduplex unwinding, transcription termination | Bacterial Rho |
| Superfamily 6 (SF6) | AAA+ | Hexamer | 3'-5' | DNA unwinding/replication | Eukaryotic/archael MCMs |

**Table 1.1: Classification of DNA helicases.** DNA helicases superfamily is shown with respective characteristics and examples.

## 1.13 Mechanism of action:

Helicases have two important activities, namely translocation along ssDNA and unwinding of the duplex. The mechanisms by which helicases couple these two activities are still a subject of debate. Different unwinding mechanisms have been proposed for various helicases in the past (figure 1.2):
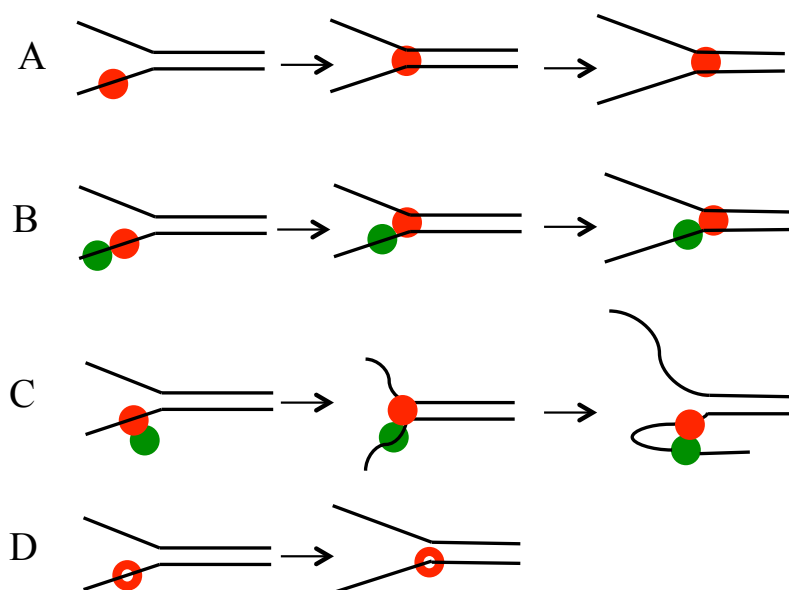
**Figure 1.2: Models for DNA helicase translocation and unwinding.** A) Inchworm model B) Co-operative inchworm model, C) Rolling model, D) Hexameric helicase model.

**A. Inchworm model:** The helicase has two non-identical DNA binding sites that bind with a defined polarity. The leading site interacts with the duplex region during successive cycles of unwinding, whereas the tail site interacts with the ssDNA. It is consistent with any oligomeric state, including monomers [7]. A dimeric inchworm mechanism has been reported for the bacterial UvrD helicase [8].

**B. Co-operative inchworm model:** Multiple helicase molecules line up along the ssDNA lattice to promote DNA unwinding. This mechanism is similar to the inchworm model, with the exception that it requires multiple helicase molecules [9, 10]. For example, the bacteriophage T4 Dda helicase is functional a monomer, but becomes more processive when there are multiple molecules acting cooperatively [10, 11].

**C. Rolling model**: Each monomer has least two identical DNA-binding sites that can bind to ssDNA and dsDNA in an alternating fashion. The rolling model requires a dimeric protein, as previously described for the bacterial Rep helicase [12].

**D. Hexameric helicase model**: The enzyme forms ring structure that encircles one strand of the duplex leaving the other strand outside the ring. The formation of a ring structure in hexameric helicases may be needed to prevent premature dissociation of the functional helicase molecule from the DNA substrate. Classical examples of hexameric helicases are the gp4 of bacteriophage T7 [13, 14], Rho of *Escherichia coli* [15, 16], and the eukaryotic minichromosomal maintenance (MCM) helicase [17-19].

## 1.2 RecQ helicases

The family of RecQ helicases is named after the RecQ gene of *Escherichia coli* discovered by Nakayama and his colleagues, more than 20 years ago [20]. RecQ helicases are highly conserved from bacteria to man. They are part of SF2 family and they all unwind DNA with 3' – 5' polarity [21]. RecQ helicases play an essential role

in the maintenance of genome stability by acting at the interface between DNA replication, recombination, and repair [22, 23] [24].

Orthologs of RecQ have been found in all kingdoms of life. Unicellular organisms, such as bacteria and yeasts only have one or two RecQ helicase genes per species, while higher eukaryotes generally express multiple RecQ enzymes [1, 22, 25, 26]. For example, four RecQ helicase genes have been found in *Caenorhabditis elegans*, five in *Drosophila melanogaster* and *Homo sapiens*, and seven in the plant species *Arabidopsis thaliana* and *Oryza sativa* [27]. Why human cells should encode five RecQ homologs, while microorganisms like *E.coli*, *S. cerevisiae* and *S.pombe* possess only one or two, remains unexplained.

## 1.21 Domain architecture:

The RecQ helicases contain the following domains (figure 1.3)

1. The core Helicase domain
2. RecQ C-terminal domain, also known as the RQC domain
3. The helicase-and-RNaseD-like-domain, also known as the HRDC domain
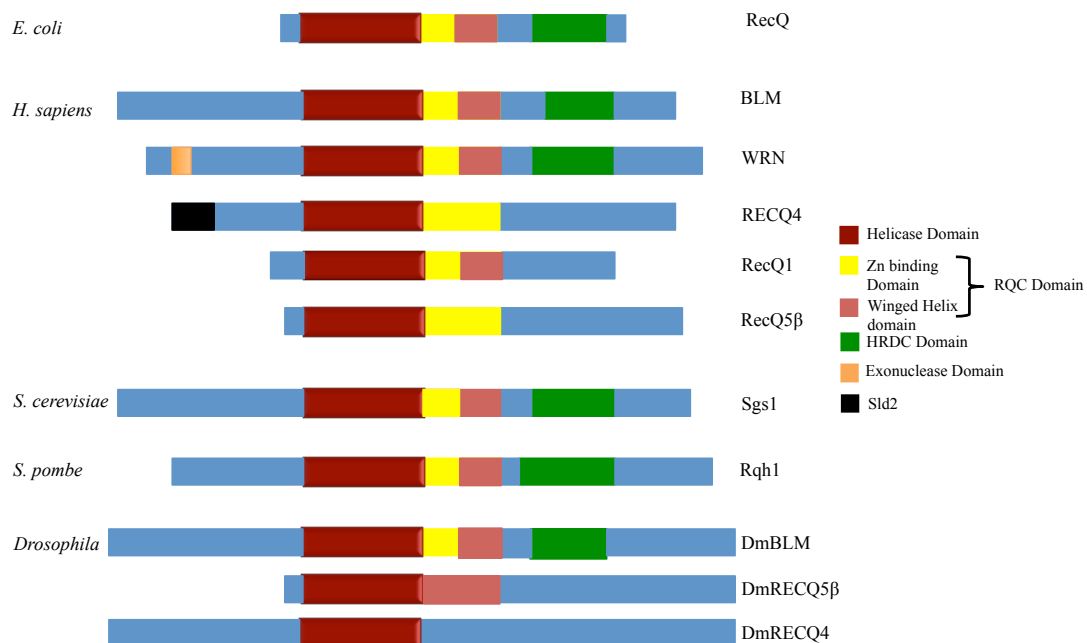


**Figure 1.3: Domain organization of various RecQ helicases from different organisms.** Proteins are aligned by their conserved helicase domain (red boxes).

16

The core helicase domain is present in all of the RecQ helicases, while the RQC and HRDC domains are present in most, but not all RecQ proteins. Although all RecQ helicases share a great degree of domain conservation, the N- and C-terminal domains are different in each protein and are involved in heterologous protein interaction, regulation of protein subcellular localization, as well as in directing protein oligomerization or in conferring additional activities such as the exo-nuclease domain in WRN [28].

**1. The helicase domain:**

As mentioned previously, helicases are enzymes that catalytically unwind double-stranded DNA duplexes by binding and hydrolyzing NTP. This characteristic function of the helicases is coordinated through a series of seven sequence motifs (I, Ia, II, III, IV, V, VI), which are the hallmark of both SF1 and SF2 family helicases. The central helicase domain of RecQ helicases are of approximately 300–450 amino acids long [29] [3, 4, 30].

X-ray crystallography of various helicases of the SF1 and SF2 family has shown that these seven motifs form the core of two RecA-like domains that function as the ATP driven "motor" of the helicase. Available structural data for the central helicase domain of the two RecQ helicases, the *E. coli* RecQ and human RECQ1 proteins, shows that the general fold of the core helicase domain of RecQ enzymes is similar to that of the other known SF1 and SF2 helicases [31, 32].

RecQ helicases possesses an additional motif 0 that is N-terminal to the motif I, in addition to these seven motifs (I, Ia, II, III, IV, V, VI) [33]. In addition, the primary sequence of the seven conserved motifs differs from those of the SF1 protein. The motif 0 is well conserved in all RecQ enzymes from different organisms and is composed of four invariant and two conserved amino acids spaced by eight non conserved residues: $Lx_3$ (F/Y/W) $Gx_3F$(R/K)$x_2Q$. The structures of *E. coli* RecQ and human RECQ1 proteins show that the motif 0 is involved in nucleotide binding, and mutagenesis studies have confirmed that this motif is important for core helicase domain function [28]. In particular, *in vitro* studies showed that the substitution of the C-terminal Gln 34 to Ala in the motif 0 of RECQ5β significantly reduces its

ATPase activity [34, 35] and that the same substitution in murine BLM inactivates the ATPase and the helicase activity of the enzyme [36]. Interestingly, the same mutation has also been reported in BS patients [37].

The mechanism by which RecQ helicases couple ATP binding/hydrolysis cycles to unidirectional translocation along ssDNA is poorly understood. Although the nucleotide bound structures of *E. coli* RecQ and human RECQ1 show that RecQ enzymes bind ATP in a conventional way, we currently have little knowledge on their physical mechanism of DNA unwinding.

*E. coli* RecQ contains a conserved aromatic-rich loop in its helicase domain which is located between motifs II and III [38]. A similar conserved aromatic-rich loop in motif III of SF1 helicases mediates both ATP and single-stranded DNA binding [39], [7]. Mutational analysis of the RecQ aromatic-rich loop provided evidence that this region is critical for coupling ATPase and DNA binding/unwinding activities [38]. The crystal structure of *E. coli* RecQ [31] has provided further insight into the functional importance of some of the conserved helicase motifs. The Motif I helps in making the canonical phosphate and metal contacts [31]. Mutations in the phosphate binding lysine residue in motif I of WRN [35], BLM [35], RECQ1 [40] and RECQ5ß [34], and the yeast Sgs1 helicase [41] seriously impair or abolish their ATPase and DNA-unwinding activities. Motif II represents the canonical Walker B motif [42] and is therefore implicated in NTP hydrolysis.

## 2. The RQC domain:

It is the second most highly conserved domain in RecQ helicases and is present in almost all of the members of the RecQ family. RECQ4 was the only human family member that was initially thought to lack this domain, but a recent bioinformatics analysis performed in our group suggested that the presence of this domain also in human RECQ4 [43]. The RQC domain is unique to the RecQ family and it can be divided into two sub-domains:

**A) Zn²⁺-binding domain:** Characterized by a pair of anti parallel helices and four Cys residues that coordinates, as the name suggests, a single $Zn^{2+}$ atom. It is responsible for the structural integrity and stability of RecQ proteins [44], [45], [46]. It is also believed that the Zn-domain might be involved in DNA and/or protein interactions, as previously suggested for other proteins that contain a similar domain [47].

A single amino acid substitution in the Zn-domain of hBLM and bacterial RecQ showed that the translated variants were insoluble and prone to degradation [44], [45], [46]. Missense mutations of the Cys residues in hBLM have been reported in Bloom Syndrome patients [37]. Moreover, the Sgs1 point mutant Cys1047Phe shows enhanced DNA-damage sensitivity and a hyper-recombination phenotype in yeast models [48].

**B) Winged helix (WH) domain:** Unlike the other sub-domains, the WH helix domains show poor degree of similarity in their primary sequences among various RecQ helicases. They have the characteristic helix-turn-helix fold that is also present in variety of DNA binding proteins, such as the transcription factors CAP and hRFX1, and the human DNA repair protein AGT [49] [50] [51] [52]. Interestingly, the WH domain of RECQ1 is characterized by the presence of a prominent ß-hairpin loop, with an aromatic residue (Tyr) at the tip, which is significantly shorter in the equivalent structures of *E. coli* RecQ and WRN. This Tyr residue acts as a pin, and abuts the end of the DNA duplex, thereby promoting strand separation. In agreement with this conclusion, *in vitro* studies with purified human RECQ1 show that the substitution of this Tyr residue with Ala in hRECQ1 abolishes the unwinding activity of the enzyme. Interestingly, the mutations of the His residue at the tip of the hairpin loop of *E. coli* RecQ does not affect its enzymatic activity [32].

The WH domain is also involved in dsDNA recognition. For example, it is required for G-quadruplex DNA binding in the case of *E.coli* RecQ and human BLM while it is needed for the interaction with Holliday junctions and forked substrates in the case of WRN [53], [54]. Perhaps surprisingly, given its small size and critical role in mediating DNA binding, studies on WRN have shown that many protein:

protein interactions are mediated by the WH domain, suggesting that this helix-turn-helix motif might also be involved in protein recognition [55].

**3) The HRDC Domain:**

The third conserved region of RecQ helicases derives its name from its similarity with the C-terminal region of the RNaseD protein, and hence is called the helicase-and-RNaseD-like-C-terminal (HRDC) domain [56]. This domain is missing in several RecQ enzymes. For example, among the five human RecQ helicases, only BLM and WRN possess a recognizable HRDC domain, which is located at the C-terminus. Interestingly, the RecQ helicase from *Rhodobacter sphaeroides* contains two HRDC domains, while other RecQ helicases from *Deinococcus radiodurans, Neisseria meningitidis*, and *Neisseria gonorrhea* are characterized by three HRDC repeats. These multiple HRDC domains regulate the enzymatic activity of *Deinococcus radiodurans* RecQ and differentially affect the ability of the enzyme to bind and unwind DNA [57].

Structural and biochemical studies have confirmed that the HRDC domain is associated with structure-specific recognition of DNA substrates and plays a crucial role in differentiating the activity and functions of the various RecQ homologs. The C-terminal fragment of BLM, encompassing the RQC and HRDC domains, is necessary for the interaction with the telomere-associated protein, TRF2, which stimulates BLM-mediated unwinding of two telomere substrates *in vitro*; a 3'-overhang and a telomere D-loop structure [58]. Collectively, these studies indicate that the HRDC domain plays an important role both in conferring some specific enzymatic activities to the individual RecQ enzymes and in DNA structure-specific recognition. In addition, it may mediate protein-protein interactions.

| Protein | Characteristics of the HRDC domain | Function |
|---------|-----------------------------------|----------|
| Sgs1 | Has a lysine- and arginine-rich patch that forms an electropositive surface important for the interaction with ssDNA [59]. | Binds both ssDNA and partially ds DNA. |
| WRN | Has a cluster of acidic and hydrophobic residues [60]. | Does not appear to interact with DNA *in vitro*. However, |

| | | a WRN fragment containing the HRDC domain and additional residues at the C-terminus (fragment 1072-1432) binds forked-duplex DNA and Holliday junctions with high affinity [54]. |
|---|---|---|
| *E. coli* RecQ | Uses electropositive surfaces to interact with DNA, but the residues that form this surface are located on a different face of the domain from that in the Sgs1 protein [61]. Characterized by a $3_{10}$ helix with a Tyr (residue 555) on its surface, which is essential for binding to ssDNA and partial duplex DNA | Binds preferentially to ssDNA over other DNA structures. |

**Table 1.2: Characteristic features and functions of HRDC domains of some RecQ helicases.**

*In vitro* studies on *E.coli* RecQ mutants lacking the HRDC domain showed that these mutants lack stable binding to partial duplex DNA. However, the HRDC domain of *E.coli* RecQ was found to be dispensable for the ATPase and unwinding activity of the enzyme. These results led the authors to suggest that, although it is dispensable for the catalytic activity of bacterial RecQ, the HRDC domain might facilitate the unwinding of long DNA duplexes by stably binding DNA [31]. Similarly, a Sgs1 truncation mutant lacking the HRDC domain was shown to be an active helicase and ATPase *in vitro* [62] [41]. However, the disruption of the HRDC domain in BLM was shown to compromise its ability to resolve HJ *in vitro*. In particular, Lys 1270 of BLM was found to play an important role in HJ disruption [63] [64]. On the other hand, this domain has a minor effect on forked-duplex unwinding activity of BLM and it is not required for ATP hydrolysis [63] [45].

 **4) The Exonuclease domain:**

An exonuclease domain is present at the N-terminus of the human WRN helicase and its orthologs in other organisms, such as *X. laevis* FFA-1. The crystal structure of this domain has also been solved [65], [66], [67], [68]. Recombinant WRN possesses 3' –5' exonuclease activity that can act on a wide variety of substrates [69]. It is very likely that the helicase and exonuclease activities of WRN

are coordinated *in vivo*, as suggested from the *in vitro* studies [70]. The exonuclease domain has a 3' − 5' proof reading activity that has been suggested to be required for DNA non-homologous end joining [68].

## 1.22 Human RecQ helicases and their associated diseases:

There are five RecQ helicases in humans—RECQ1, BLM, WRN, RECQ4 and RECQ5, with RECQ5 existing in two different forms due to alternative mRNA splicing [71]. Mutations in the genes of three out of the five human RecQ helicases are associated with well-defined cancer predisposition and premature aging disorders. In particular, Bloom syndrome is associated to *BLM* gene mutations, Werner syndrome to *WRN* gene mutations and Rothmund–Thomson syndrome, RAPADILINO and Baller Gerold syndrome are all caused by mutations in *RECQ4* gene [37, 72-74], [75].

### 1.22.1 Bloom syndrome:

Bloom Syndrome (BS) is an autosomal recessive disorder caused by defects in the *BLM* helicase gene. BS is a rare disorder and BS patients are characterized by proportionate pre- and post-natal growth deficiency, sun-sensitive telangiectatic hypo- and hyper-pigmented skin, immune deficiency, predisposition to malignancy and chromosomal instability. BS patients also show a very high incidence of cancers of various types including leukemias, lymphomas, and carcinomas [76].

**Murine model:**

Several groups have tried to generate BS mouse models. In one model, ES cells where a fragment of the *BLM* gene upstream of the helicase domain was replaced with a neomycin resistance cassette were transferred into blastocysts and crossed with WT mice to form the Blm$^{+/-}$ heterozygous mice. These mice are characterized by growth defects and micronuclei similar to human BS patients [77]. In a second model, ES cells with the exons 10–12 of the *BLM* gene replaced with HPRT (hypoxanthine–guanine phosphoribosyltransferase) were injected into the blastocyst and crossed with WT mice to generate heterozygous Blm$^{Cin/-}$. These mice

showed a slight increase in the frequency of micronuclei [78]. In addition, both mouse models were characterized by a shorter life span. Allan Bradley's group generated knockout models using an embryonic stem cell method. They generated different mutant alleles of the mouse homologue of human BLM: $Blm^{m1}$ (lacking the appropriate in frame translation start site), $Blm^{m2}$ (producing a truncated BLM polypeptide) and $Blm^{m3}$ (producing a truncated BLM polypeptide). The heterozygous mice with $Blm^{m2}$ or $Blm^{m3}$, the compound heterozygous $Blm^{m2/m3}$, and the homozygous $Blm^{m3/m3}$ were viable and fertile. However, the homozygous $Blm^{m2/m2}$ did not develop to term. The $Blm^{m3/m3}$ mice served as better model for BS and closely recapitulated the cellular phenotype of BS patients, such as increased SCE in somatic cells and predisposition to cancer [79].

**Cellular phenotype:**

Cells from patients with BS and the cells derived from *BLM* knockout mice exhibit chromosome instability. BS patients cells are characterized by an increased numbers of chromatid gaps, breaks, chromosome structural rearrangements and sister chromatid exchanges (SCE). It has been reported that BS cells as well as $BLM^{-/+}$ fibroblasts show a tendency for the formation of spontaneously induced micronuclei [80, 81]. Moreover, these cells display a significantly lower rate of chain elongation during DNA synthesis [82]. In addition, BS cells are sensitive to UV radiation and hydroxyurea (HU) [83]. *BLM* deficient mouse embryonic fibroblast (MEF) cells also showed elevated mitotic recombinations with the increased SCE [79]. Such elevated level of chromosomal disruptions observed in BS cells and *BLM* deficient MEF cells can likely be the reason for high incidence of cancer in BS patients.

**1.22.2 Werner syndrome:**

Werner syndrome (WS) is caused by a defective *WRN* gene, and similar to the BS is characterized by premature aging and cancer predisposition. WS is an autosomal recessive condition characterized by an early onset of age-related symptoms that include ocular cataracts, premature graying and loss of hair, arteriosclerosis and atherosclerosis, diabetes mellitus, osteoporosis, and a high

incidence of cancers [84] . The predominant cancers in WS are soft-tissue sarcoma, osteosarcoma, myeloid disorders, thyroid cancer, and benign meningiomas [85].

**Murine model:**

Two WS mouse models have been generated so far. The first model, where exons that encode motifs III and IV of the helicase domain were targeted, shared phenotypes similar to those of human WS patients. Similar to WS patients, the knockout mice acquired myocardial fibrosis, T cell lymphoma, and were prone to cancer [86]. The second model carries a mutation that eliminates the expression of the C-terminus of the helicase domain of WRN and didn't show any organismal phenotype that resembles WS patients. However, p53$^{-/-}$ WRN$^{-/-}$ double-knockout mice died earlier and the lack of p53 accelerated the mortality of WRN$^{-/-}$ or WRN$^{-/+}$ mice [87] [88].

**Cellular phenotype:**

Primary Cells from WS patients undergo replicative senescence more rapidly than normal cells and are highly sensitive to cross-linking agents, especially to 4-nitroquinoline 1-oxide (4-NQO). They also loose their proliferative capacity at an accelerated rate. Additionally, cultured fibroblasts from such patients have an extended S-phase of the cell cycle [89]. Telomere dysfunction likely contributes the premature senescence because serially passaged WS fibroblasts shorten telomeres more rapidly than controls and senesce prematurely. The expression of telomerase hTERT in WS cells leads to the immortalization of cells and reduces their sensitivity towards cross-linking agents [89, 90]. At the chromosome level, WS cells carry an increased number of chromosomal translocations and deletions. Such chromosomal aberrations observed in WS cells and *WRN* deficient MEF cells can explain the cancer phenotype of WS patients and *WRN* knockout mice.

**1.22.3 RECQ4 deficiency:**

Defects in the *RECQ4* gene are associated with three genetic disorders Rothmund-Thomson syndrome (RTS), Baller-Gerald syndrome (BGS) and RAPADILINO syndrome. Mutations in helicase domain of *RECQ4* gene lead to

RTS. The RTS patients show poikiloderma, growth deficiency, juvenile cataracts, premature aging and a predisposition to malignant tumors, particularly osteosarcomas [91-93]. Mutations in the exon 9 of the *RECQ*4 gene lead to BGS. The clinical features of the patients are radial aplasia/hypoplasia and craniosynostosis [94]. Mutations which leads to an in-frame deletion of exon 7 of the *RECQ4* gene are the cause of RAPADILINO syndrome, where the patients show RAdial hypo-/aplasia, PAtellae hypo-/aplasia and cleft or highly arched palate, DIarrhoea and Dislocated joints, LIttle size and LImb malformation and Nose slender [73].

**Murine model:**

Three *RECQ4* knockout mouse models have been reported so far. The first model carries a knockout of exon 5-8 of *RECQ4*, covering the N-terminal tail. This deletion is embryonic lethal [95] suggesting an essential function of the N-terminal domain of RECQ4. In the second mouse model part of exon 13, which codes for part of the helicase domain, was deleted. These mice showed severe growth retardation and other organismal phenotypic characteristics resembling RTS patients [96]. The third mouse model where exons 9 to 13 were deleted showed typical RTS clinical features such as hypo-/hyperpigmented skin, skeletal limb defects and palatal patterning defects [97]. The existence of two mouse models carrying deletions in the helicase domain and displaying a phenotype similar to RTS patients support the notion that mutations in the helicase domain of RECQ4 are associated with RTS.

**Cellular phenotype:**

The cells derived from RTS patients show genomic instability, including trisomy, aneuploidy and chromosomal rearrangements. Likewise, cytogenetic analysis of the embryonic fibroblasts (MEF) derived from *RECQ4* knockout mice revealed an overall aneuploid phenotype and a significant increase in the frequency of premature centromere separation [96]. Such wide range of disruptions of the chromosome can be one of the reasons for the carcinoma associated with RTS, BGS, and RAPADILINO. Additionally, RTS cells are sensitive to ionizing radiation and oxidative stress/damage suggesting a possible role in DNA repair. Acute deletion of

RECQ4 protein in primary murine embryo fibroblasts leads to defects in DNA synthesis and cell proliferation [98], which is consistent with embryonic lethality of RECQ4 knockout mice.

## 1.3 Biochemical properties of RecQ helicases

### 1.31 Helicase activity:

RecQ helicases unwind ds-DNA with $3' - 5'$ polarity with respect to the strand to which the enzyme is bound. They are characterized by wide substrate specificity that differs among the different RecQ helicase members, supporting the notion that the five human RecQ helicases play distinct roles in the maintenance of genome stability. The ranges of substrates they can act upon are schematically shown in figure 1.4.

| Blunt-ended duplex | 5' – tailed duplex | 3' – tailed duplex | Duplex containing bubble |

| Forked duplex | A classic helicase substrate | G4 DNA | D - loops |

| Holliday Junction | 3' and 5' flap DNA substrates | | Replication Fork like substrate |
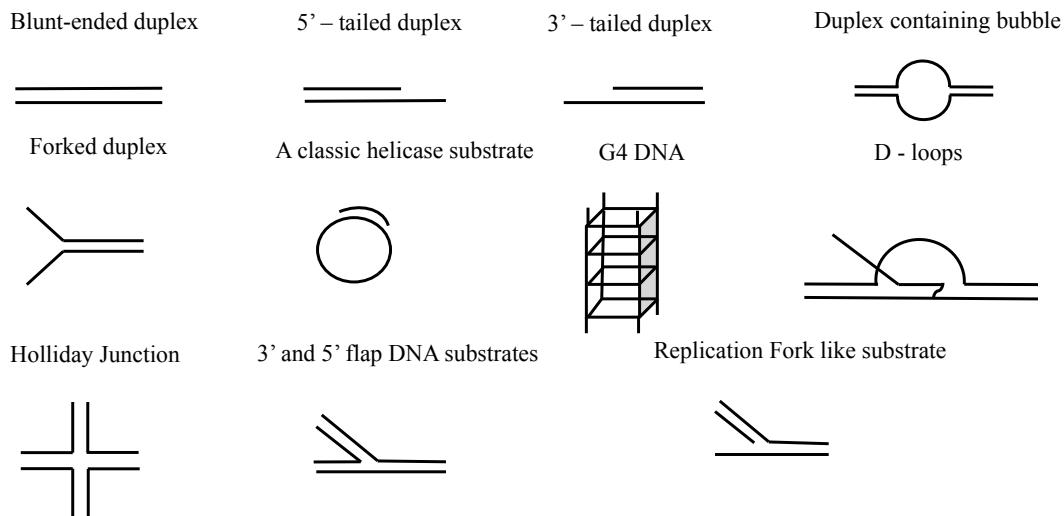
**Figure 1.4: Various DNA substrates used for the biochemical characterization of RecQ helicases.**

The unwinding activity is fueled by ATP hydrolysis. Consistent with the presence of Walker A and B boxes (ATPase motifs I and II), all members of the RecQ helicase family characterized thus far exhibit ATPase activity. This activity is dependent on a bivalent cation, which is generally $Mg^{2+}$, and is normally stimulated by DNA binding [99].

## 1.32 Annealing activity:

The human RecQ helicases RECQ5β [34], RECQ1 [40], WRN, BLM [100, 101], and RECQ4 [102], as well as the *dm*RECQ5b protein [100], are also able to mediate the annealing of complementary ssDNA molecules in the absence of ATP. On the contrary, nucleotide (ATP) binding inhibits the strand annealing of RecQ helicases [34, 40, 101]. Unlike the annealing activity of human RAD52, the annealing activity of human RecQ helicases is inhibited by human Replication Protein A (hRPA) binding [103].

The biological significance of the strand annealing activity of RecQ helicases remains, however, poorly understood. Conceivably, strand annealing by RecQ helicases may be important for replication fork regression (formation of a 'chicken foot' structure at blocked replication forks), strand exchange on homologous duplexes, or in a specific HR repair pathway such as synthesis-dependent strand annealing (SDSA) that involves both DNA-unwinding and strand annealing activities. Moreover, RecQ helicases were shown to promote strand exchange of partially homologous oligonucleotides *in vitro* by the coordinated action of the unwinding and strand annealing activities [100], suggesting that RecQ helicases are structurally designed to accomplish strand exchange on complex replication or recombination intermediates, such as two-way or three-way junctions.

## 1.33 Exonuclease activity:

Out of the five human RecQ helicases, WRN is the only one characterized by an intrinsic exonuclease activity. The 3'-5' exonuclease activity of WRN is conferred by an N-terminal exonuclease domain. This activity has been suggested to be required to proof read during non-homologous end-joining reactions mediated by WRN in combination with Ku70/80 and DNA-PKcs [68].

## 1.34 Functional forms of hRecQ helicases:

RECQ helicases exists under different oligomeric states that range from monomers to hexamers. DNA and/or ATP binding regulate the equilibrium between

these different states. Recent studies suggested that these different oligomeric states are associated with distinct functions. The following table provides an overview of the different states and their activities:

| RecQ helicase | Oligomerization state and their role | Region responsible for Oligomerization |
|---|---|---|
| RECQ1 | Monomer/dimer: DNA unwinding Tetramer: Strand Annealing; interact with and/or branch migrate HJ [104] [105] | Amino acids: 1-48, controlled by ssDNA and ATP binding |
| BLM | Monomer: DNA unwinding Hexameric ring: Strand Annealing [101] | Amino acids: 1290 – 1350 |
| WRN | Monomer: DNA unwinding [69] Tetramer: Binding to HJ or forked duplexes [106] | Amino acids: 1072 – 1150 [107]; controlled by DNA binding |
| RECQ5 | Monomer: in both DNA bound and unbound state [34] | - |

Table 1.3: Functional forms of RecQ helicases and their corresponding functions.

# 1.4 RecQ helicases in DNA repair

### 1.41 DNA damage repair (DDR):

Five major DNA repair pathways reverse DNA damage. They can be broadly classified as:

1. **Double-strand break (DSB) repair:** DSBs are the most dangerous of all types of DNA damage; when unrepaired, DSBs can be lethal and trigger apoptosis. There are 2 major pathways for DSB repair, each of which has 2 sub-pathways:

A)**Non-homologous end-joining (NHEJ):** NHEJ repair is the result of the direct ligation of the free ends of the DNA DSB. NHEJ is preferred in G0/G1. NHEJ may require end trimming that makes it less accurate [108-111]. The choice between classic NHEJ and the alternate NHEJ pathway is regulated by 53BP1 [109], which promotes classic NHEJ, and PARP1, which promotes alternative NHEJ [110]. Table 1.4 gives an overview of the classic and the alternative pathways of NHEJ.

28

| Process | Classic NHEJ | Alternative NHEJ |
|---|---|---|
| Initiated by | Ku70/86 and DNA-PKcs | PARP1 |
| End-resection by | Artemis, Metnase | MRN complex (MRE11/RAD50/NBS 1), CtIP tumor-suppressor |
| Microhomology involved | Little/No | Yes |
| Ligation of ends by | Ligase IV/XRCC4/XLF protein complex | Ligase III/XRCC1 |
| Suppression by 53BP1 | No | Yes |
| Fidelity (relative to each other) | More | Less |

**Table 1.4: Classic versus alternative NHEJ pathway.**

B) **Homologous recombination (HR):** HR uses strand invasion of the homologous chromatid to synthesize DNA across the DSB using this homologous chromatid sequence as a template. Thus, HR can take place only after DNA replication, in S/G2 cell-cycle phases. Because HR uses a homologous template to repair a DSB, it is more accurate than NHEJ [108-111].

HR requires extensive single-strand end-resection to allow for the invasion of the homologous template by the single-stranded DNA. End resection occurs in 2 phases. First, MRN/CtIP initiates a limited resection. This is followed by a more extensive resection mediated by the BLM helicase in complex with the EXO1 and DNA2 exonucleases [112].

**Accurate HR:** Homologous DNA sequences are used as templates to copy genetic information for repair. As mentioned, homologous sequences are typically sister chromatids in S/G2 cell cycle phases, but may be homologous chromosomes or linked or unlinked repeated sequences. After resection, accurate HR involves binding of RPA to single strands, and BRCA2-mediated replacement of RPA with RAD51 to form a RAD51 nucleoprotein filament, which searches for and invades the

homologous template [113]. The invading strand is extended by synthesis of new DNA. The newly synthesized strand can then anneal with the other resected end, and additional synthesis and ligation completes high-fidelity repair.

**Inaccurate HR:** Also termed single-strand annealing (SSA), in which extensive resection exposes complementary sequences in linked direct repeats, which anneal in a reaction promoted by RAD52 [114]. SSA is inaccurate because it deletes one of the repeats and the intervening sequence. In addition, SSA can result in translocations when 2 DSBs occur within or near repeats on different chromosomes.

**2. Nucleotide lesion repair:** There are three major repair pathways devoted to fix DNA lesions that occur on the single strands. In all cases, the complementary strand serves as the repair template.

A) **Base excision repair (BER)**: BER repairs base damage and is initiated by several glycosylases that produce apurinic or apyrimidinic (AP) lesions that recruit PARP1, followed by strand nicking by APE1 and deoxyribophosphodiesterase, repair synthesis, and ligation.

B) **Nucleotide excision repair (NER):** NER repairs bulky lesions by excising 30 nt oligonucleotides containing the lesion. NER is a multistep process that involves lesion recognition, helicase, and nuclease activities, followed by synthesis/ligation.

C) **Mismatch repair (MMR):** MMR is also an excision-based repair mechanism involving mismatch recognition, excision directed from induced or existing nicks, and synthesis/ligation.

**1.42 Defects in DDR:**

Defects in each of these repair pathways can lead to malignant transformation, as described earlier. Moreover, defects in these pathways can also give a proliferative advantage to cancer cells. The finding that cancer cells are defective in some of these repair pathways has led to the concept of synthetic lethality. The concept of synthetic lethality originated during genetic studies in the fruit-fly *Drosophila*, where the loss of one gene was compensated by over reliance to

another [115, 116]. This discovery prompted scientists to extend the same concept for cancer treatment, since it was evident that most of the cancer cells were deficient in one of the repair pathways, which made them dependent exclusively on an alternative pathway, which can be targeted to promote cell death. Since normal cells have both the pathways active, the loss of one of the pathways during treatment can be compensated by the presence of the other pathway. In other words, synthetic lethality is exploiting the vulnerability of tumor cells, which have lost one DNA repair pathway by targeting a second repair pathway. This represents a new emerging and interesting therapeutic approach. The following table gives a few examples of the concept of synthetic lethality exploited in certain diseases involving compromised repair pathways.

| Syndrome /Disease | Affected Repair pathway(s) | Proteins involved | Drugs exploiting the defective DDR |
|---|---|---|---|
| Xeroderma pigmentosum | NER | ERCC4, ERCC1 | Platinum salts |
| Breast, ovarian, pancreatic cancers | HR | BRCA1, BRCA2, PALB2, ATM CHEK1, CHEK2 RAD51 | PARP inhibitors, Platinum salts |
| Colorectal cancer | MMR | MSH2, MLH1 | Methotrexate |
| Glioma | Direct reversal | MGMT | Temozolomide |

**Table 1.5: Examples of drugs exploiting synthetic lethality of cells**

**1.43 Role of RecQ helicases in DNA repair:**

**BLM:**

The BLM helicase plays an essential role in regulating several recombination events. BLM has a role in suppressing recombination events, which is evident by the hyper-recombination phenotype of BS patient cells and of cells derived from *BLM* knockout mice. This increased recombination events are connected to the tumor susceptibility of *BLM* knockout mice [117]. The major characteristic phenotypes of BS cells are an elevated level of SCEs [37], associated with defects in homologous recombination. To initiate HR, blunt-ended DSBs have to be resected to create 3'

single stranded DNA. HR occurs via two major steps; strand exchange and resolution. RAD51, a highly conserved recombinase protein, binds to ssDNA ends and exchanges strands between homologous regions. After strand exchange, a triple-stranded intermediate, termed a D-loop, is formed. D-loops can either be destroyed by an unwinding reaction, or be converted into four-way junctions (Holliday junctions) [118]. BLM interacts with RAD51 and may suppress homologous recombination by unwinding the invading strand from the D-loop [119]. If the D-loops are converted into Holliday junctions, these junctions have to be resolved, otherwise the recombining molecules will remain covalently intertwined. BLM promotes the resolution of Holliday junctions to generate exclusively or predominantly non-crossover products. In particular, the BLM-TopIIIα-BLAP75/RMI1 complex was shown to resolve double-Holliday junctions without crossover in ATP-dependent manner [120-122].

Following the observation that BS cells have an abnormally high frequency of anaphase bridges, micronuclei formation and mitotic abnormalities, Chan et al. have also found that this BLM complex is recruited during anaphase to catenated DNA structures that persist following DNA replication. The BLM complex is required to resolve these catenated structures and permit faithful sister-chromatid disjunction [123].

Moreover, Ashutosh Rao et al. reported that BLM-deficient cells and primary BS fibroblasts display an endogenously activated DNA double-strand break checkpoint response [124]. In particular, BS cells show increased levels of phosphorylated histone H2AX (γH2AX), Chk2 (pT68Chk2), and ATM (pS1981ATM) co-localizing in nuclear foci. Moreover, the mitotic fraction of γH2AX foci did not seem to be higher in BLM deficient cells, indicating that the DNA lesions must have been formed transiently during the interphase.

BLM deficiency was also shown to be associated with a strong cytidine deaminase defect, leading to pyrimidine pool imbalance. Nucleotide pool normalization of BLM-deficient cells was shown to reduce SCE frequency and was also sufficient to fully restore the replication fork velocity but not the fork restart defects [125].

**WRN:**

WRN has been implicated in telomere maintenance. A number of studies suggest that WRN play important roles in recombination-mediated mechanisms of telomere elongation or alternative lengthening of telomeres (ALT). These processes are essential to maintain/elongate telomeres in the absence of telomerase [126]. Consistently, the forced expression of exogenous telomerase in WS fibroblasts rescued the premature senescence phenotype of these cells [127]. It is also reported that WRN readily alleviates G-quadruplex secondary structures, which are predicted to be formed in the G-rich telomeric regions [128]. These structures are more likely to impede the progress of the lagging-strand replication machinery. So, if these structures are unresolved, they can prevent the complete synthesis of the daughter strand [129] and hence, cells lacking a functional WRN helicase show a more rapid telomere shortening that occurs stochastically with each cell cycle [130]. Compared with normal fibroblasts, WS cells exhibit an increase in sister-telomere loss (STL) or telomere-free ends (TFE) at some of chromosome ends. Although infrequent, telomere defects (TDs) can significantly impair the cell viability and activate damage signalling and subsequent processing by non-homologous end joining, potentially forming dicentric chromosomes and causing genome instability [129, 131, 132]. Thus, telomere defects are a consistent, well-recognized feature of WRN-deficient cells.

Improper remodelling of forks in the absence of WRN may result in DNA breakage and thus activation of the DNA damage response branch of the cell cycle checkpoint. In agreement with this, chromosomal rearrangements, breaks, and persistent γ-H2AX foci are more frequent in WRN-deficient cell [133]. Several studies suggested that WRN is involved in different DNA repair pathways including BER, SSBR (single-strand break repair), HR, and NHEJ. This conclusion is mainly based on the observations that WRN interacts with key proteins involved in these pathways. However, the exact role of WRN in all these repair pathways is yet to be elucidated.

The involvement of WRN in BER/SSBR is supported by the observation that WS cells are sensitive to hydrogen peroxide and they accumulate increased damage

after endogenous oxidative stress. In addition, WS cells show reduced BER activity *in vitro* [134, 135]. Consistently, WS cells are sensitive to number of methylating agents such as MMS, methylexitropsine, and telozolomide. WS cells are also sensitive to SSB producing agents such as CPT and 4-NQO [136, 137].

The exact role of WRN in NHEJ is still unclear. WRN is not an essential component of NHEJ, but it might act in a NHEJ sub pathway on sub-genomic regions such as telomeres or ribosomal (r) DNA [23]. Moreover, an alternative NHEJ pathway for DSB repair involving DNA ligase IIIα and WRN was discovered in chronic myeloid leukemia cells [138].

**RECQ5:**

Available literature suggests that RECQ5 is a tumour suppressor protein. In particular, it minimizes the propensity of oncogenic rearrangements by suppressing the accumulation of DSBs and attenuating HR by disrupting inappropriate RAD51 presynaptic filaments [139]. The association of RECQ5 with RNAP II *in vivo* points to a possible role of RECQ5 in transcription. The exact mechanism of transcription regulation by RECQ5 is not yet clear. Thus, RECQ5 has been proposed to promote genome stability through two parallel mechanisms: by participation in homologous recombination-dependent DNA repair and by regulating initiation of RNAPII to reduce transcription-associated replication impairment and recombination [140].

In line with its proposed functions in transcription and homologous recombination, RECQ5 interacts with various proteins involved in these two pathways. In particular, RECQ5 is the only member of the human RecQ helicase that interacts with RNA polymerase II (RNAPII). Strikingly, RNAPII is the major protein complex associated with RECQ5 when purified from human chromatin under physiological conditions. RECQ5 is able to associate with both the hypo- and hyper-phosphorylated forms of RNAPII and the RPB1 subunit of RNAPII and the C-terminal domain of RECQ5 mediate this interaction [141]. *In vitro* transcription assays and small interfering RNA (siRNA) studies have shown that the RecQ5-RNAPII interaction inhibits transcriptional initiation and elongation [141].

Recent findings from Weidong Wang's lab using chicken DT40 cells inactivated for RECQ5 demonstrate that the interaction with RNAPII is critical for the RECQ5-dependent suppression of SCE and resistance of CPT-induced cell death. Their studies shows that, both the helicase activity of RECQ5 and the association with the initiation polymerase is essential for RECQ5 function because the mutants lacking either of the two activities were partially defective in the suppression of SCE and the double mutants were completely defective. Hence they proposed that *RecQL5* could promote genome stabilization in two ways: by participation in HR-dependent DNA repair and by regulating the initiation of Pol II to reduce transcription-associated replication impairment and recombination [142].

RECQ5 seems to be recruited by MRE11–RAD50–NBS1 (MRN) complex, a primary sensor of DNA double-strand breaks to sites of DNA damage [143] where it interacts physically with the RAD51 recombinase and disrupts RAD51 presynaptic filaments in a reaction dependent on its helicase activity [144]. Thus RECQ5 also regulates homologous recombination.

**RECQ4:**

RECQ4 is implicated in different DNA metabolic processes, as suggested by three different genetic diseases associated with *RECQ4* mutations. RECQ4 has been shown to participate in various DNA repair pathways. Petkovic *et al.* reported that after etoposide treatment RECQ4 nuclear foci coincide with the foci formed by RAD51 [145]. In addition, fibroblasts from RTS patients (RTS cells) are sensitive to ionizing radiation [146] and Kumata *et al.* recently provided evidence that RECQ4 participates in DSB repair in *Xenopus* egg extracts [147]. Vilhelm Bohr's group also suggested that RECQ4 is involved in NER and showed that the complementation with wild-type RECQ4 rescues the UV sensitivity of RTS cells [148]. Moreover, it has been recently reported that RECQ4 plays a role in oxidative stress response and particularly in BER [149].

RECQ4 also interacts with PARP1 and PARP1 poly(ADP-ribosyl)ates RECQ4 suggesting that the interaction with PARP1 might be required to withstand the oxidative stress [150]. Consistently, biochemical experiments indicate that

RECQ4 specifically stimulates the apurinic endonuclease activity of APE1, the DNA strand displacement activity of DNA polymerase β, and the incision of a 1- or 10-nucleotide flap DNA substrate by Flap Endonuclease I. All these enzymatic processes are important for the removal of oxidized bases [149]. Moreover, RECQ4 is recruited to the UV-DNA damaged sites by a direct association with XPA and it is required for the optimal repair of UV-induced DNA lesions [151].

A recent study by Avik K.Ghosh *et al*. reported that RTS patients have elevated levels of fragile telomeric ends in their cells and that RECQ4-depleted human cells accumulate fragile sites, SCE's and DSB's at the telomeric sites. They have also shown that RECQ4 localizes to the telomeres and associates with the shelterin proteins TRF1 and TRF2 [152]. In agreement with these observations, a recent *in vitro* study shows that RECQ4 could repair thymine glycol lesions *in vitro* and this activity is slightly enhanced by the TRF2 shelterin protein [153].

**RECQ1:**

The increased load of DNA damage and the elevated sister chromatid exchanges in the RECQ1 deficient cells suggest that RECQ1 is involved in maintaining chromosomal stability playing an anti-recombinative role and suppressing the formation of recombination intermediates that arise during replicative stress [154]. A role of RECQ1 in DNA repair has also been suggested by the ionic radiation sensitivity of RECQ1 deficient cells and by the interaction of endogenous RECQ1 with some DNA mismatches repair proteins [155].

Several DNA repair proteins such as MSH2/6, MLHI-PMS2, EXO1 and RAD51 have been shown to associate with RECQ1 helicase by co-imunoprecipitation experiments. The functional role of these interactions is still unknown [154, 155]. RECQ1 was also shown to play an important role in DNA replication that will be discussed in the next paragraph.

# 1.5 RecQ helicases in DNA replication

## 1.51 DNA replication:

Genome is an integral aspect of every living organism, and it contains all of the biological information needed to build and maintain a living example of that organism. The genome is inherited to the next generation by a process called as DNA replication, and hence it is rightly called as the basis of biological inheritance. Prior to cell division, the DNA has to be duplicated to guarantee that the daughter cell gets the same amount of DNA as the parent cells. DNA replication is semi-conservative and it involves different steps.

First, the double helical structure of the DNA has to be partially unwound to initiate the replication process. This occurs at specific site called the "origins" of DNA replication, which are usually "A, T" rich. The unwound strands are prevented from re-annealing by the binding of single stranded binding proteins (SSB's) to the single strands. Bacteria and prokaryotes have only one DNA replication origin that is fired once during each cell cycle. However, owing to the complexity of their genome, the eukaryotic cells have multiple origins of replication and the timing of origin firing as well as the origin firing efficiency varies among the different origins. All eukaryotic organisms studied so far seem to have excess origins, leading to the suggestion that there are some "dormant origins" which are fired only when the other origins are inactivated [156].

Next, the DNA assumes a forked or a Y-shaped structure where replicative polymerases load to duplicate the DNA. The two strands, called the leading and lagging strand, serve as a template for the synthesis of daughter strands.

- On the leading strand, the DNA polymerase—Pol III in prokaryotes and Pol ε in eukaryotes—reads the DNA and adds nucleotides to the 3' – OH of the previous nucleotide. The leading strand moves towards the fork and is synthesized continuously.

- The lagging strand is discontinuous and moves away from the fork. The primase reads DNA and adds RNA primers along the strand, which is faithfully extended by the DNA pol III in prokaryotes or Pol δ in eukaryotes. The RNA primers are subsequently removed and replaced with DNA nucleotides. The pieces of DNA synthesized, called Okazaki fragments, are joined together by DNA ligase I.

Since eukaryotes initiate DNA replication at multiple points, the replication forks terminate when they meet the adjacent replication forks. They also terminate when they encounter the telomeres which are the physical ends of chromosome [157].

DNA replication is a tightly regulated process to ensure that the DNA divides once and only once during a cell cycle. Cell division is laid out in the format of a cycle and in every cycle the DNA is replicated only at the S-phase. The cell cycle is in turn regulated by checkpoints that help to maintain high fidelity by stabilizing the replication forks and preventing the cell cycle progression during replication stress or damage [158].

Finally, DNA replication has to be monitored carefully to guarantee a faithful transmission of genetic information and protect the integrity of the replicating DNA. Thus, the cells must be able to initiate adequate DNA repair processes if the replication forks are damaged or stalled. Hence, genetic mutations that affect the enzymes involved in replication or those involved in post replication repair, results in the accumulation of mutations or DNA intermediates that triggers genome instability and recombination. And it is not surprising that these defects eventually lead to diseases and ageing.

**1.52 Replication stress and fork stability:**

There are a wide variety of agents, both endogenous and exogenous that challenges the replication fork integrity. A damaged or stalled replication fork is called "arrested" when it is capable of restart once the lesion has been removed, whereas it is called "collapsed" when it cannot restart due to the dissociation of the replication machinery or the formation of a DSB [159] .

Some common endogenous agents that could damage/stall replication forks are:

- ❖ ROS – Reactive oxygen species which are generated by normal cellular metabolism
- ❖ Base depurination and deamination
- ❖ Unusual DNA structures (triplex H-DNA, left handed Z- DNA)
- ❖ Collision with the transcription machinery
- ❖ DNA-protein complexes

Some common exogenous agents that could damage/stall replication forks agents are:

- ❖ Ultraviolet rays (Thymidine dimer formation)
- ❖ Ionizing radiation (SSB and DSB)
- ❖ Cigarette smokes (e.g., nitrosamines, polycyclic aromatic hydrocarbons)
- ❖ Industrial chemicals (e.g., vinyl chloride, hydrogen peroxide)
- ❖ Drugs used in chemotherapy (e.g., cyclophosphamide, etoposide)

The replication checkpoint stands out as the prime regulator of RF stability after genotoxic stress. The replication check-point is composed of a network of sensors and transducers that detect, transmit, and amplify the DNA damage and replication stress signal, and then promote a DNA damage response that ensures the stabilization of RFs, DNA repair and cell cycle arrest [159]. The ATM kinase (Ataxia telangiectasia mutated) with its regulator MRN complex (Mre11-Rad50-NBS1) and the ATR kinase (ATM and Rad3-related protein) with its regulator ATRIP (ATR-interacting protein) are the two major players involved in check-point response.

The ATM pathway is typically activated by double strand breaks. Collapsed replication forks generate DSBs that also activate ATM [160]. Following DSB formation, the histone H2AX is phosphorylated at the serine 139 ($\gamma$-H2AX) by ATM. This represents as one of the earliest events in DDR [161]. The MRN (MRE11-RAD50-NBS1) complex, which is one of the first complexes to be recruited to DSBs, acts as a damage sensor that also physically bridges the ends of the DSB [162]. MRE11 plays a role in end resection while the NBS1 interacts with ATM, and

this interaction is required for the recruitment and retention of ATM to DSBs [163-167]. ATM phosphorylates and modulates the activity of several protein kinases, which in turn phosphorylate their own substrates and the most notable among the kinases is the checkpoint kinase 2 (CHK2) [168]. The components of the MRN complex are also phosphorylated and contribute to the timely activation of various DDR branches [169-173].

The ATR checkpoint responds to exposed single-stranded breaks coated with hRPA (Replication protein A) and promotes their stabilization [174-177]. Stalled forks generated by helicase-polymerase uncoupling generally presents exposed ssDNA regions coated by the single-strand binding protein RPA (replication protein A), which in turn recruits the active ATR-ATRIP (ATR-interacting protein) complex [178]. In spite of the numerous substrates, the main signal arising from the ATR cascade is the phosphorylation-activation of Chk1, a serine-threonine kinase. Globally Chk1 activation leads to cell cycle arrest by phosphorylation-modulation of CDK regulators CDC25-A, CDC25-B, CDC25-C, and p53 activation. In addition, the ATR pathway promotes local fork stabilization through phosphorylation of several targets such as replication components, nucleases, and DNA helicases, which are required to maintain replisome integrity and prevent fork collapse [178, 179].

The activation ATM and ATR kinases trigger the checkpoint response through the phosphorylation of targets that are implicated in various downstream processes [180, 181]. About 25 ATM and ATR substrates have been identified [182], many as candidates based on known roles in damage signaling.

BLM is a substrate of ATR and is phosphorylated on Thr99 and Thr122 in HU treated cells [183]. BLM was shown to co-localize with ATR and co-immunoprecipitate with ATR from cell extracts following DNA replication arrest. The authors propose that phosphorylation of BLM on Thr-99 and Thr-122 by ATR is an important component of the response of cells undergoing replication fork arrest and that it is subsequently essential for adequate cellular recovery from the replication stress [183]. WRN was shown to be phosphorylated after replication arrest in an ATR-dependent manner and also both ATR and WRN were shown to be acting together in a common pathway to stabilise common fragile sites [184, 185].

The same group reported the role of both ATM and ATR in promoting the recovery from replication perturbation by differently regulating WRN at defined moments of the response to RF arrest. They reported that suppression of ATR-mediated phosphorylation of WRN prevented the proper accumulation of WRN in nuclear foci, co-localisation with RPA and caused breakage of stalled forks, whereas inhibition of ATM kinase activity led to the retention of WRN in nuclear foci and impaired recruitment of RAD51 recombinase resulting in reduced viability after fork collapse [186].

**1.53 Roles of RecQ helicases in DNA replication:**

DNA replication is a complex process that can be divided in different steps such as assembly of the replication machinery, replication initiation, and replication fork progression. This process is highly controlled by checkpoint proteins. RecQ helicases are involved in most DNA replication steps.

Role of RecQ helicases in initiation of DNA replication was first shown for RECQ4. The first 200 amino acids of human RECQ4 share homology with the yeast DNA replication initiation factors Drc1 (*Schizosaccharomyces pombe*) and Sld2 (*S. cerevisiae*) [98, 187, 188]. Moreover, Matsuno *et al.* and Sangrithi *et al.* showed that depletion of *RECQ4* from *Xenopus laevis* egg extracts prevents initiation of DNA replication and suggested that this might be due to a defect in the loading of RPA to chromatin [98, 189]. Interestingly, the N-terminal Sld2-like domain of human RECQ4 has been also shown to possess an intrinsic DNA helicase activity [188], although this result has not been confirmed by future studies [190]. Our group showed that RECQ4 is recruited to replication origins at late G1 after the origin recognition complex (ORC) [191]. In agreement with this finding, Yilun Liu's group showed that human RECQ4 interacts with the MCM [192], while J.K.Lee's group showed that RECQ4 is essential for replisome assembly [193]. Our group also showed that RECQ4 is required for the loading of PCNA and the ssDNA binding protein RPA onto the replication fork, supporting the notion that RECQ4 is an essential factor for replication initiation [191]. The notion that RECQ4 plays an essential role during DNA replication is supported by the embryonic lethality of *RecQ4* knockout mice [95]. Moreover, a recent study suggested that the helicase and

the C-terminal domain of RECQ4 facilitate DNA replication elongation in cells that have been exposed to IR [194]. Given that all the *RECQ4* mutations identified in RTS patients are located within or after the exons encoding the central helicase domain, it is possible that these patients still express a truncated RECQ4 protein with an intact Sld2-like domain required for replication initiation. Therefore, all of the *RECQ4* mutations associated with disease might be hypomorphic [92, 96].

While RECQ4 is important for origin firing, BLM can suppress origin firing. In eukaryotic cells, there are multiple DNA replication origins with a different, but regulated order of activation. Some of the origins are dormant and are normally suppressed [195]. Upon replication inhibition, these dormant origins can fire, probably to compensate for the slower overall DNA replication rate and/or to permit replication of loci to be rescued by a converging fork. Davies *et al* showed that BS cells have high origin firing frequency after release from HU stress. They showed that BLM is required for the efficient restart of the stalled replication forks and for the suppression of dormant origin firing [196]. These activities require the helicase activity of BLM and phosphorylation of the Thr 99 residue targeted by stress-activated kinases (ATR in the context of replication blockade) [183].

Several evidence support the notion that the human RECQ1 helicase might also play a role during DNA replication. Wang *et al.* employed a DNA affinity purification and mass spectrometry procedure to show that RECQ1 is physically associated with KSHV ori-Lyt through the viral proteins K8 and RTA; they speculated that RECQ1 is not only an integral component of the pre-replication complex, but also the so long-sought helicase that unwinds origin DNA in the initiation of KSHV lytic DNA replication [197]. Later it was found that RECQ1 is also associated with the ori-Lyt and Zta of another virus, Epstein–Barr virus (EBV). Depletion of RECQ1 by shRNA resulted in reduced lytic DNA replication [198]. Successively, our group showed by chromatin imunoprecipitation approaches that RECQ1 physically associates with replication origins in a cell cycle-regulated fashion in unperturbed cells [191]. However, the exact role of RECQ1 during DNA replication remained to be determined and my thesis and our recent paper provide new clues on the role of RECQ1 in this process [199].

Various studies suggested a possible role of RecQ helicases during replication fork progression. For example, depletion of BLM or RECQ1 was shown to reduce the replication fork speed [191, 200, 201], while BS cells are known to accumulate abnormal replication intermediates [202]. Conversely, depletion of WRN or RECQ4 does not seem to influence the fork progression rate [191, 201]. RecQ helicases seem to be particularly important for replication fork progression when there is a replication blockage. In particular, the acute depletion of several human RecQ family members is associated with an increased sensitivity to several DNA damaging agents and replication inhibitors [203]. For example, RECQ1, BLM, WRN, RECQ4 and RECQ5 depleted cells are sensitive to CPT [151, 154, 199, 203-205] and HU treatment (except RECQ5) [192, 196, 201, 203, 206]. RECQ4 depleted cells are sensitive to UV damage [151]. In addition, RecQ helicases localize at damaged replication sites upon replication perturbation. For example, BLM translocate from PML bodies to damaged replication forks upon DNA damage induction, while WRN translocate from the nucleolus to nucleoplasmic foci upon UV exposure [207].

BLM and WRN have been shown to be phosphorylated during replication stress to fine-tune their function at the replication fork. BLM depleted cells or BS cells show reduced efficiency of replication fork restart after HU or aphidicolin treatment, demonstrating a key role for BLM helicase through its helicase activity for replication restart. Mechanistically, BLM was suggested to restart replication forks by transporting p53 to RAD51 sites at the stalled replication forks [208]. BLM forms a complex with topoisomerase III alpha, RMI1, RMI2 and replication protein A, called the 'BLMcx' [209]. This complex has been shown to be recruited to the replicating chromatin during normal S-phase and members of the complex are phsophorylated in response to DNA damage. During replication stress, BLM from the BLMcx and FANCD2 cooperate to promote restart of stalled replication forks while suppressing firing of new replication origins [209]. BLM was also shown to co-localize with ATR and co-immunoprecipitate with ATR from cell extracts following DNA replication arrest. The authors propose that phosphorylation of BLM on Thr-99 and Thr-122 by ATR is an important component of the response of cells undergoing replication fork arrest and that it is subsequently essential for adequate cellular recovery from the replication stress [183].

WRN cells are sensitive to treatment with replication inhibitors and DNA damaging agents that cause replication fork stalling such as aphidicolin, HU, CPT, etoposide, MMS, cisplatin, mitomicin C and γ-irradiation [86, 210-214]. When cells are challenged with genotoxic agents additional WRN-dependent deficiencies are revealed. These can reflect replication problems in other susceptible areas, such as fragile sites, satellite repeats, or any genomic segments that replicate unidirectionally [185]. Finally, systemic deregulation of replication, by genotoxic drugs [201] or oncogenes such as hyperactive Myc [215], can elicit severe S-phase defects in WRN-depleted cells [201]. In addition to the restart defects, the restarted forks progressed slowly in the absence of WRN. WRN was also shown to be phosphorylated after replication arrest in an ATR-dependent manner and also both ATR and WRN was shown to be acting together in a common pathway to stabilise common fragile sites [184, 185]. The same group reported the role of both ATM and ATR in promoting the recovery from replication perturbation by differently regulating WRN at defined moments of the response to RF arrest. They reported that suppression of ATR-mediated phosphorylation of WRN prevented the proper accumulation of WRN in nuclear foci, co-localisation with RPA and caused breakage of stalled forks, whereas inhibition of ATM kinase activity led to the retention of WRN in nuclear foci and impaired recruitment of RAD51 recombinase resulting in reduced viability after fork collapse [186].

A variety of DNA structures such as G-quadruplexes and hairpins can serve as "road-blocks" and impede the progression of the repliosome, especially if they are present in the leading strand template. It is known that several human RecQ helicases can resolve these substrates, thereby enabling the smooth progression of the repliosome [216]. Replication problems might also occur at an increased frequency in telomeric regions, because of the intrinsic inability of the lagging strand DNA replication machinery to function at the very end of chromosomes. Hence, a specialized reversed transcriptase called telomerase adds G-rich repeat sequence to the telomere ends. WRN has been shown to be required for telomere lagging strand synthesis [129]. WRN associates with the telomeric TTAGGG region, and possibly unwinds G-quadruplexes formed therein to allow the replication forks to progress to the chromosome ends. In cells lacking a functional telomerase, there is an alternative pathway termed alternative lengthening of telomeres, which requires sgs1 in *S.*

*cerevisiae* [217] [218] [219]. The alternative lengthening of telomeres pathway is dependent on the HR factors Rad50 and Rad52, but not on RAD51. WRN is able, through the combined use of its helicase and exonuclease activities, to resolve the D-loop HR intermediate to release the 3′ invading tail. This activity might be used to disrupt recombination events at telomeres or to disrupt the natural telomeric T-loop (a specialized D-loop) in order to permit replication of the telomeric end.

## 1.6 Replication fork regression and restoration

The effects of DNA lesions on replication fork progression vary based on the strand in which the lesions are. For example, the lesions on the discontinuously synthesized lagging strands can be skipped over and a new Okazaki fragment can be re-initiated downstream of the lesion to be repaired after completion of DNA replication [220, 221]. On the other hand, lesions on the leading strand are more likely to block fork progression. In response to this threat, DNA damage tolerance pathways have evolved to enable DNA polymerases to bypass lesions on the leading DNA strand template.

Stalling of the replication fork at a lesion on the leading strand template can result in the uncoupling of leading and lagging strand synthesis; DNA synthesis continues only on the undamaged lagging template strand generating ssDNA gaps that may activate HR [222]. Alternatively, DNA lesion bypass can occur through the template strand switch mechanism [223]. This mechanism includes conversion of the fork into a reversed fork structure reminisce of a Holliday junction (known as the 'chicken foot' structure) [220, 224] and this process is called as "fork regression" (figure 1.5).
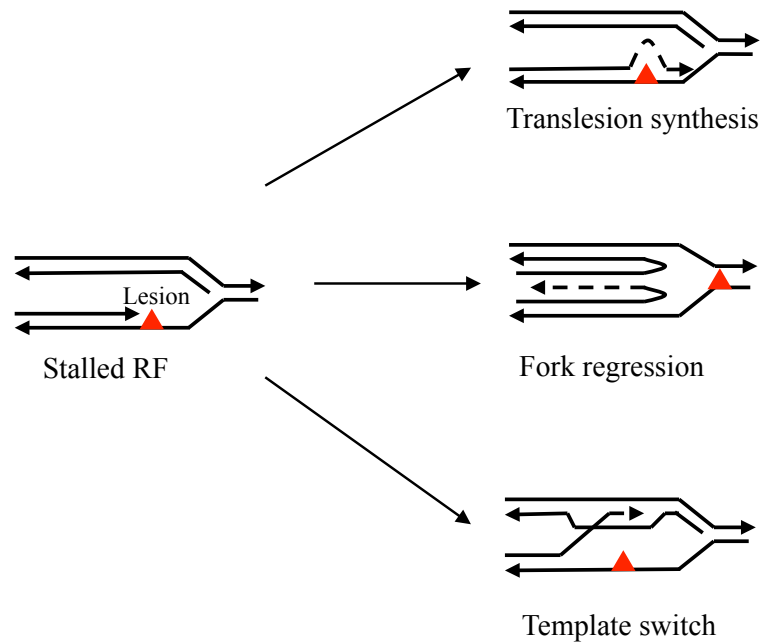
**Figure 1.5: Mechanisms of DNA damage tolerance to lesions on the leading strand.** The lesion in the leading strand could be either by-passed by translesion synthesis or by template switch mechanism, or alternatively by re-modelling the fork into a chicken-foot like structure by a process called fork regression.

Following fork regression, the DNA lesion is repaired and a reverse branch migration reaction takes place to re-establish a functional fork structure. Alternatively, the extended lagging daughter strand is used as a template for the synthesis of the leading strand followed by reverse branch migration to bypass the blocking lesion and re-establish the functional replication fork. Part of this thesis focuses on investigating the roles of human RecQ helicases in fork regression and restoration.

RECQ1, WRN, and BLM are all able to bind and branch migrate Holliday junctions *in vitro* [225-228]. In addition, BLM and WRN also able to promote fork regression and restoration *in vitro* [225, 227, 229-232] suggesting that RecQ helicases could play an essential role in the formation and resolution of these replication structures in cells. Alternatively, the regressed forks could be resolved by Holliday junction resolvases, causing fork collapse [233] [234]. These broken forks must be repaired by HR through DNA strand invasion to re-establish a functional replication fork [235] [236].

This reaction is promoted *in vitro* by RecQ helicases, including BLM and WRN, which might allow the bypass of a DNA lesion blocking the fork and the restart of DNA replication. Once the regressed fork is formed, a four-way Holliday junction is generated, which could potentially be migrated back by RECQ1, BLM or WRN to restore a functional replication fork.

## 1.61 Top1 inhibitors and replication fork reversal:

DNA topoisomerases are enzymes that relax DNA torsional strain generated during replication, transcription, recombination, repair, and chromosome condensation [237], and hence are vital to all cells undergoing division. The relaxation of DNA supercoiling by topoisomerase I (Top1) is enabled by a mechanism of controlled rotation around a transient DNA single-strand break [238, 239]. During this process, the enzyme forms an intermediate covalent complex with the DNA, mediated by a bond between the active site tyrosine (Tyr723 in human Top1) and the cleaved phosphate group [237]. Top1 and Top2 inhibitors rely on the transient trapping of these specialized nucleases on their 3'-single-strand and 5'-double-strand DNA substrate, respectively, thus preventing the religation step [237]. Because of the high proliferation of cancer cells, drugs that target Top1 such as camptothecin, or Top2 such as etoposide, are potential chemotherapeutics and some of them have been already clinically approved for cancer treatment [240, 241]. In particular, the S-phase dependent cytotoxicity of Top1 inhibitors was thought to arise from replication run-off at Top1-DNA frozen complexes located on the leading strand, triggering to the accumulation of lethal one-side DSBs [242]. This model was recently challenged by the work of Koster *et al.* where using a combination of single-molecule and *in vivo* experiments, the authors demonstrated that Top1 inhibitors hinder the uncoiling activity of Top1, thus promoting positive supercoiling formation and replication fork slowing. They also proposed that the resulting accumulation of positive supercoils ahead of the replication machinery is the major mechanism of fork collapse and cell death upon camptothecin exposure [243, 244].

Recently, the group of Massimo Lopes in Zurich has extended this observation by demonstrating that clinically relevant doses of Top1 inhibitors are associated with replication fork slowing, without DSBs formation. By exploiting a combination of *in vivo* psoralen cross-linking and EM analysis to directly visualize

replication intermediates, they were able to detect a high frequency of regressed forks upon Top1 poisoning in yeast, *Xenopus laevis* egg extract, and mammalian cells. In contrast to previous findings, they found that the replication fork slowing and reversal associated with Top1 inhibitors are not checkpoint or recombination dependent. Moreover, they discovered that poly(ADP-ribose) polymerases 1 (PARP1) activity, at least in *X. laevis* egg extract and mammalian cells, is essential to slow the replication forks on CPT-damaged templates by promoting the accumulation of regressed forks. PARP1 depletion or inhibition revert this effect of Top1 poisoning, leading to the formation of DSBs likely by replication run-off at Top1-DNA covalent complexes (Top1cc) (figure 1.6) [245]. PARP1 plays a critical role in mediating the cellular sensitivity to camptothecin derivatives and several clinical trials are currently investigating the potential advantages of combined therapies with PARP and Top1 inhibitors [246, 247].
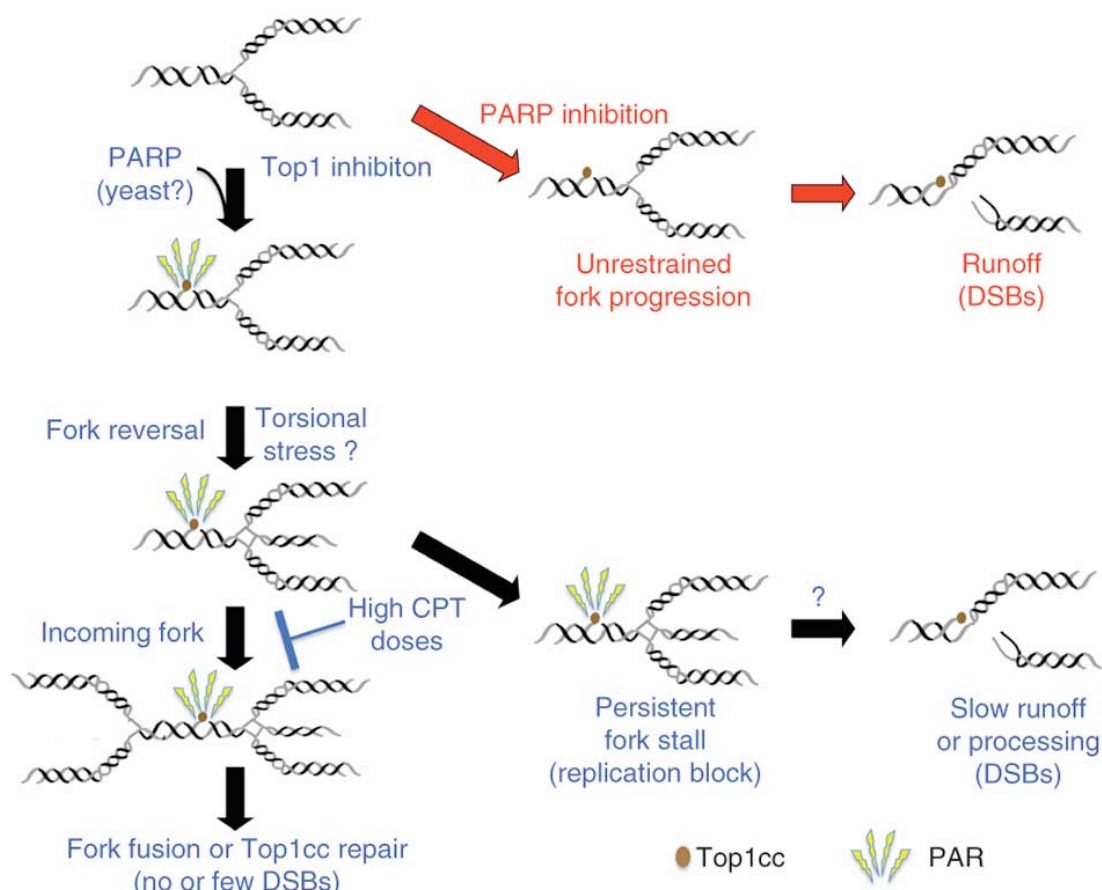


**Figure 1.6. Model for replication interference by Top1 poisons and their synergistic effects with PARP inhibitors.** Upon Top1 inhibition, replication forks rapidly experience slowed progression and reversal, mediated by PARP activity in higher eukaryotes (and unknown factors in yeast) and promoting Top1 covalent complex (Top1cc) repair and replication completion. PARP inactivation

leads to increased DSBs, owing to unrestrained fork runoff at Top1cc. High CPT doses lead to incomplete replication and persistent fork stalling, causing DSBs by eventual fork collapse and/or processing; PAR, poly(ADP-ribose) Adapted from Ray Chaudhuri A., 2012 [245].

The results of Dr. Lopes' group provide a new rationale for the synergic effect of these inhibitors on actively proliferating cancer cells. They also point to fork reversal as a general strategy that allows the repair enzymes to fix the lesion before the replication resumes, thus avoiding replication fork collision with single, and possibly, double strand breaks. Nevertheless, this work opens several relevant biological questions: 1) since PARP1 is just a signaling molecule without motor activity, what other factors are involved in PARP-mediated fork reversal? 2) Which are the cellular factor responsible for the restart of the reversed forks? My thesis provides answers to these questions by pointing to an essential role of the human RECQ1 helicase in this process.

# 2. MATERIALS AND METHODS

## 2.1 Antibodies and chemicals:

The antibodies used were rabbit anti-His antibody (sc-803) from Santa Cruz, rabbit anti-RECQ1 polyconal antibody was custom made against the full length sequence of the protein.

$NAD^+$, ATP, ATPγS, TCEP, imidazole were all from Sigma. Protease inhibitor cocktail tablets were from Roche. The radioactive $[^{32}γP]$-ATP was from PerkinElmer. The antibiotics were from Sigma. Bluo-gal was from Invitrogen. The restriction enzymes and polymerases were from NEB and Agilent technologies respectively. For protein purification, the TALON Cobalt resin was from Clontech and the gel filtration columns were from GE healthcare. The BioSpin columns for the removal of extra nucleotides were from Bio-Rad. All other chemicals were of reagent grade or higher from various vendors.

## 2.2 Cell culture and transfection:

The Sf9 cells were grown at 27°C in SFM II media (Invitrogen). Sf9 cells were transfected using cellfectin II (invitrogen) following the supplier's protocol. Briefly 8 X $10^5$ cells were transfected with 1 μg of bacmid using cellfectin II and incubated at 27ºC. The virus was collected 72 hours post transfection and stored protected from light at 4°C (short term storage) or -80°C (long term storage).

## 2.3. Expression and purification of recombinant proteins:

### 2.3.1. RECQ1 overexpression and purification:

RECQ1 was overexpressed and purified from Sf9 cells as already described [248]. RECQ1 bacmid was isolated from DH10Bac (Invitrogen) cells after transposition, confirmed by PCR and was transfected into Sf9 cells using cellfectin II reagent. After 72 hours, the medium containing the baculovirus was collected,

centrifuged to remove the cell debris and stored protected from light. To increase the titre, the baculovirus was amplified 3 - 4 times by infecting log-phase Sf9 cells, followed by collecting the media containing the viral particles. For RECQ1 overexpression, a litre of the Sf9 cell suspension culture at a density of 150 X $10^4$ cells /ml was infected with the appropriate amount of the baculovirus and the infected cells were collected 72 hours post infection. The pellet was washed with phosphate buffered saline (PBS) and stored at - 80°C until use.

For protein purification, the infected cells were re-suspended in lysis buffer (20 mM Tris–HCl, pH 7.4, 400 mM KCl, EDTA free protease inhibitor, 5 mM β-mercaptoethanol) and sonicated on ice five times at maximum amplitude for 30 s with a 30 s gap. The lysate was cleared by centrifugation at 15,000 rpm for 45 minutes. Meanwhile, the TALON cobalt resin (Clontech) was washed twice with Milli Q water and equilibrated in the lysis buffer. The cleared lysate was allowed to bind to the resin (1 ml resin / 5 mg protein) for 2 hours at 4°C in a nutator. After binding, the resin was washed thrice with high salt buffer (20 mM Tris–HCl, pH 7.4, 500 mM KCl, 12.5 mM imidazole, 5 mM β-mercaptoethanol) and twice with low salt buffer (20 mM Tris–HCl, pH 7.4, 150 mM KCl, 12.5 mM imidazole, 5 mM β-mercaptoethanol). The resin was loaded into a column and the polyhistidine tagged RECQ1 was eluted using 120 mM imidazole in the elution buffer (20 mM Tris-HCl, pH 7.4, 100 mM KCl, 5 mM β-mercaptoethanol,). The eluted fractions were run on a SDS-PAGE gel and the fractions containing the protein were pooled and dialyzed at 4°C against 150 mM KCl, 1 mM DTT and 20 mM Tris-HCl pH: 7.4 three times for two hours each. The dialyzed protein was quantified, aliquoted and stored at -80°C after flash freezing in liquid nitrogen.

## 2.3.2 Site directed mutagenesis and purification of RECQ1 mutants:

The ATPase mutants K119R-RECQ1, E220Q-RECQ1 and the annealing mutants L18P-RECQ1 and L28P-RECQ1 were prepared using the wild-type pFASTBAC1-RECQ1 recombinant plasmid as template. The mutations were done using the QuickChange XL site-directed mutagenesis kit (Stratagene) following the manufacturer's protocol. The respective bacmids were produced in DH10Bac cells,

verified by PCR and sequencing. The bacmids were isolated and transfected into Sf9 cells for protein overexpression and purification following the protocol used for the wild-type RECQ1 (section 2.3.1).

### 2.3.3. Preparation of the truncated RECQ1:

The RECQ1$^{T1\ (49\text{-}616)}$ cloned into the pNIC-CTHF vector was transformed and expressed in BL21(DE3)-R3-pRARE *E.coli* expression strain. The protein was overexpressed and purified as already described [32]. The expressed protein has an additional Methionine at the N-terminus and an AENLYF*SHHHHHHDYKDDDDK C-terminal extension containing the TEV protease cleavage site and a His tag followed by a FLAG tag. The protein was overexpressed in Terrific Broth modified medium (sigma) by IPTG induction. 2-3 $OD_{600}$ cells were induced with 0.2 mM IPTG and then grown at 18°C overnight. The cells were collected by centrifugation and lysed in lysis buffer (50 mM HEPES pH: 7.5, 500 mM NaCl, 10 mM imidazole, 1 mM TCEP, 5 % glycerol and protease inhibitors) by sonication (4 times; 30 s pulse with 30 s gap). The lysate was cleared by centrifugation and incubated with Ni-NTA resin (Qiagen) for 2 hours at 4°C in a nutator. The protein bound resin was washed with the lysis buffer supplemented with 30 mM imidazole and eluted with the lysis buffer supplemented with 500 mM imidazole. The eluted protein was confirmed on a SDS-PAGE gel and the protein containing fractions were pooled and dialyzed against 20mM Tris pH: 7.4, 150 mM KCl, 1 mM TCEP.

### 2.3.4 Determination of protein concentration:

The absorbance of the protein was recorded at 280 nm in a nanodrop. The theoretical extinction coefficient of the protein was determined from Expasy employing the Protparam tool (http://ca.expasy.org/tools/protparam.html). Protein concentrations were determined using Beer-Lamberts law:

Protein concentration (M) = $Abs_{280}$ (cm$^{-1}$) / Extinction coefficient (M$^{-1}$cm$^{-1}$)

## 2.4 Oligonucleotides:

All the oligonucleotides used in this study were chemically synthesized (Integrated DNA Technologies) and HPLC purified. Stock solutions were made by re-suspending the oligonucleotides in autoclaved MilliQ water (DNase/RNase free) and stored at -20°C. The sequence of the oligos used in the preparation of various substrates used in this study is listed below in Table 2.1.

| Name | Length (nt) | Sequence 5' → 3' |
|:---:|:---:|:---|
| A | 81 | CTT TAG CTG CAT ATT TAC AAC ATG TTG ACC TTC AGT A/isodC/A ATC TGC TCT GAT GCC GCA TAG TGT CAT GCC AGA GCT TTG TAC |
| B | 81 | CGG GTG TCG GGG CGC ATG ACA CTA TGC GGC ATC AGA GCA GAT TGT ACT GAA GGT CAA CAT GTT GTA AAT ATG CAG CTA AAG |
| C | 43 | GTA CAA AGC TCT GGC ATG ATA CTA TGC GGC ATC AGA GCA GAT T |
| D | 50 | TCA GTA CAA TCT GCT CTG ATG CCG CAT AGT ATC ATG CGC CCC GAC ACC CG |
| E | 49 | GTA CAA AGC TCT GGC ATG ATA CTA TGC GGC ATC AGA GCA GAT TGT ACT G |
| F | 60 | CAC TGT GAT GCA CGA TGA TTG ACG ACA GTA GTC AGT GCT GCA GTG GTC AGG TGT CAT CAC |
| G | 60 | CCT GCA TAC AGA TGT TGA CCC AGC ACT GAC TAC TGT CGT CAA TCA TCG TGC ATC ACA GTG |
| H | 60 | GTG ATG ACA CCT GAC CAC TGC AGC ACT GAC TAC TGT CGT CGA TCA TCG TGC ATC ACA GTG |
| I | 60 | CAC TGT GAT GCA CGA TGA TCG ACG ACA GTA GTC AGT GCT GGG TCA ACA TCT GTA TGC AGG |
| J | 60 | GTG ATG ACA CCT GAC CAC TGC AGC ACT GAC TAC TGT CAC TGA TCA TCG TGC ATC ACA GTG |

| | | |
|---|---|---|
| K | 60 | CAC TGT GAT GCA CGA TGA T**CA GT**G ACA GTA GTC AGT GCT GGG TCA ACA TCT GTA TGC AGG |
| L | 50 | GAC GCT GCC GAA TTC TGG CTT GCT AGG ACA TCT TTG CCC ACG TTG ACC CG |
| M | 50 | CGG GTC AAC GTG GGC AAA GAT GTC CTA GCA ATG TAA TCG TCT ATG ACG TC |
| N | 50 | GAC GTC ATA GAC GAT TAC ATT GCT AGG ACA TGC TGT CTA GAG ACT ATC GC |
| O | 50 | GCG ATA GTC TCT AGA CAG CAT GTC CTA GCA AGC CAG AAT TCG GCA GCG TC |
| P | 50 | GAA CGA ACA CAT CGG GTA CGT TTT TTT TTT TTT TTT TTT TTT TTT TTT TT |
| Q | 50 | TTT TTT TTT TTT TTT TTT TTT TTT TTT TTT CGT ACC CGA TGT GTT CGT TC |
| X12-1 | 50 | GAC GCT GCC GAA TTC TGG CTT GCT AGG ACA TCT TTG CCC ACG TTG ACC CG |
| X12-2 | 50 | CGG GTC AAC GTG GGC AAA GAT GTC CTA GCA ATG TAA TCG TCT ATG ACG TC |
| X12-3 | 50 | GAC GTC ATA GAC GAT TAC ATT GCT AGG ACA TGC TGT CTA GAG ACT ATC GC |
| X12-4 | 50 | GCG ATA GTC TCT AGA CAG CAT GTC CTA GCA AGC CAG AAT TCG GCA GCG TC |
| X26-1 | 60 | CCG CTA CCA GTG ATC ACC AAT GGA TTG CTA GGA CAT CTT TGC CCA CCT GCA GGT TCA CCC |
| X26-2 | 60 | TGG GTG AAC CTG CAG GTG GGC AAA GAT GTC CTA GCA ATC CAT TGT CTA TGA CGT CAA GCT |
| X26-3 | 60 | GAG CTT GAC GTC ATA GAC AAT GGA TTG CTA GGA CAT CTT TGC CGT CTT GTC AAT ATC GGC |
| X26-4 | 61 | TGC CGA TAT TGA CAA GAC GGC AAA GAT GTC CTA GCA ATC CAT TGG TGA TCA CTG GTA GCG G |

**Table 2.1.** Sequences of the oligonucleotides used in the study of fork regression and restoration. Bold red letters indicate the nucleotides that form mismatched pairs in the branch migration products.

## 2.5 Preparation of DNA substrates:

One of the strands in each substrate was 5'-end labelled with $[\gamma^{32}P]ATP$ (3000 Ci/mmol) for 45 minutes using $T_4$ polynucleotidyl kinase (NEB) and the reaction was terminated by heat inactivating the enzyme at 95°C for 6 minutes. The unincorporated $[\gamma^{32}P]ATP$ was removed using the Bio-spin 30 columns (Bio-Rad). For the preparation of the helicase assay substrate (forked duplex), the labelled strand P (table 2.1) was annealed with 1.4 of excess of the unlabelled complementary strand Q (table 2.1) in annealing buffer (10 mM Tris-HCl pH 8.3, 50 mM NaCl) followed by heating at 95°C for 6 minutes and then slowly cooling to room temperature. For the annealing assay the labelled strand P (table 2.1) was used as a substrate.

For the preparation of Holliday junction substrate for branch migration (X12), the labelled strand X12-1 (table 2.1) was annealed with 1.5 fold excess of the three complementary unlabelled strands X12-2, X12-3, X12-4 (table 2.1) in annealing buffer (supplemented with 5 mM $MgCl_2$) followed by heating at 95°C for 6 minutes and then slowly cooling to room temperature. The Holliday junction was purified in a sepharose 4B (5ml) column and the collected fractions were analysed on a 10 % PAGE gel. The fractions were selected based on their purity. A similar protocol with oligos F, G, H, I/J (table 2.1) was followed for the preparation of HJ (1) and HJ (4) with mis-matches. To prepare the Holliday junction substrates for EMSA, labelled oligonucleotide L (table 2.1) and 1.5-fold excess of unlabelled oligonucleotides M, N, O (table 2.1) were incubated in annealing buffer supplemented with 5 mM $MgCl_2$ for 30 min at 37°C and for a further 30 min at room temperature.

For analytical ultracentrifugation experiments, the X26 Holliday junction substrates were prepared by annealing the four strands X26-1, X26-2, X26-3 and X26-4 (table 2.1) in annealing buffer, followed by heating at 95°C for 6 minutes and then slowly cooling to room temperature. The annealed products were run on a PAGE gel and visualised by staining with Stains all (Sigma). The band corresponding to the Holliday junction was excised and the Holliday junction was

purified from the gel by "crush and soak" method [249]. Briefly, the gel slices were frozen and crushed into small pieces and buffer was added to the tubes. The tubes were incubated at 37°C with gentle shaking and after a few hours, the buffer containing the HJ was pipetted out, quantified and stored for further use.

## 2.5.1 Construction of the replication fork and the chicken-foot like structure:

For the fork regression and restoration assays, we used the same substrate previously utilized by the group Dr. Alexander Mazin to characterize the fork regression activity of the human Rad54 protein [250]. Four oligos (oligos A - E, table 2.1) were annealed in different combinations to form the chicken-foot and the replication fork like structures. The oligo B was end-labelled with $^{32}$P and purified.

For the preparation of the chicken-foot structure, the $^{32}$P labelled oligo B was initially annealed with oligo A in annealing buffer (10 mM Tris-HCl, pH 8.3, 50 mM NaCl). In a separate reaction, oligos C or E (where oligo E is six nucleotide longer than oligo C) were annealed with oligo D in annealing buffer. Successively, two substrates were annealed in annealing buffer supplemented with 5 mM MgCl$_2$ at 37°C for 30 minutes followed by a 30 minutes incubation at room temperature (Fig. 2.1).
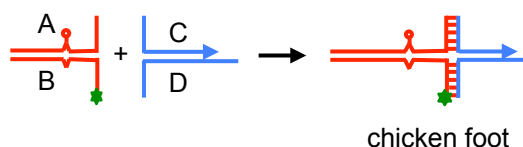


Figure 2.1: Schematic of the preparation of chicken-foot like structure.

For the replication fork like structure, the $^{32}$P labelled oligo B was initially annealed with oligo D in annealing buffer (10 mM Tris-HCl, pH 8.3, 50 mM NaCl). In a separate reaction, oligos C or E (oligo E is six nucleotide longer than oligo C) were annealed with oligo A in annealing buffer. Successively, the two substrates were annealed in annealing buffer supplemented with 5 mM MgCl$_2$ at 37°C for 30 minutes followed by a 30 minutes incubation at room temperature (Fig. 2.2).
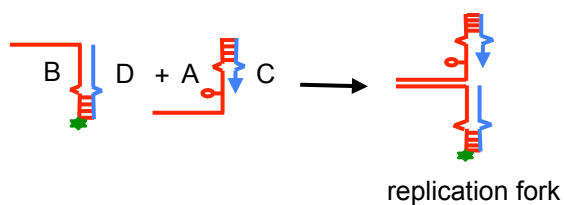
Figure 2.2: Schematic of the preparation of replication fork like structure.

Figure 2.3 shows a gel with all the intermediates and the final products of the reaction. The Figure also explains how we can distinguish the bands corresponding to a regressed fork from the band corresponding to a functional replication fork
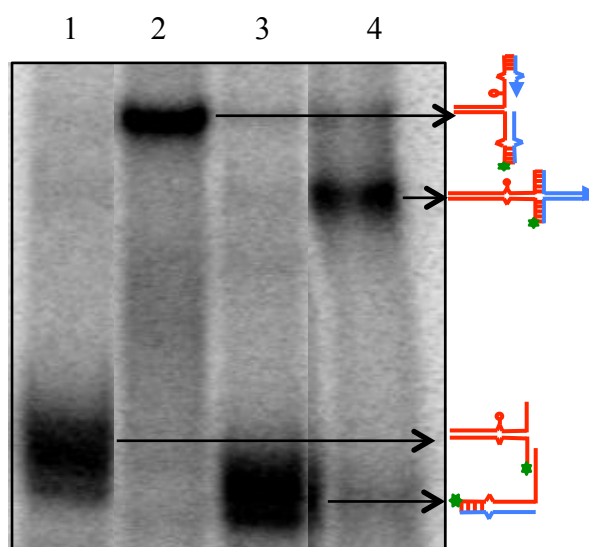


Figure 2.3: Preparation of replication fork and chicken foot like structure. Lane 1: annealed oligos B and D. Lane 2: chicken-foot like structure. Lane 3: annealed oligos A and B. Lane 4: replication fork like structure.

Note that the two terminal regions of the vertical arms contained different, complementary but mutually exclusive sequences to ensure that the "chicken foot" (or reversed fork structure) structure is converted to a replication fork structure and prevent complete separation of the two strands (shown by lined regions). In addition, we inserted a single isocytosine (iso-C) residue in the oligonucleotide that represents a replication fork leading strand (denoted with a circle) and two mismatches on the substrate vertical arms (shown by carets) to prevent spontaneous fork regression and restoration.

## 2.6. Radiometric biochemical assays:

### 2.6.1 Helicase assay:

In the helicase assay we measure the release of a $^{32}$P-labeled ss-DNA fragment from the partial duplex DNA substrate by the RECQ1 helicase. The 20 µl reaction mix typically contained the $^{32}$P-labeled DNA substrate (0.5 nM) in the helicase buffer (20 mM Tris- HCl (pH 7.5), 8 mM DTT, 5 mM MgCl2, 10 mM KCl, 80 mg/ml BSA, 10% Glycerol) with 5 mM ATP. The reaction was initiated by the addition of the required amounts of RECQ1, and the mixture was incubated at 37°C for 20 min. In case of time dependent assays, 5 nM of RECQ1 was used and at the indicated time points 20 µl of the reaction mix was withdrawn. The reactions were terminated by the addition of 20 µl of (0.4 M EDTA pH 8.0, 10% glycerol, 10% SDS). The reaction products were resolved on a native 10 % PAGE and visualised by autoradiography.

### 2.6.2 DNA strand annealing assay:

The strand-annealing activity of RECQ1 was measured using partially complementary synthetic oligonucleotides (0.5 nM). Strand annealing reactions (20 µl) containing the labelled strand (20U) and the indicated concentration of protein were carried out at 37°C in the helicase buffer in the absence of ATP and were initiated by adding the unlabelled DNA strand. Reactions were terminated by the addition of 20 µl of quenching solution (0.4 M EDTA pH 8.0, 10% glycerol, 10% SDS). Reaction products were subsequently resolved on native 10 % PAGE and visualised by autoradiography.

### 2.6.3 *In vitro* fork regression and restoration assays:

Reactions were performed in a 20 µl volume with 2 nM substrate and the indicated protein concentrations in branch migration buffer (35 mM Tris-HCl pH 7.5, 20 mM KCl, 5 mM MgCl$_2$, 0.1 mg/ml BSA, 2 mM DTT, 15 mM phosphocreatine, 30 U/ml creatine phosphokinase, 5% glycerol) at 37$^{\circ}$C for the

indicated time. The reaction was initiated by the addition of 2 mM ATP. For the poly(ADP-ribosyl)ation experiments, the indicated concentrations of PARP1 and 200 μM NAD$^+$, or 100 nM purified PAR, were added to the reaction mixture prior to the addition of ATP and pre-incubated with RECQ1 and the substrate for 10 min at 37$^°$C . The reaction was then started by the addition of 2 mM ATP. DNA substrates were de-proteinized by adding 3X stop buffer (1.2 % SDS, 30 % glycerol supplemented with proteinase K (3 mg/ml)) followed by incubation at room temperature for 10 min prior to being resolved on an 8 % native PAGE. Labelled DNA fragments were detected by autoradiography.

**2.6.4 Electrophoretic mobility shift assay (EMSA):**

Purified proteins were incubated with 0.5 nM $^{32}$P labelled DNA in binding buffer (20 mM Hepes-KOH pH 7.6, 75 mM KCl, 2 mM MgCl$_2$, 2 mM ATPγS, 1 mM DTT, 0.25 mM EDTA, 20 μg/ml BSA, 5% glycerol, 0.1% NP-40) for 30 minutes at room temperature. When indicated 200 μM NAD$^+$ and 100 nM PAR were added. The protein-DNA complexes were resolved on 5 % native PAGE. Labelled DNA fragments were detected by autoradiography.

**2.6.5 Resolving radioactive reactions on native PAGE:**

The reactions were analysed on 8 % or 10 % native PAGE gels run in 1 X Tris-Borate EDTA (89 mM Tris Base, 89 mM boric acid and 2 mM EDTA) buffer at 4°C. After electrophoresis, the gels were exposed to a phospho screen at 4°C overnight and the screen was visualised in a Typhoon imager (GE Healthcare). For EMSA assays the gel was run in 0.5 X TBE buffer for 3 hours at 4°C.

**2.6.6 Quantification and graphs:**

The autoradiography images acquired through Typhoon imager were quantified using OptiQuant software (PerkinElmer) and the values were exported to Origin (Microcal software) for calculations. GraphPad prism was used for plotting graphs and for further analysis.

## 2.7 Purified PAR production:

PAR polymer was produced and purified as previously described [251]. Briefly poly (ADP-ribosyl)ation reaction was set up as above and the DNA was digested by adding 10 U/ml of DNAseI (Fermentas) for 30 min at 37°C to the reaction. Next, the protein was digested using 50 U/ml of proteinase K (Roche) and 1% SDS, followed by incubation for 1.5 hour at 55°C. After phenol–chloroform extraction, the water-soluble polymer was washed twice with diethyl ether, precipitated with ethanol, air-dried and dissolved in TBS (Tris-HCl pH 7.5, 150 mM NaCl). PAR concentration was determined spetrophotometrically using the following equation:

$$[PAR] = A_{258}\,(cm^{-1}) \, / \, 13{,}500\,(M^{-1}\,cm^{-1})$$

## 2.8 Western blotting:

Total cell extracts obtained after sonication of cells in their respective lysis buffer were quantified by Bradford assay (Biorad). Proteins were resolved in a SDS-PAGE, transferred onto PVDF membranes (GE Healthcare) and probed using the appropriate primary and secondary antibodies. The secondary antibody coupled to horseradish peroxidase (Dako, Pierce) was detected with ECL reagents (Pierce) following the manufacturer's protocol.

## 2.9 Analytical ultracentrifugation:

Sedimentation velocity experiments were carried out at 8°C on a Beckman XL-I analytical ultracentrifuge equipped with a Ti-50 rotor. Protein samples were studied at different concentration in 10 mM HEPES pH 7.4, 150 mM KCl, 0.5 mM TCEP, 2% (v/v) glycerol and 5 mM MgCl$_2$ . After equilibration at 8°C for 2-3 hours, the speed was increased to 40,000 r.p.m. and radial absorbance scans were taken every 2 min at 280 nm and 260 nm. In the case of DNA/Holliday junction binding, the scans were recorded at 280 nm and 260 nm. Information from scans 5–50 was used for analysis. Data were analysed using SEDFIT to calculate c(s) distributions. The software package SEDNTERP (http://www.jphilo.mailway.com) was used in

order to normalize the obtained sedimentation coefficient values to the corresponding values in water at 20°C. Graphs were plotted using Origin.

Analytical ultracentrifugation (AUC) sedimentation equilibrium experiments were performed at 8°C, with protein concentrations of 6 μM and 4 μM , dialysed against 10 mM HEPES pH 7.4, 150 mM KCl, 0.5 mM TCEP, 2% (v/v) glycerol and 5 mM MgCl$_2$. The samples were centrifuged at 7000 r.p.m. for 22 h and scanned; a further scan after 2 h was performed to confirm that equilibrium had been attained. The speed was then increased to 9000 r.p.m., and the chambers were scanned after 18 and 20 h. Finally, the speed was increased to 26000, to achieve meniscus depletion, providing a baseline for the analysis. Data was analyzed using SEDFIT and SEDPHAT.

## 2.10 Gel filtration chromatography:

Size exclusion chromatography experiments were performed on a ÄKTA FPLC system (GE Healthcare) using a 10/30 Superdex 200 HR gel filtration column (GE Healthcare), as described previously [105]. Briefly, the column was equilibrated at a flow rate of 0.5 ml/min with 20 mM Tris (pH 7.5), 150 mM KCl and 1 mM DTT. Approximately 150–200 μg of recombinant protein was loaded on the column and detected using an UV detector at 280 nm. The Superdex column was calibrated using calibration standards (Bio-Rad). A standard curve was generated from the plot of average molecular weight against elution volume and fit using the standard exponential fit equation. Using the equation, the molecular weight of the protein that eluted at appropriate elution volume was determined.

## 2.11 Cryo-EM:

Our collaborator Dr. Alessandro Costa, London Research Institute helped us by doing the cryo-EM experiments. Briefly, RECQ1 molecules were retained by biotinylated HJs on a streptavidin 2D crystal matrix and imaged. The Fourier-transformed (FFT) images were computed and the diffraction spots were masked to erase any streptavidin lattice information. Then, the single particles were selected on

the filtered image transformed back (FFT$^{-1}$) into real space and thereafter processed by established reconstruction approaches.

## 2.12 *In silico* analysis:

Multiple sequence alignments were performed using the T-Coffee multiple sequence alignment tool (http://tcoffee.crg.cat/apps/tcoffee/do:regular). The coiled-coil analysis was done using the Multicoil program (http://groups.csail.mit.edu/cb/multicoil/cgi-bin/multicoil.cgi).

# 3. RESULTS

## 3. 1 Biochemical characterization of RECQ1:

### 3.11 Expression and purification of hRECQ1 from Sf9 insect cells:

The human RECQ1 protein (649 aa) was overexpressed in Sf9 insect cells using the baculovirus expression system as previously described [252]. The recombinant protein contains an N-terminal tag consisting of six His residues followed by a thrombin cleavage site and a short linker sequence (MGSSHHHHHHSSGLVPRGSHMAS). The His-tagged hRECQ1 protein was purified from the cell lysate by $Co^{2+}$-affinity chromatography and the purity of the eluting fractions was verified by SDS-PAGE gel as described in the materials and methods (section 2.3.1). The final product was dialyzed to remove the imidazole. Finally, its purity was determined by coomassie blue staining (figure 3.1A) and its identity confirmed by Western blot analysis using either anti-RECQ1 or anti-His antibodies (figure 3.1B). The purified recombinant hRECQ1 appears as a major band at 75kDa on a SDS-PAGE gel along with few minor bands at the top. Mass spec analysis indicated that these top bands correspond to hRECQ1 suggesting that they might contain higher oligomer forms hRECQ1, which do not dissociate in the gel.
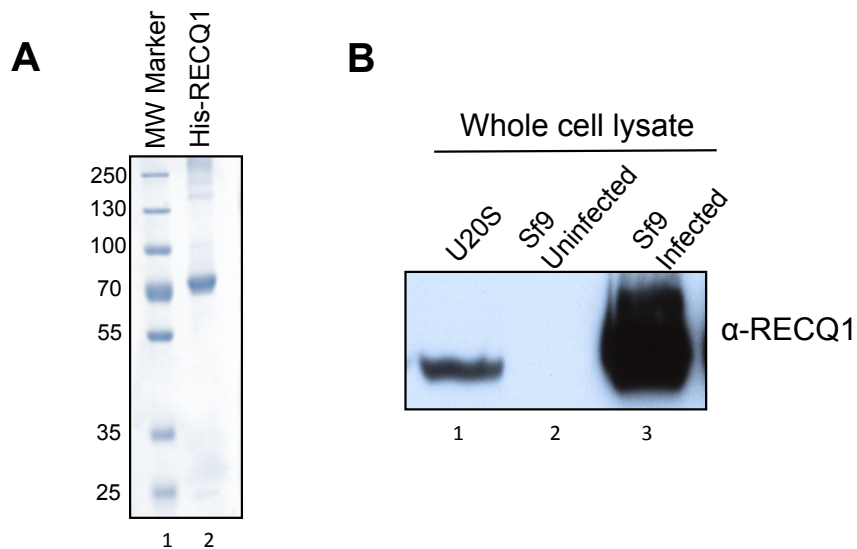


**Figure 3.1:** A) SDS-PAGE analysis of purified hRECQ1 after dialysis (8% polyacrylamide (PA) gel, coomassie staining). Lane 1: Molecular weight (MW) marker; Lane 2: Purified RECQ1. B) Western blot analysis of the cell lysates from the infected (lane 3) and the uninfected (lane 2) Sf9 cells using specific antibodies against hRECQ1. Human osteosarcoma cell (U-2 OS) lysate (lane 1) was used as a positive control.

## 3.12 Biochemical characterization of the hRECQ1 helicase:

All purified RECQ1 samples were initially tested to confirm that they retain normal unwinding and annealing activity, and that there is no exonuclease contamination. The enzyme activity was tested using our standard helicase and DNA annealing assays using $[^{32}\gamma P]$-ATP labelled model DNA substrates (Table 2.1). The exonucleases are a common contaminant of His-tagged proteins purified from insect cells and it is important to make sure that they are absent because they would otherwise interfere with all the activity assays involving DNA [253]. Normally, binding of the exonuclease to the resin is avoided by saturating the resin with the recombinant protein.

### 3.12A Helicase assays using the forked duplex:

I assayed the unwinding activity of the enzyme as a function of protein concentration using a $[^{32}\gamma P]$-ATP forked duplex with a 20 bp arm and a $dT_{30}$ tail (Table 2.1). The reactions were initiated by the addition of indicated concentration of RECQ1 to a solution containing 0.5 nM substrate. The results showed that the helicase activity increases as a function of the protein concentration and that 5 nM RECQ1 is sufficient to unwind almost 100% of the substrate within 15 minutes (figure 3.2A). The graph below shows the helicase activity measured as a function of protein concentration for three different RECQ1 preparations (figure 3.2B).
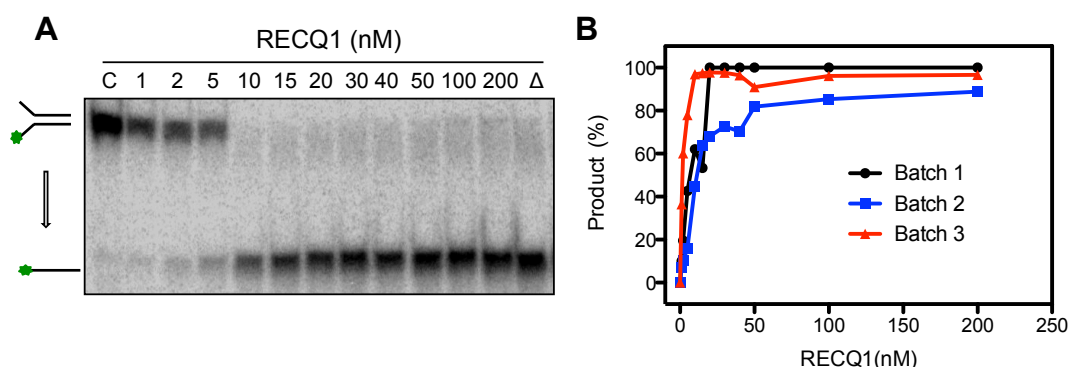


**Figure 3.2: Analysis of the unwinding activity of RECQ1 using forked duplex DNA substrate on a 10% Native PAGE.** A) Unwinding assay using various concentrations of RECQ1 (1 – 200 nM) and 0.5 nM of the forked duplex substrate. The reactions were incubated for 20 minutes at 37°C and stopped by the addition of quenching solution. B) Plot of the unwinding activity as a function of RECQ1 concentration showing the comparison of the activity of different RECQ1 preparations.

### 3.12B Strand annealing assays:

The ability of RECQ1 to anneal two complementary strands (strand annealing) was analysed as a function of increasing protein concentrations. The reactions were carried out in the absence of ATP. The results showed that the strand annealing activity of RECQ1 increased with increasing protein concentrations and reached a plateau at 15 nM RECQ1 (figure 3.3A). Different RECQ1 preparations displayed very similar annealing activity, as shown in the graph below (figure 3.3B).
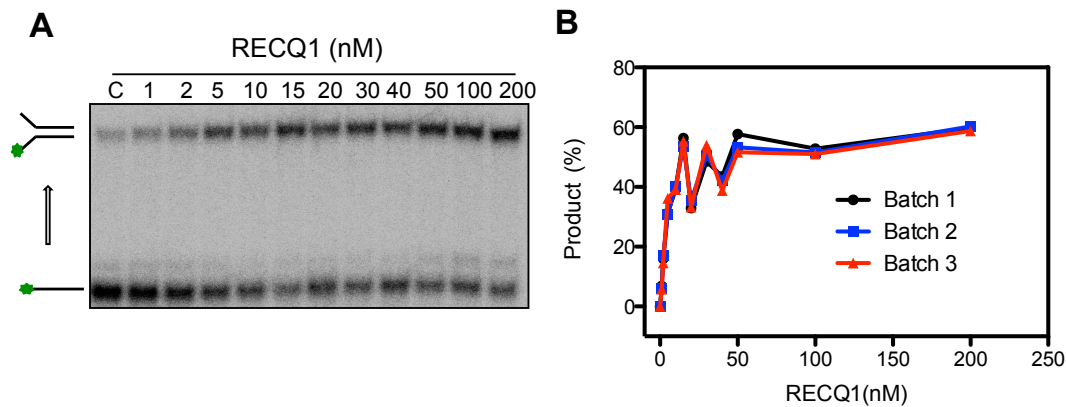


**Figure 3.3: Analysis of the DNA strand annealing activity of RECQ1.** A) DNA strand annealing assay using various concentration of RECQ1 (1 – 200 nM) and 0.5 nM labelled single strand DNA. The reactions were initiated by the addition of 1.2 nM complementary unlabelled strand in the absence of ATP and incubated for 30 minutes at 37°C. B) Plot of the annealing activity as a function of RECQ1 concentration showing the comparison of the activity of different RECQ1 preparations.

## 3.2 Role of RECQ1 in replication fork restart:

### 3.21 RECQ1 promotes restart of reversed replication forks *in vitro*:

Our group demonstrated that RECQ1 interacts with the DNA replication origins and that the amount of RECQ1 loaded on the origins increases during the early S-phase of the cell cycle when replication origins begin firing and the replication forks are formed [191]. We also showed that RECQ1 deficient cells are characterized by a slower replication fork progression and are sensitive to certain DNA damaging agents that interfere with DNA replication [191]. These data support the notion that RECQ1 plays an important role at the replication fork.

Replication fork restoration/regression is an emerging mechanism to explain how replication forks are processed following DNA damage induction. Thus, we

decided to test if RECQ1 could promote fork restoration and/or fork regression *in vitro*. To perform these experiments, I used a set of four oligonucleotides, which could be annealed in two alternative ways to mimic either a replication fork like structure or a "chicken-foot" like structure [250]. Owing to the difference in their structures, the two substrates migrate differently in a gel, enabling us to differentiate between the two forms and to compare the fork restoration *versus* fork regression activity of RECQ1 (figure 3.4). The two terminal regions of the vertical arms contained different, complementary but mutually exclusive sequences to ensure that the "chicken foot" (or HJ structure) structure is converted to a replication fork structure and prevent complete separation of the two strands. In addition, a single isocytosine (iso-C) residue in the oligonucleotide that represents a replication fork leading strand (denoted with a circle) and two mismatches on the substrate vertical arms (shown by carets) were inserted to prevent spontaneous fork regression and restoration.

## A    Fork restoration



chicken foot

## B    Fork regression



replication fork
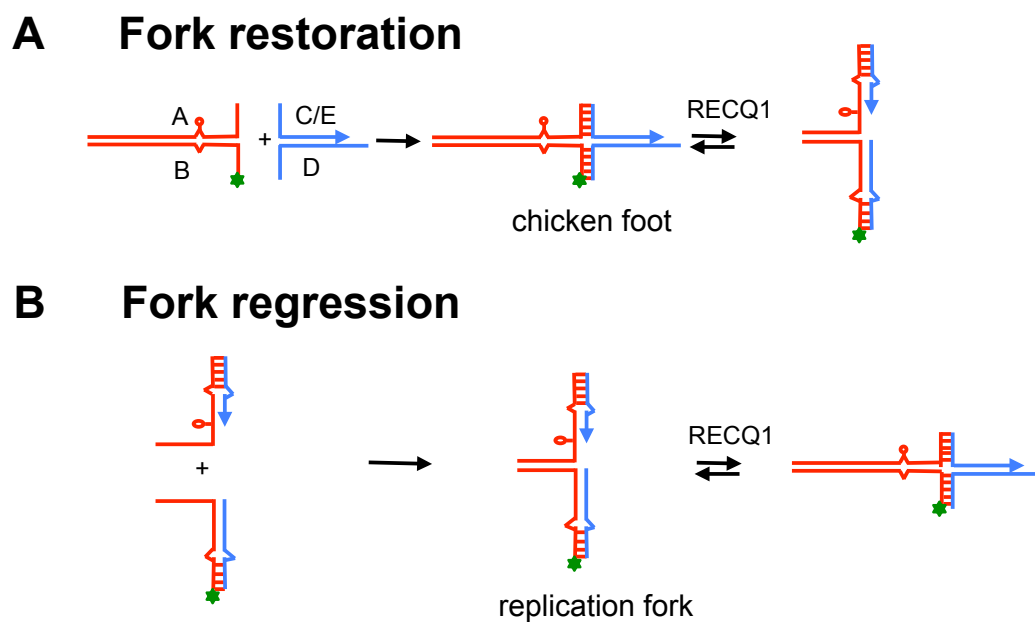
**Figure 3.4:** A) The scheme for the preparation of the reversed fork substrate (chicken foot). The circle indicates the position of iso-C that mimics a lesion on the leading DNA strand template. Unpaired single DNA bases are shown by carets. Hatched regions denote heterologous DNA terminal regions that prevent complete strand separation during fork regression. Stars indicate [γ-32P]ATP-labelled 5' ends. B) The scheme for the preparation of the model replication fork.

Fork restoration and regression assays were started by the addition of indicated amounts of RECQ1 to a solution containing 2 nM of the labelled substrate. The results showed that while RECQ1 efficiently converted a "chicken-foot" to a replication fork like structure (fork restoration), it is unable to convert a replication

fork into a "chicken-foot" like structure (fork regression). RECQ1 promoted fork restoration in a concentration dependent fashion (figure 3.5). 50 nM RECQ1 was sufficient to convert more than 75% of the "chicken-foot" structure into a replication fork like structure, whereas RECQ1 did not display any regression activity even at the highest protein concentration (200 nM). To exclude the possibility that RECQ1 could not regress the replication forks due to the presence of a 6-nucleotide single-stranded gap on the leading-strand template of the substrate, I repeated these experiments using a variant of the same substrate that lacked the single-stranded gap and found that RECQ1 was still unable to perform fork regression (figure 3.6).
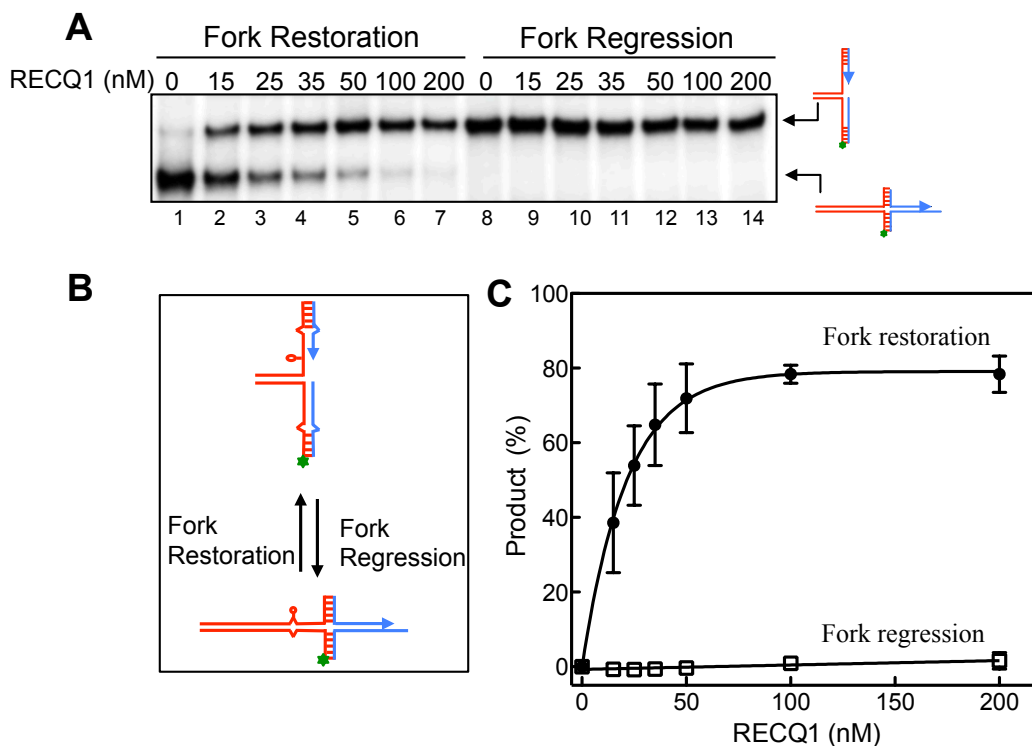


**Figure 3.5: Analysis of the fork restoration and fork regression activity of RECQ1.** A) Fork restoration assays (lanes 1–7) and fork regression assays (lanes 8–14) performed using indicated RECQ1 concentrations and 2 nM of chicken-foot substrate or replication fork structure. See paragraph 2.5.1 of the Materials and Methods for more details on the procedure for the correct assignment of the identity of the bands shown in the gel. B) Schematic of the restoration and regression reactions and their products. The circle indicates the position of iso-C that mimics a lesion on the leading DNA strand template. Unpaired single DNA bases are shown by carets. Hatched regions denote heterologous DNA terminal regions that prevent complete strand separation during fork regression. Stars indicate [$\gamma$-$^{32}$P]ATP-labelled 5' ends. C) Percentage of fork restoration and regression products plotted as a function of protein concentration. The data points represent the mean of three independent experiments with the standard deviation indicated by error bars.
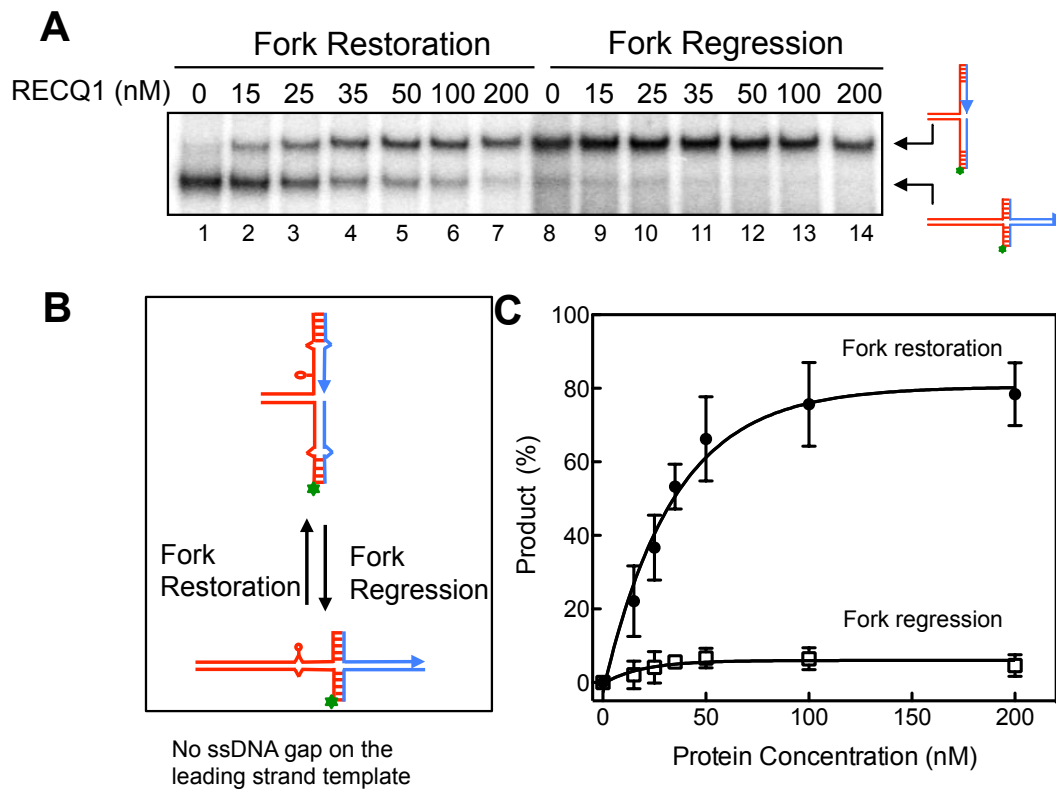
**Figure 3.6: Analysis of the fork restoration and fork regression activity of RECQ1 using a substrate that lacks 6 nucleotide single strand gap.** A) Fork restoration assays (lanes 1–7) and fork regression assays (lanes 8–14) performed using indicated RECQ1 concentrations and a 2 nM of chicken-foot substrate or replication fork structure lacking the 6 nucleotide single strand gap. B) Schematic of the restoration and regression reactions and their products. The substrates lack the 6 nucleotide single strand gap. The circle indicates the position of iso-C that mimics a lesion on the leading DNA strand template. Unpaired single DNA bases are shown by carets. Hatched regions denote heterologous DNA terminal regions that prevent complete strand separation during fork regression. Stars indicate [γ-$^{32}$P]ATP-labelled 5' ends. C) Percentage of fork restoration and regression products plotted as a function of protein concentration. The data points represent the mean of three independent experiments with the standard deviation indicated by error bars.

## 3.22 ATPase activity of RECQ1 is essential for its fork restoration activity:

To confirm that ATP hydrolysis is required for the fork restoration activity of RECQ1, I used two previously characterized ATPase deficient mutants of RECQ1, namely E220Q RECQ1 and K119R RECQ1 [105]. The results showed that both mutants failed to promote fork restoration. The same results were obtained using the poorly hydrolysable analogue of ATP, ATPγS, and the non-hydrolysable analogue of ATP, AMP-PNP (figure 3.7).
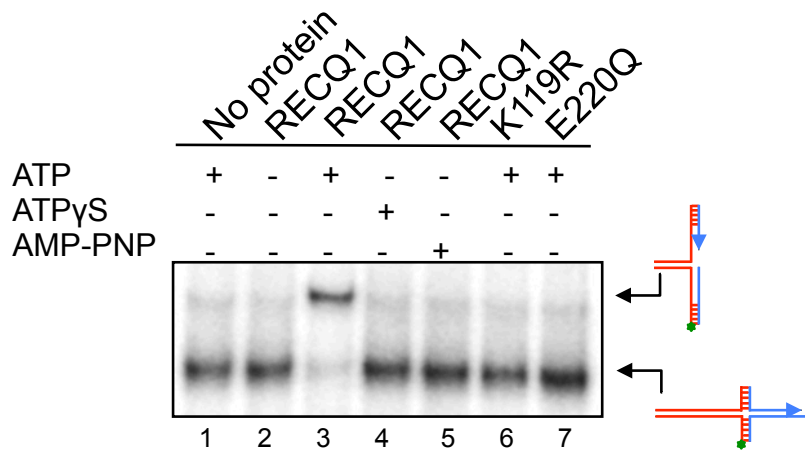
**Figure 3.7: Fork restoration assays using non-hydrolysable ATP analogues or ATPase deficient RECQ1 mutants.** Fork restoration assays were performed in the presence of ATP or different ATP analogues using wild-type RECQ1 (lanes 2-5) or the ATPase deficient RECQ1 mutant, K119R (lane 6) and E220Q (lane 7). The protein concentration was 50 nM for all the experiments.

## 3.23 RECQ1 can by-pass DNA heterology:

To test whether RECQ1 can bypass regions of heterology, I used Holliday junction (HJ) substrates containing 1 or 4 mismatches. RECQ1 efficiently branch migrated these substrates in a concentration dependent manner. However, the efficiency of branch migration was reduced almost 50 % when heterology length was increased from 1 to 4 bases (figure 3.8). The ability of RECQ1 to bypass regions of heterology suggests that the helicase activity of RECQ1 is involved in the resolution of these structures.
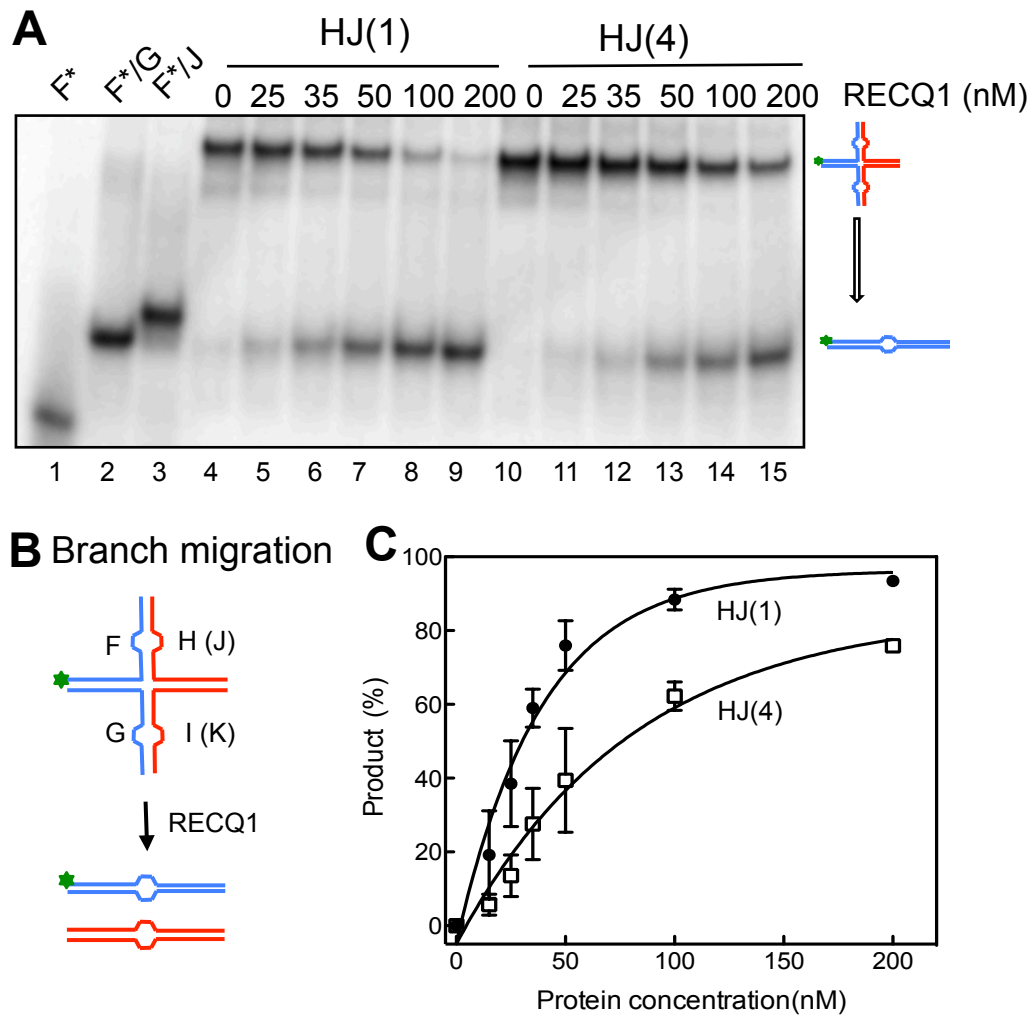
**Figure 3.8: Analysis of the branch migration activity of RECQ1 on Holliday junction substrates with mis-matches.** A) Branch migration assays were performed with HJ substrates with heterology regions of 1 (HJ (1)) or 4 bases (HJ (4)). Lanes 1-3: DNA migration markers. Lanes 4-9: branch migration assays performed using increasing RECQ1 concentrations and a fixed concentration of HJ (1) (2 nM). Lanes 10-15: branch migration assays using increasing RECQ1 concentrations and a fixed concentration of the HJ(4) (2 nM). All the reactions were stopped after 20 min. B) Schematic representation of the branch migration reaction of HJ with 1 and 4 mismatches by RECQ1. C) Plot of the branch migration reaction as a function of protein concentration. The data points represent the mean of three independent experiments with the standard deviation indicated by error bars.

## 3.24 PARP1 – a key RECQ1 interactor, inhibits the fork restoration activity of RECQ1 *in vitro:*

Recent studies in our lab identified PARP1 as one of the most prominent RECQ1 interactors. Given that PARP1 plays an important role in replication stress response, we decided to investigate the combined roles of RECQ1 and PARP1 at the replication fork [245, 254].

First, we decided to test *in vitro* the effect of PARylated PARP1 on the fork restoration activity of RECQ1. PARP1 PARylates itself after DNA binding and this PARylation reaction plays an important role in mediating the accumulation of PARP1 at regressed forks after DNA damage [199, 245]. The results showed that PARylated PARP1 inhibited the fork restoration activity of RECQ1. At 40 nM RECQ1 concentration, the fork restoration activity was reduced from 80 % to < 30% upon addition of equimolar concentrations of PARylated PARP1 (figure 3.9).
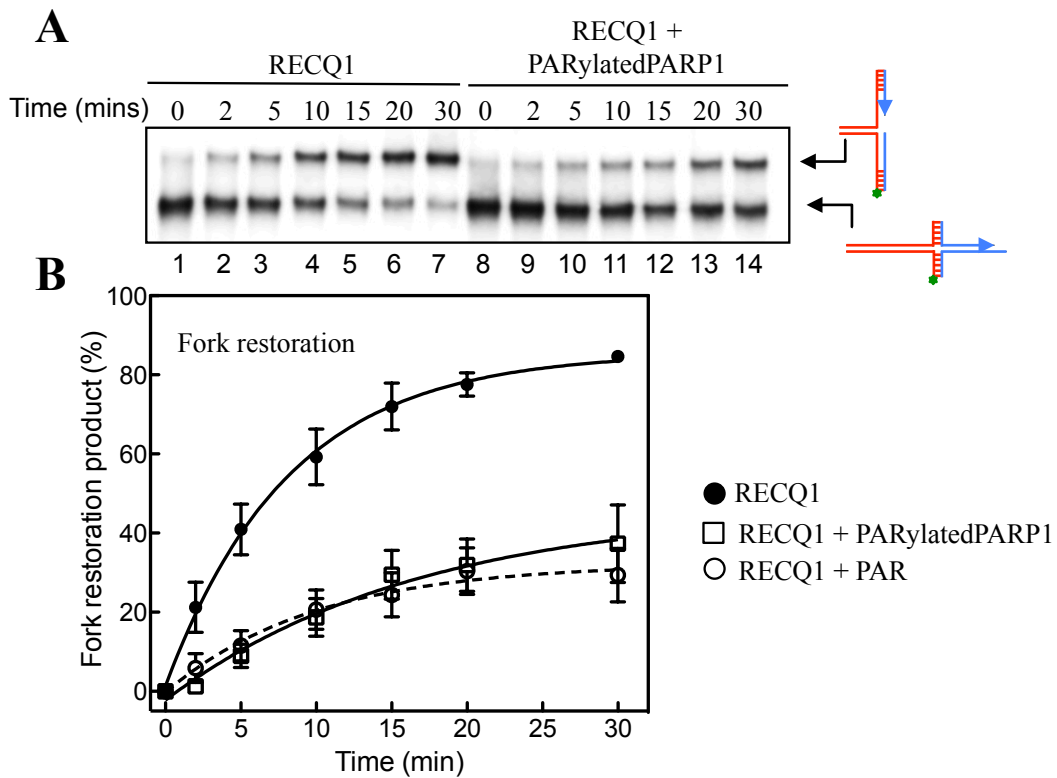


**Figure 3.9: Analysis of the effect of PARylated PARP1 on the fork restoration activity of RECQ1.** A) Kinetic experiments using 40 nM RECQ1 and 2 nM chicken-foot substrate, visualized by gel electrophoresis. Lanes 1–7: RECQ1 alone; lanes 8–14: RECQ1 in the presence of PARylated PARP1 (40 nM); B) Plot representing percentage of fork restoration for RECQ1 alone and RECQ1 in the presence of PARylated PARP1 as a function of reaction time. The data points represent the mean of three independent experiments with the standard deviation indicated by error bars.

Experiments performed at increasing concentration of PARylated PARP1 showed that a two-fold excess of PARylated PARP1 did not inhibit the reaction further, indicating that equimolar concentrations are sufficient for maximal inhibition (figure 3.10). PARylated PARP1 had a similar inhibitory effect on the branch migration activity of RECQ1 using Holliday junction substrates (figure 3.11).
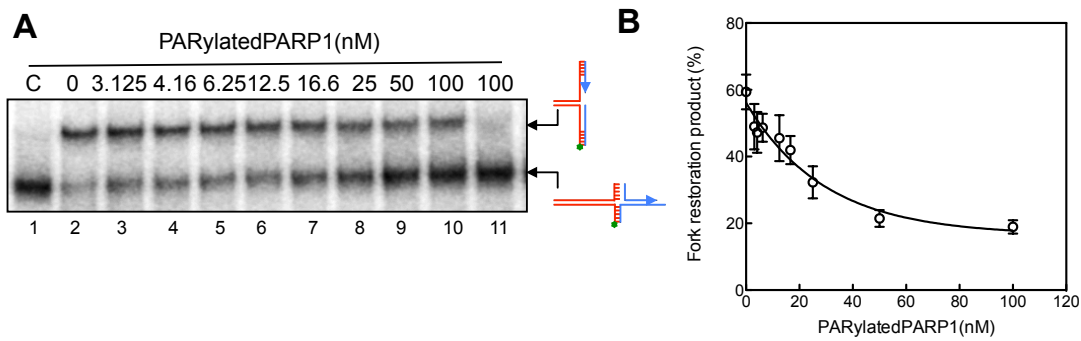
**Figure 3.10: Inhibition of the *in vitro* fork restoration activity of RECQ1 by increasing concentrations of PARylatedPARP1.** A) Lane 1: substrate alone. Lane 2: RECQ1 alone (50 nM). Lanes 3-10: fork restoration assays performed using increasing PARylatedPARP1 concentrations (3.125, 4.16, 6.25, 12.5, 16.6, 25, 50 and 200 nM) and a fixed concentration of RECQ1 (50 nM). Lane 11: PARylatedPARP1 alone (100 nM). All the reactions were stopped after 20 min, and the products were analyzed by electrophoresis in an 8% polyacrylamide gel. B) Plot of the fork restoration. The data points represent the mean of three independent experiments and the error bars indicate standard deviation.
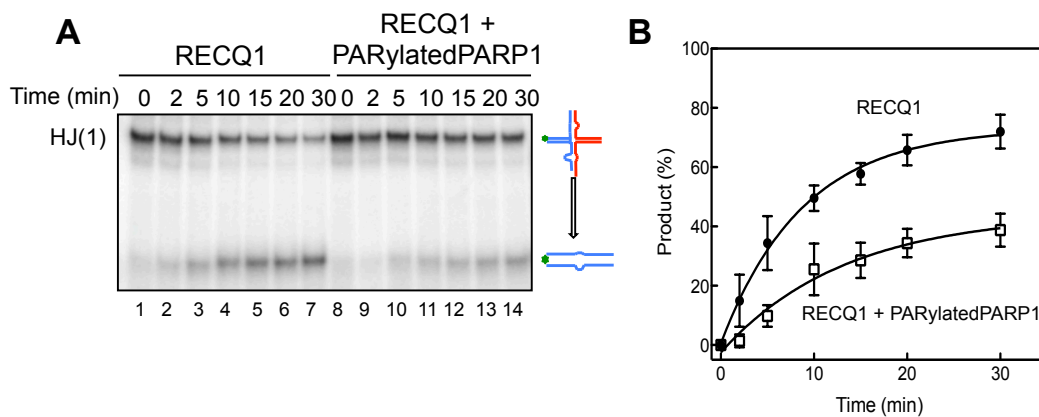


**Figure 3.11: Effect of PARylatedPARP1 on RECQ1 branch migration activity using the HJ(1) substrate.** A) Lanes 1-7: kinetic experiments performed using 50 nM RECQ1 and the HJ (1) (2 nM). Lanes 8-14: kinetic experiments performed in the presence of PARylatedPARP1 (50 nM). B) Plots of the branch migration assays performed in the presence and absence of PARylatedPARP1. The data points represent the mean of three independent experiments. Error bars indicate s.e.m.

## 3.25 PAR polymer is responsible for the inhibitory effect of PARylated PARP1 on the fork restoration activity of RECQ1:

Electrophoretic mobility shift assays (EMSA) with increasing PARylated PARP1 concentrations confirmed the previous finding [255] that PARylated PARP1 binds DNA with low affinity (figure 3.12 A, B). This excludes the possibility that the inhibitory effect of PARylated PARP1 on RECQ1 could be due to the competition between the two proteins for DNA binding. To test whether the PAR polymer is also able to inhibit the fork restoration activity of RECQ1, we purified PAR from

PARylated PARP1 as described in materials and methods (section 2.7). Then, I repeated the fork restoration assay using purified PAR instead of PARylated PARP1. The results showed that the inhibitory effect of PAR was similar to that observed in the presence of PARylated PARP1 supporting the notion that the interaction between RECQ1 and the PAR polymer regulates RECQ1 activity (figure 3.12 C).
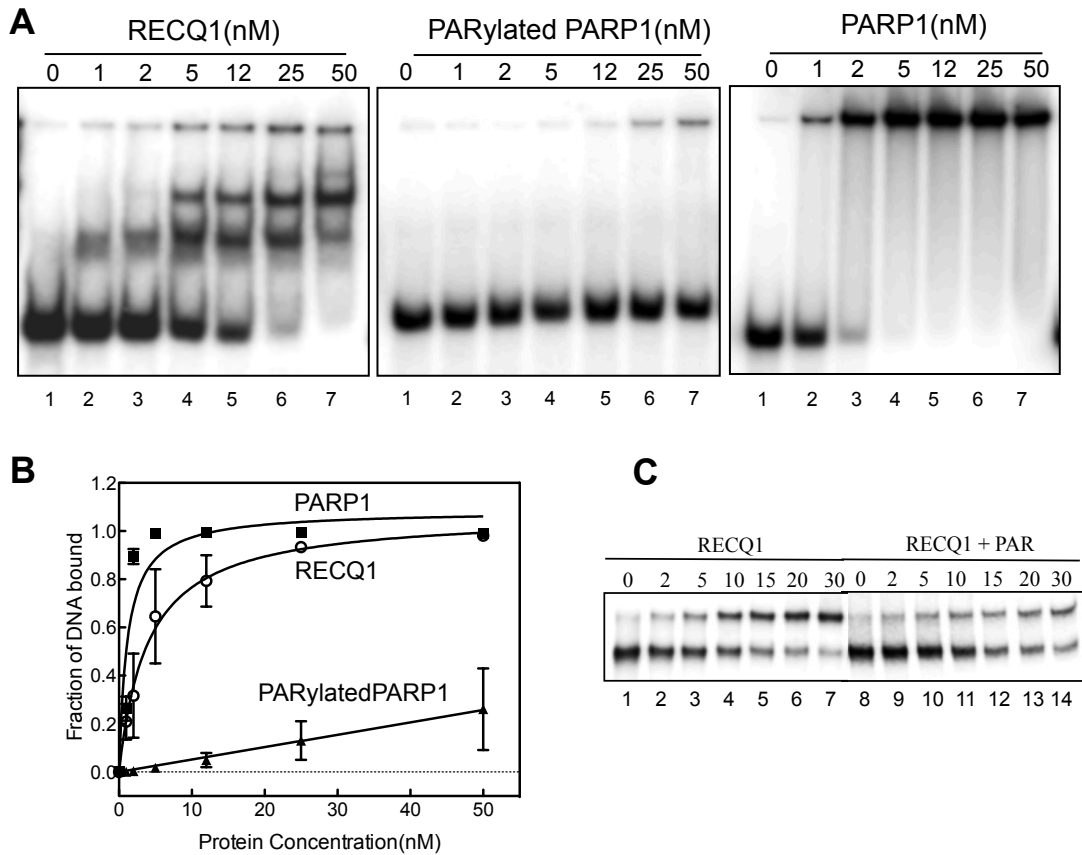


**Figure 3.12** A) DNA binding assays at increasing protein concentrations using the HJ probe. EMSA experiments performed using a HJ substrate with a 12-bp homologous core (0.5 nM). Lane 1: substrate alone. Lanes 2-7: experiments at increasing RECQ1, PARylated PARP1 and PARP1 concentrations (1, 2, 5, 12, 25, 50 nM). PARylated PARP1 was prepared by incubating PARP1 in the presence of NAD. B) The plots are the average of three independent experiments. Error bars indicates s.e.m. C) Effect of the inhibitory effect of PAR on the fork restoration activity of RECQ1. Kinetic experiments using 40 nM RECQ1 and 2 nM chicken-foot substrate, visualized by gel electrophoresis. Lane 1-7: RECQ1 alone; Lane 7-14: RECQ1 in the presence of 100 nM PAR.

### 3.26 PARylated PARP1 inhibits the DNA unwinding activity of RECQ1:

We also analyzed the effect of PARylated PARP1 on the unwinding activity of RECQ1 using our standard forked duplex substrate. The results show that equimolar concentrations of PARylated PARP1 inhibit the helicase activity of RECQ1 by approximately 50 % (figure 3.13).
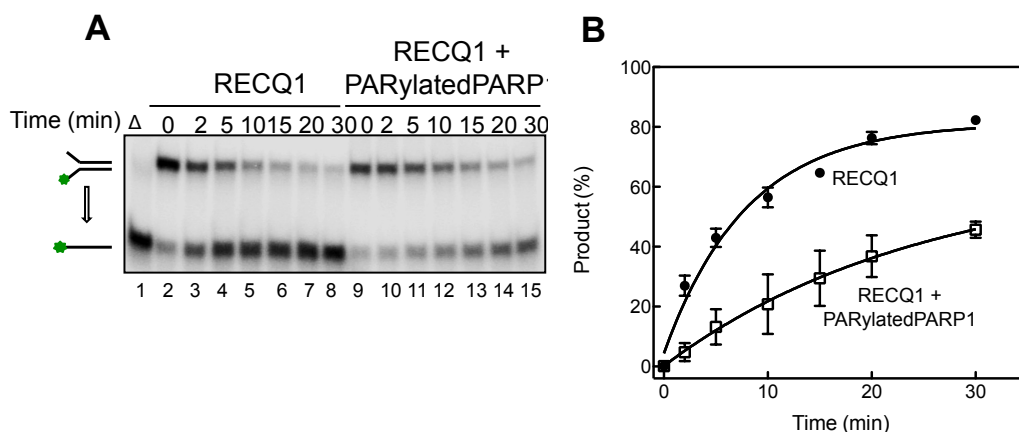
**Figure 3.13:** A) DNA unwinding assays using the forked duplex substrate. Lane 1: Heat denatured substrate. Lanes 2-8: kinetic experiments performed using 50 nM RECQ1 and the forked duplex substrate (2 nM). Lanes 9-14: kinetic experiments performed in the presence of PARylatedPARP1 (50 nM). B) Plots of the unwinding assays performed in the presence and absence of PARylatedPARP1. The data points represent the mean of three independent experiments. Error bars indicate s.e.m.

## 3.27 PARylated PARP1 specifically inhibits the activity of RECQ1:

The human WRN was previously shown to interact with PARP and to be able to regress and restore replication forks *in vitro* [230, 256, 257]. Thus, we investigated whether the inhibitory effect of PARylated PARP1 was specific to RECQ1. To test this, I repeated the fork restoration assays using the exonuclease-deficient WRN mutant - E84A. WRN-E84A promoted both fork regression and restoration efficiently with a slight bias towards fork restoration (figure 3.14A, B). The results for experiments performed in the presence of PARylated PARP1 showed that the inhibitory activity of PARylated PARP1 was specific to RECQ1 because PARylated PARP1 did not inhibit the fork restoration activity of WRN-E84A (figure 3.14C). The results were in agreement with the previous study performed with different sets of oligonucleotides [257].
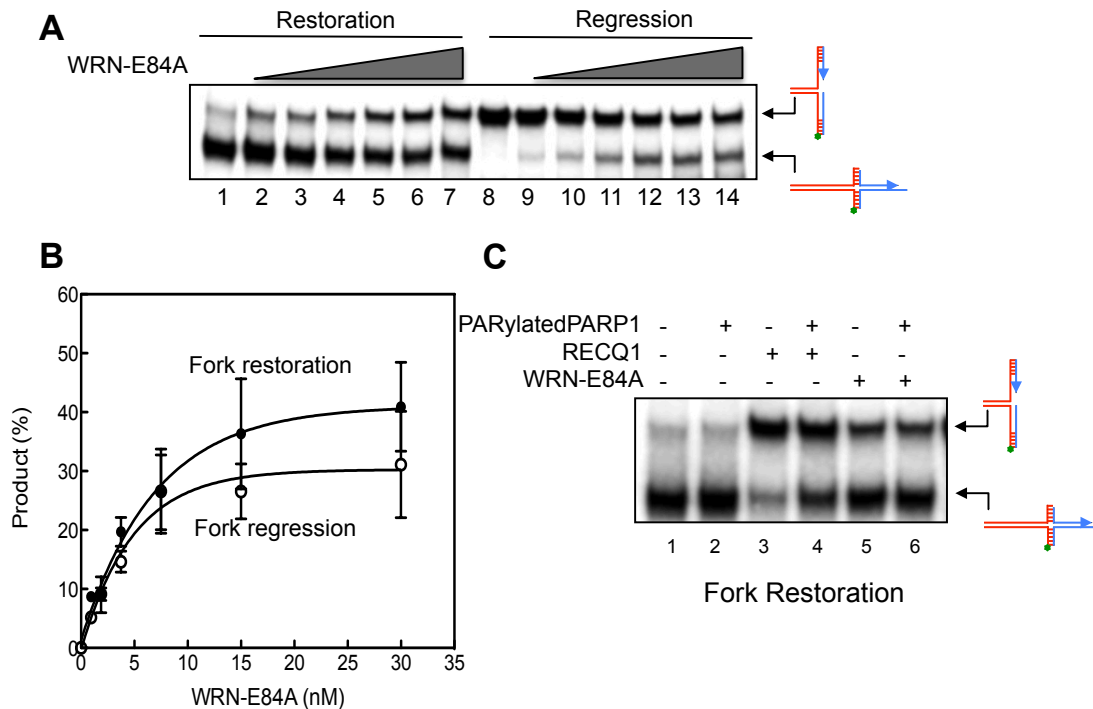
**Figure 3.14: Fork restoration and regression assays using human WRN-E84A.** A) These experiments were performed using exonuclease-deficient WRN-E84A mutant that allows following the branch migration reaction without possible complications arising form the substrate digestion. Lanes 1-7: fork restoration assays performed at increasing WRN-E84A concentrations (0, 0.9375, 1.875, 3.75, 7.5, 15, and 30 nM) and a fixed concentration of the chicken foot substrate (2 nM). Lanes 8-14: fork regression assays at increasing WRN-E84A concentrations (0, 0.9375, 1.875, 3.75, 7.5, 15, and 30 nM) and a fixed concentration of the replication fork structure (2 nM). All the reactions were stopped after 20 min. B) Plot of the fork restoration and regression activity as a function of protein concentration. The data points represent the mean of three independent experiments. Error bars indicate s.e.m. C) Fork restoration assays performed in the presence (lanes 2, 4, 6) and absence (1, 3, 5) of PARylatedPARP1 (50 nM) using wild-type RECQ1 (50 nM, lanes 3,4) or WRN-E84A (20 nM, lane 5,6). All the reactions were incubated for 20 min.

## 3.3 Architecture of RECQ1 assemblies with the Holliday junctions:

Understanding the mechanism of HJ branch migration is critical to explaining how cells resolve this universal HR intermediate. Many eukaryotic factors have been proposed to be involved in HJ branch migration [230, 256, 258-260]. However, our current knowledge of the actual mechanisms by which these factors branch migrate HJ structures is extremely limited. We recently discovered that RECQ1 plays a key role in the restart of reversed replication forks that regressed upon TOP1 inhibition [199]. However, the mechanism by which RECQ1 promotes the branch migration of reversed forks to restore a functional replication fork is unknown, and why other

human RecQ helicases do not share the same function of RECQ1 in reversed fork restart is unclear. Determining the RECQ1 mechanism of reversed fork branch migration is essential to shedding light on how eukaryotic proteins resolve cruciform structures.

**3.31 Analytical ultracentrifugation experiments on RECQ1 bound to Holliday junction:**

My studies with the annealing mutants Leu18Pro and Leu28Pro confirmed our previous conclusion that higher-order oligomers are required for the branch migration activity of RECQ1 (figure 3.30). In order to directly measure the oligomeric state of RECQ1 in complex with a Holliday junction (HJ) substrate, I performed sedimentation velocity analytical ultracentrifugation (AUC) experiments of RECQ1 in complex with HJs. The scans were acquired both at 280 nm and 260 nm to differentiate between the signals originating from RECQ1 alone (280 nm) and RECQ1 in complex with HJs (260 nm).

First, I performed sedimentation velocity AUC runs using different concentrations of the RECQ1 protein alone. The results showed that RECQ1 exists as two different oligomeric forms which sedimented at 6.8 S and 9.9 S respectively (figure 3.15 A-C). Sedimentation equilibrium experiments confirmed that these two forms have an estimated molecular weight of 130.5 kDa and 298.9 kDa, corresponding to dimers and tetramers, respectively, as previously reported [104]. Further sedimentation velocity experiments showed that the ratio of RECQ1 tetramers *versus* dimers increases at increasing protein concentrations in agreement with our previous gel filtration chromatography studies [105] (figure 3.16).

In order to study the RECQ1 complex with the HJ substrates, the scans were also acquired at 260 nm where the RECQ1 protein alone has a low absorbance even at the highest concentration of protein tested (figure 3.15 A, B, C). On the other hand, the AUC sedimentation profile for the HJ alone showed that the absorbance at 260 nm is much higher than its absorbance at 280 nm. The HJ sedimented as a single species at 5.8 S (figure 3.15D).
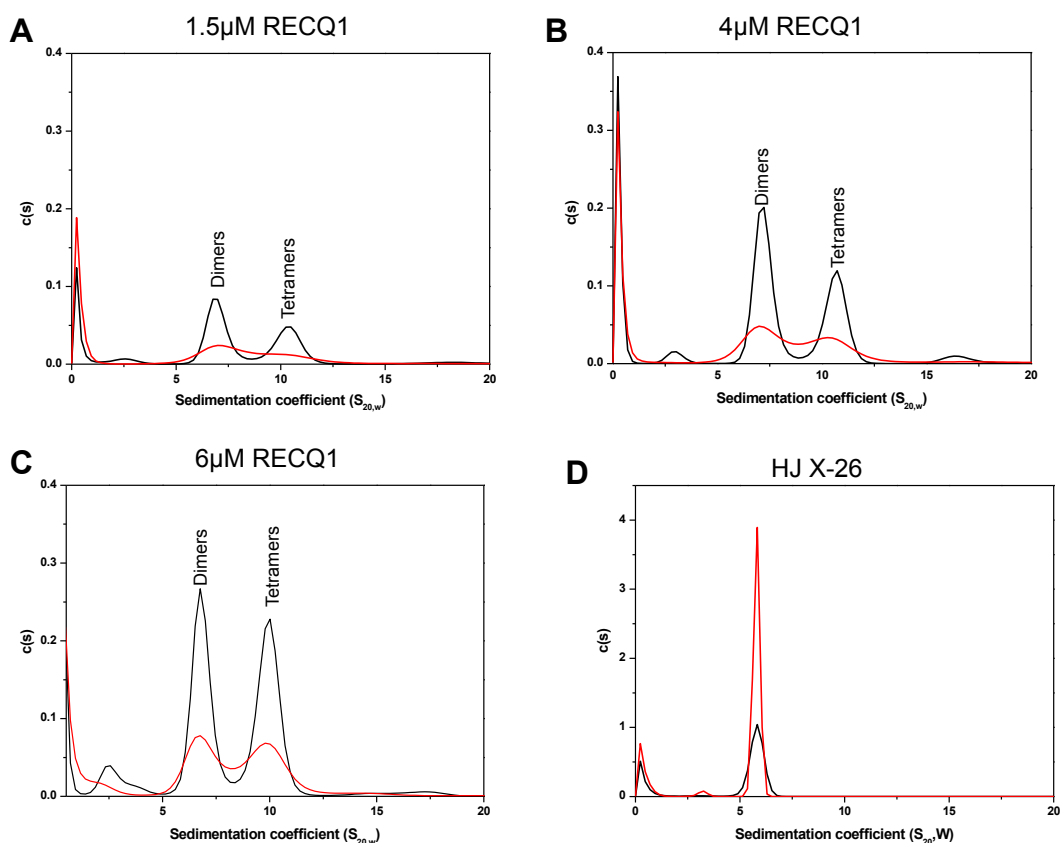
**Figure 3.15: Sedimentation velocity of RECQ1 and HJ in AUC.** RECQ1 in solution sedimented as two separate species. Continuous c(s) distributions as a function of sedimentation coefficient calculated from the sedimentation velocity profiles collected at 260 nm (red) and 280 nm (black) for A) 1.5 μM RECQ1, B) 4 μM RECQ1, C) 6 μM RECQ1, D) 1 μM HJ X-26. The data were analyzed using continuous c(s) distribution of Lamm equation (SedFit).
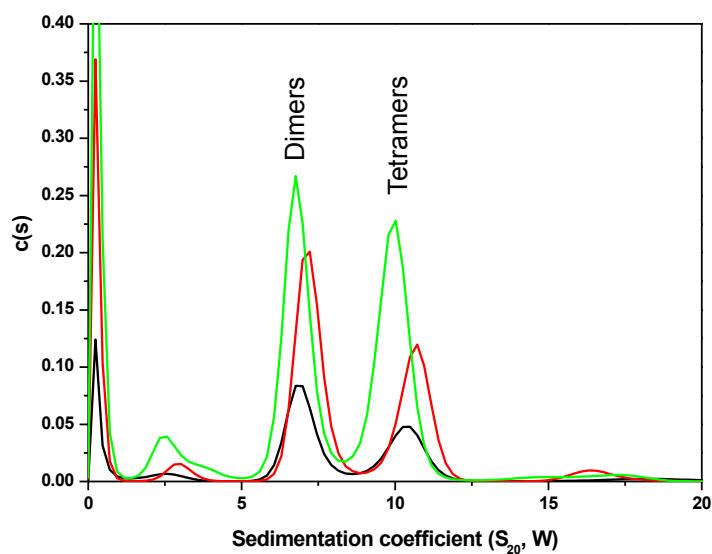


**Figure 3.16: Sedimentation velocity of RECQ1 in AUC.** The tetramer: dimer ratio of RECQ1 is concentration dependent. Continuous c(s) distributions as a function of sedimentation coefficient calculated from the sedimentation velocity profiles collected at 280 nm for 1.5 μM RECQ1 (black),

4 µM RECQ1 (red) and 6 µM RECQ1 (green) to analyze the effect of protein concentration on the ratio of tetramers *versus* dimers. 6 µM RECQ1 showed the highest ratio, followed by 4 µM and then by 1.5 µM RECQ1. The data were analyzed using continuous c(s) distribution of Lamm equation (SedFit).

Next, I performed AUC sedimentation velocity experiments of a mix containing both the HJ substrate and RECQ1 in a molar ratio of 1:6. The experiments clearly show an additional species that sedimented at 13.8 S corresponding to an estimated molecular weight of 352 kDa (figure 3.17). The appearance of this additional peak was associated with the disappearance of the peak corresponding to the RECQ1 tetramers, whereas the size of the dimer peak was not affected by the addition of the HJ. This data suggest that RECQ1 tetramers bind to the HJ and thereby there is a shift in the S value from 9.9 S (RECQ1 tetramers alone) to 13.8 S (RECQ1 tetramers + HJ). On the other hand, the RECQ1 dimers do not seem to interact with the HJ.
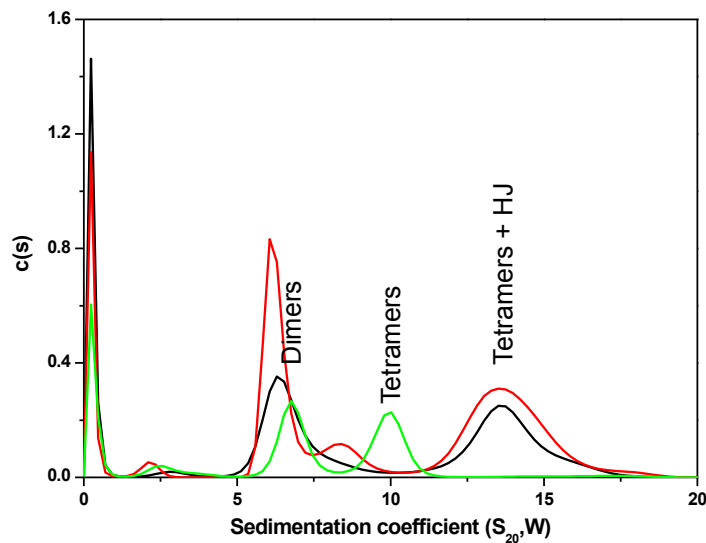


**Figure 3.17: Sedimentation velocity of RECQ1 in complex with HJ in AUC.** Continuous c(s) distributions as a function of sedimentation coefficient calculated from the sedimentation velocity profiles collected for 1µM HJ + 6µM RECQ1: RECQ1 alone at 280 nm (green), RECQ1 + HJ at 280nm (black) and 260nm (red), to analyze the functional form of RECQ1 binding to the HJ. The data were analyzed using continuous c(s) distribution of Lamm equation (SedFit).

Collectively, the above AUC experiments with the wild-type and the mutant proteins suggest that the oligomeric form of RECQ1 that interacts with HJ is mainly a tetramer. RECQ1 dimers might also be able to bind HJ, but with much lower affinity.

Our preliminary results from the cryo-EM experiments performed by our collaborator Dr. Alessandro Costa at the London research institute confirmed that RECQ1 binds HJs as a homo-tetramer (figure 3.19). The cryo-EM experiments performed by the group of Dr. Alessandro Costa, employed a novel method called the DNA-affinity grid method (figure 3.18) that aims at purifying functional nucleic acid engaged RECQ1 oligomers on the EM grid [261]. It would be interesting to extend this study using the mutants of RECQ1. In this method biotin labeled DNA is immobilized on a streptavidin layer, to form what is termed as the functionalized 2-D streptavidin crystals and upon adding the protein of interest, the 3-D model of the bound protein can be retrieved [261]. Immobilizing the DNA in this way, contrary to DNA adsorption (where the DNA interacts with a surface through it whole length), maintains the ability of the DNA to interact with proteins [261]. Since the protein is bound to the immobilized DNA, the samples contain a more homogenous population and also the chances of multiple proteins or DNA molecules binding to each other is greatly reduced. The ability to immobilize the DNA while retaining the accessibility of interacting proteins opens up the possibility to remove any reagents that might interfere with the analysis and to study the equilibrium of the interaction under different reaction conditions [261].
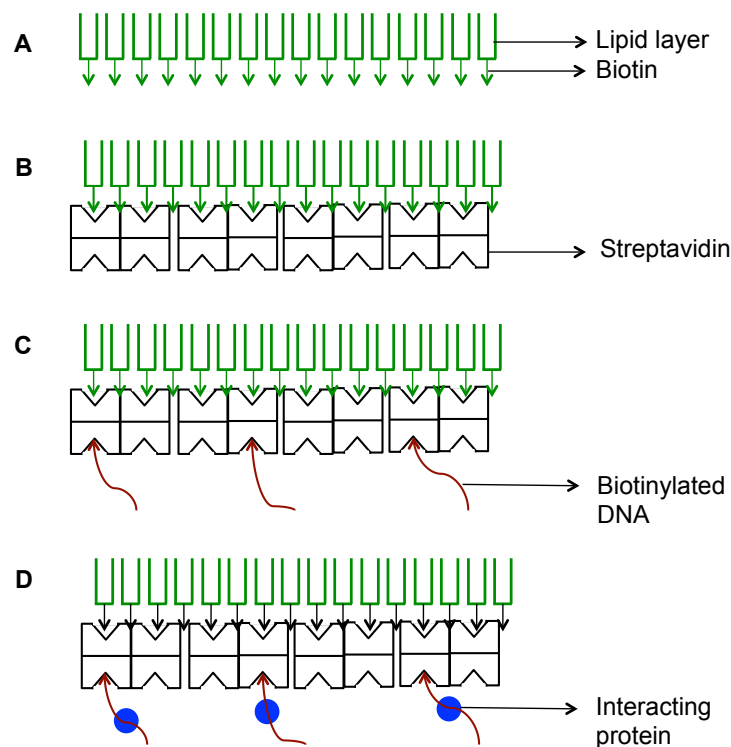


**Figure 3.18: Schematic description of the DNA-affinity grid method.** A) Lipid layer functionalized with biotin that is spread at the air-water interface. B) Addition of streptavidin and interaction of the

tetrameric streptavidin to the biotin moiety forming the 2-D crystals. C) Access to the biotin binding sites of streptavidin by the biotinylated DNA. D) The immobilized DNA is accessible to the interacting protein. Adapted from [261].
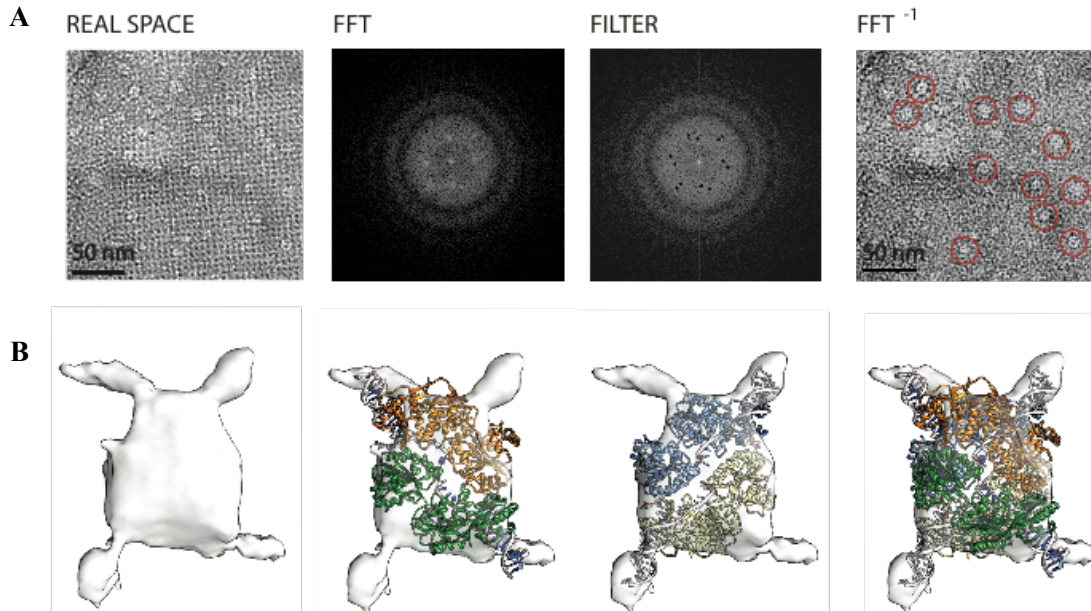


**Figure 3.19: RecQ1 on a DNA affinity EM grid.** A) Micrograph depicting RECQ1 molecules retained by biotinylated HJs on a streptavidin 2D crystal matrix (column 1). Fourier-transformed (FFT) images are computed and diffraction spots masked to erase any streptavidin lattice information (column 2 and 3). Single particles are selected on the filtered image transformed back (FFT$^{-1}$) into real space (column 4) and thereafter processed by established reconstruction approaches. B) Preliminary single-particle reconstruction of an HJ-bound RECQ1 assembly. Two copies of a DNA-associated RECQ1 dimer can be accommodated into the EM map, supporting a stoichiometry of four RECQ1 protomers per HJ molecule.

## 3.4 Identification of a coiled-coil region in RECQ1 and biochemical characterization of the coiled-coil mutants:

### 3.41 Identification of coiled-coil region in the N-terminus of RECQ1:

Previous studies in our lab identified two distinct oligomeric forms of RECQ1 associated with its DNA unwinding and single strand annealing activities. We showed that the dimers are associated with DNA unwinding and the tetramers are associated with DNA strand annealing [104, 105]. Our previous studies also showed that RECQ1 tetramers are mediated by two independent protein-protein contacts. One is mediated by the N-terminus of RECQ1, as suggested from our previous size exclusion chromatography analysis of truncated versions of the protein lacking the first 48 or 56 residues [32]. The other is mediated by the interaction of a

patch of residues that are clustered on one face of the helicase domain with a region of a second molecule that includes residues in the C-terminal Zn and WH domains (figure 3.20).
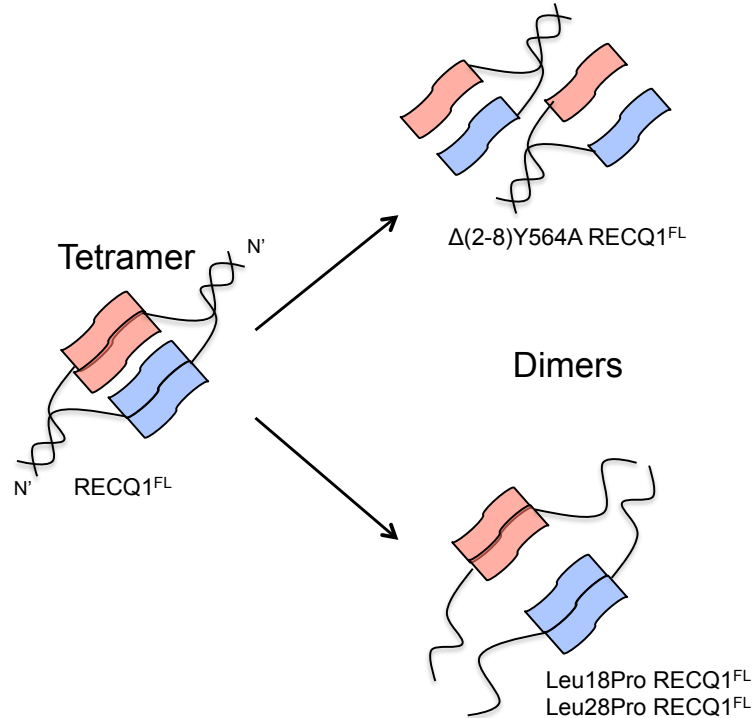


**Figure 3.20:** Schematic of the dimerization regions of RECQ1 and the assembly states of the proteins upon mutation at the respective regions.

Inspection of the human RECQ1 amino acid sequence using the Multicoil program revealed the presence of coiled-coil regions in the N-terminal region of RECQ1 (figure 3.23A). Coiled-coil motifs often function to mediate protein-protein interactions and protein multimerization [262]. Further analysis of this motif revealed the presence of hydrophobic amino acids predominating the positions 1 and 4, in the N-terminal region of the protein. The nonpolar nature of the 1 and 4 repeats of the coiled-coils has shown to facilitate dimerization along one face of each helix. Moreover, is has been reported that the degree hydrophobicity correlates with the stability of the coiled-coil [263]. The amino acids at the positions 1 and 4 also dictate the number of helices in a coiled-coil. A repeating pattern of isoleucine at position 1 and leucine at position 4 in a heptad repeat gives rise to dimeric coiled-coil [264]. The heptad repeats present in the RECQ1 sequence are consistent with the formation of dimeric-coiled-coil (figure 3.21).

```
hRECQ1 3 VSALTEELDSITSELHAVEIQIQELTERQQELIQKKKVLTKKIKQCL 50
```

**Figure 3.21: Sequence of the identified coiled-coil region in the N-terminus of RECQ1**. The amino acids at the position 1 and 4 of the helix are given in red and blue colors respectively.

## 3.42 Identification of conserved Leucine residues in the coiled-coil region:

Multiple sequence alignment of the coiled-coil N-terminal region of human RECQ1 with its orthologues in other organisms, showed the presence of two conserved Leu residues at positions 18 and 28 (figure 3.22).

```
sp|P46063|RECQ1_HUMAN  1 MASVS--ALTEELDSITSELHAVEIQIQELTERQQELIQKKK---VLTKKIKQCLE 50
tr|D7FHZ5|D7FHZ5_ECTSI 1 MGGLL--RGTFGLSSWRT--NQKEIVNATLSGRDAFVVMRTGGGKSLCYQLPALLK 50
sp|Q6AYJ1|RECQ1_RAT    1 MASIP--ALTDELESVSSELHAVDIQIQELTERQHELLQRKS---VLTKRIKQCLE 50
tr|Q28GA8|Q28GA8_XENTR 1 MDSEEAAALVDELESVSSELQAVEIQLQELLERQQELIQRKR---LLNKKIQRLSE 50
```

**Figure 3.22:** Multiple sequence alignment of human RECQ1 amino acid 1 – 50 with *Ectocarpus siliculosus, Rattus norvegicus* and *Xenopus tropicalis* RECQ1 homologues shows conserved Leucine 18 and 28 residues (boxed).

*In silico* analysis of the Leu 18 to Pro and Leu 28 to Pro mutated N-terminal sequence of RECQ1 using the Multicoil program showed reduced and abolished coiled-coil formation for the Leu18Pro and Leu28Pro mutants (figure 3.23 B, C). Thus, I performed mutagenesis studies to test whether the Leu18 and Leu28 residues are indeed involved in the higher-order oligomer assembly of RECQ1 through the formation of coiled-coils.
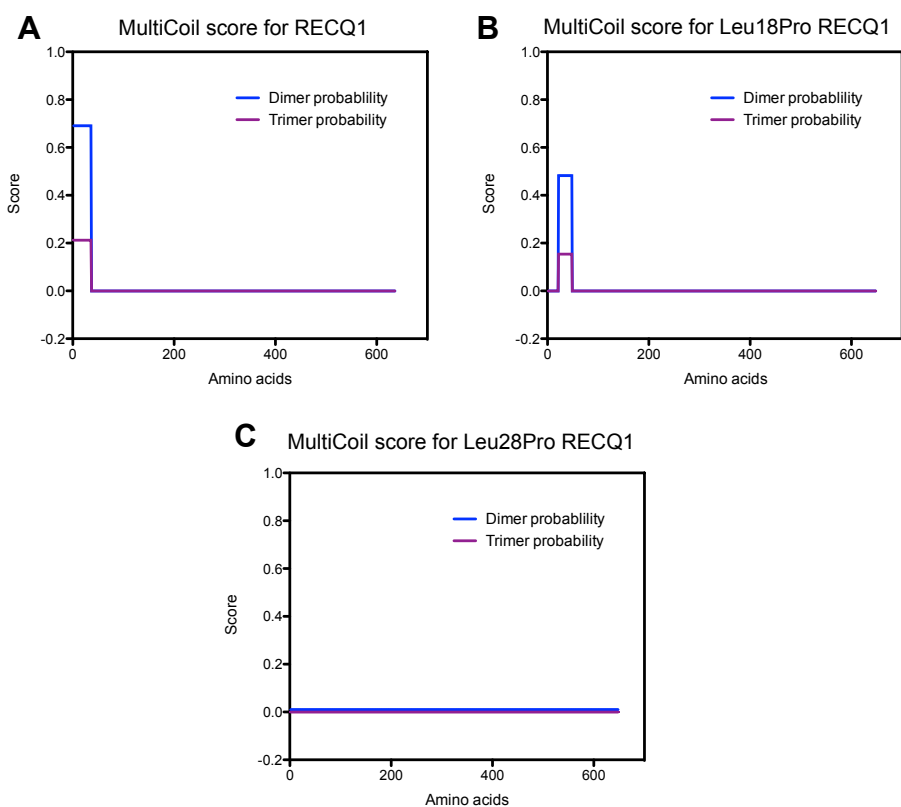
**Figure 3.23: Coiled-coil prediction for RECQ1 and the mutants Leu18Pro and Leu28Pro using MultiCoil program.** A) Coiled-coil score for the RECQ1-WT B) Coiled-coil score for the mutant RECQ1 Leu18Pro and C) Coiled-coil score for the mutant RECQ1 Leu28Pro.

## 3.43 Expression and purification of the Leu18Pro and the Leu28Pro RECQ1 mutants:

I introduced the Leu to Pro point mutations by site directed mutagenesis and prepared the respective bacmids from DH10Bac cells following the manufacturer's protocol. The proteins were overexpressed and purified following the same protocol that was used for the wild-type RECQ1. The protein expression was optimum at 72 hours after infection and the protein was purified to near homogeneity as evident from the coommassie stained SDS-PAGE gels (figure 3.24A). The blots involving the mutant proteins were detected using anti-His antibody (figure 3.24B).
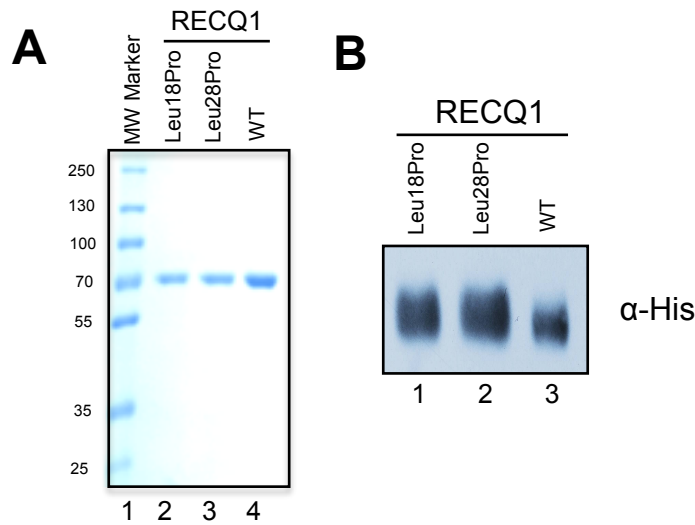
**Figure 3.24:** A) SDS-PAGE of purified RECQ1 WT and the mutants Leu18Pro and Leu28Pro over-expressed in Sf9 and purified by Cobalt affinity purification. Lane 1: Molecular weight marker (in kDa); lane 2: purified RECQ1 Leu18Pro mutant; lane 3: purified RECQ1 Leu28Pro mutant; lane 4: purified RECQ1 WT. The 8% SDS-PAGE was stained with commassie brilliant blue. B) Western Blot of RECQ1 WT lysate and the mutants Leu18Pro and Leu28Pro over-expressed in Sf9 and purified by Cobalt affinity purification: Lane 1: lysate from cells infected with RECQ1 Leu18Pro bacmid. Lane 2: lysate from cells infected with RECQ1 Leu28Pro; Lane 3: lysate from cells infected with RECQ1 bacmid. The blot was probed with rabbit anti-His antibody.

### 3.44 The Leu to Pro mutation abolishes the formation of tetramers:

The point mutants Leu18Pro and Leu28Pro showed, respectively, decreased and abolished coiled-coil formation *in silico*. Thus, I tested whether these mutations prevent indeed the formation of RECQ1 tetramers, by gel filtration chromatography. In agreement with our previous results [105], I found that the wild-type RECQ1 eluted as two peaks at a volume consistent with the tetrameric (305 kDa) and dimeric (156 kDa) form of the protein. As expected, the Leu18Pro and Leu28Pro mutants eluted as a single peak at a volume corresponding to a RECQ1 dimer (156 kDa and 163 kDa, respectively) (figure 3.25). These results were further confirmed by analytical ultracentrifugation experiments. The sedimentation coefficients measured for the wild-type protein were 6.8 S and 9.9 S, corresponding to the dimers and the tetramers, respectively. The Leu18Pro and Leu28Pro mutants sedimented as a single species with a sedimentation coefficient of 5.7 S and 6 S, respectively, confirming that the mutants can only exist as dimers (figure 3.26). Collectively, these data confirm that the coiled-coil region containing Leu18 and Leu28 is involved in the formation of RECQ1 tetramers via the N-terminal domain.
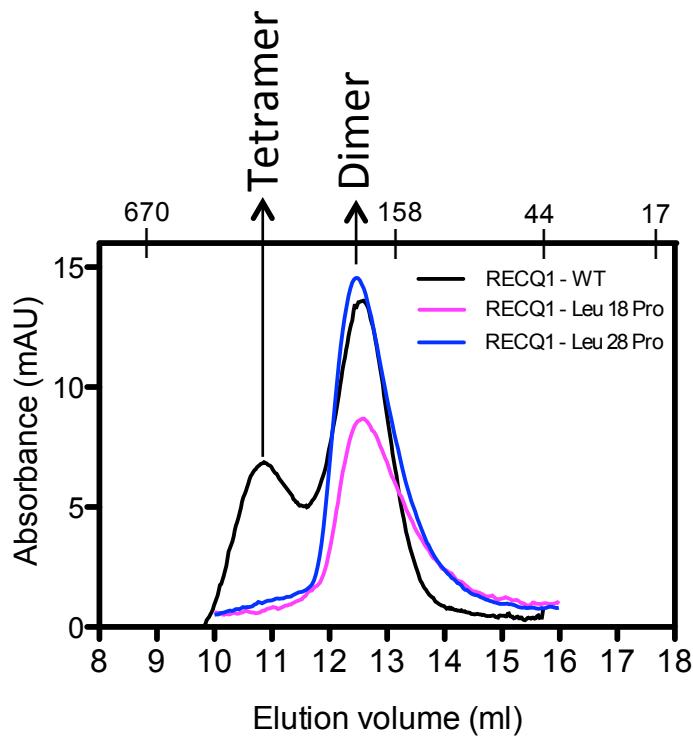
**Figure 3.25: Analysis of the oligomeric property of the mutants.** Size exclusion chromatography profiles of purified RECQ1 - WT (black), RECQ1 - Leu18Pro (pink) and RECQ1-Leu28Pro (blue). The elution volume of protein molecular weight standards (in kDa) and the position of tetramers and dimers are shown at the top of the panel.
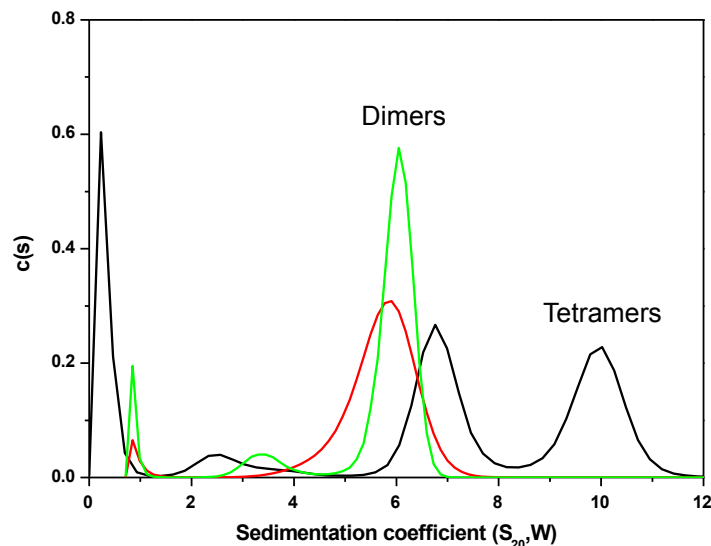


**Figure 3.26: Sedimentation velocity analytical ultracentrifugation of the wild-type and the mutant RECQ1.** The wild-type RECQ1 sedimented as two species whereas the mutants sedimented as a single species. Continuous c(s) distributions as a function of sedimentation coefficient calculated from the sedimentation velocity profiles collected for RECQ1WT (black), RECQ1-Leu18Pro (red) and RECQ1-Leu28Pro (green) at 280nm. The data was fit using continuous c(s) distribution of Lamm equation (SedFit).

Our lab has reported previously that the ratio of tetramers *versus* dimers increases in the presence of ssDNA for RECQ1 [105]. So, I tested if the mutants

Leu18Pro and Leu28Pro could form tetramers in the presence of ssDNA, by AUC sedimentation velocity experiments. I found that the mutants did not form tetramers even in the presence of ssDNA. The mutants Leu18Pro and Leu28Pro sedimented as a single species at 5.7 S and 6 S respectively. Upon addition of 1 μM ssDNA, they still sedimented as a single species at 6.6 S and 7.3 S, respectively. The peak observed in the presence of ssDNA corresponds to the dimer bound to DNA since it is also detectable at 260 nm (figure 3.27).
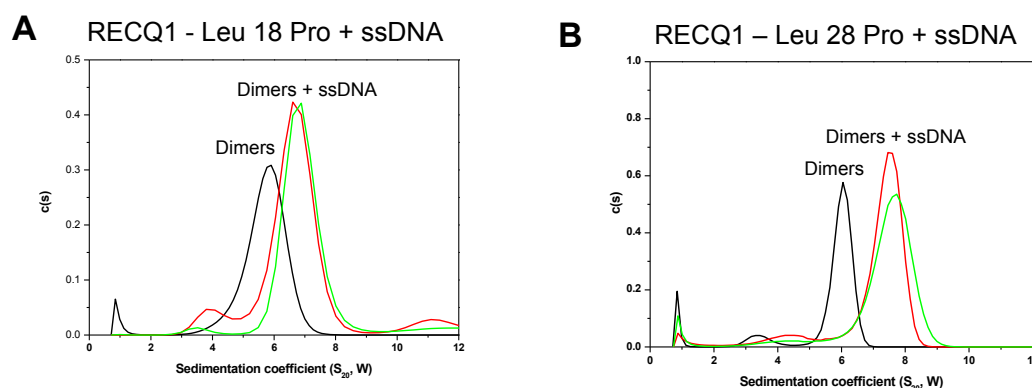


**Figure 3.27: Sedimentation velocity of Leu18Pro and Leu28Pro RECQ1 in complex with ssDNA in AUC.** Continuous c(s) distributions as a function of sedimentation coefficient calculated from the sedimentation velocity profiles collected for A) 1μM of ssDNA and 6μM of Leu18Pro RECQ1: Leu18Pro RECQ1 alone at 280nm (black), Leu18Pro RECQ1+ssDNA at 280nm (red) and 260nm (green) B) 1μM of ssDNA and 6μM of Leu28Pro RECQ1: Leu28Pro RECQ1 alone at 280nm (black), Leu18Pro RECQ1+ssDNA at 280nm (red) and 260nm (green). The data were analyzed using continuous c(s) distribution of Lamm equation (SedFit).

## 3.45 Biochemical characterization of the Leu18Pro and Leu28Pro mutants:

### 3.45A Helicase activity of the Leu18Pro and Leu28Pro mutants:

I analyzed the helicase activity of the Leu18Pro and Leu27Pro mutants using our standard forked duplex substrate. Both the mutants were active as helicases (figure 3.28 A, B) and their activities were comparable to that of the wild-type protein (figure 3.28 C). The mutants showed a concentration dependent unwinding activity.
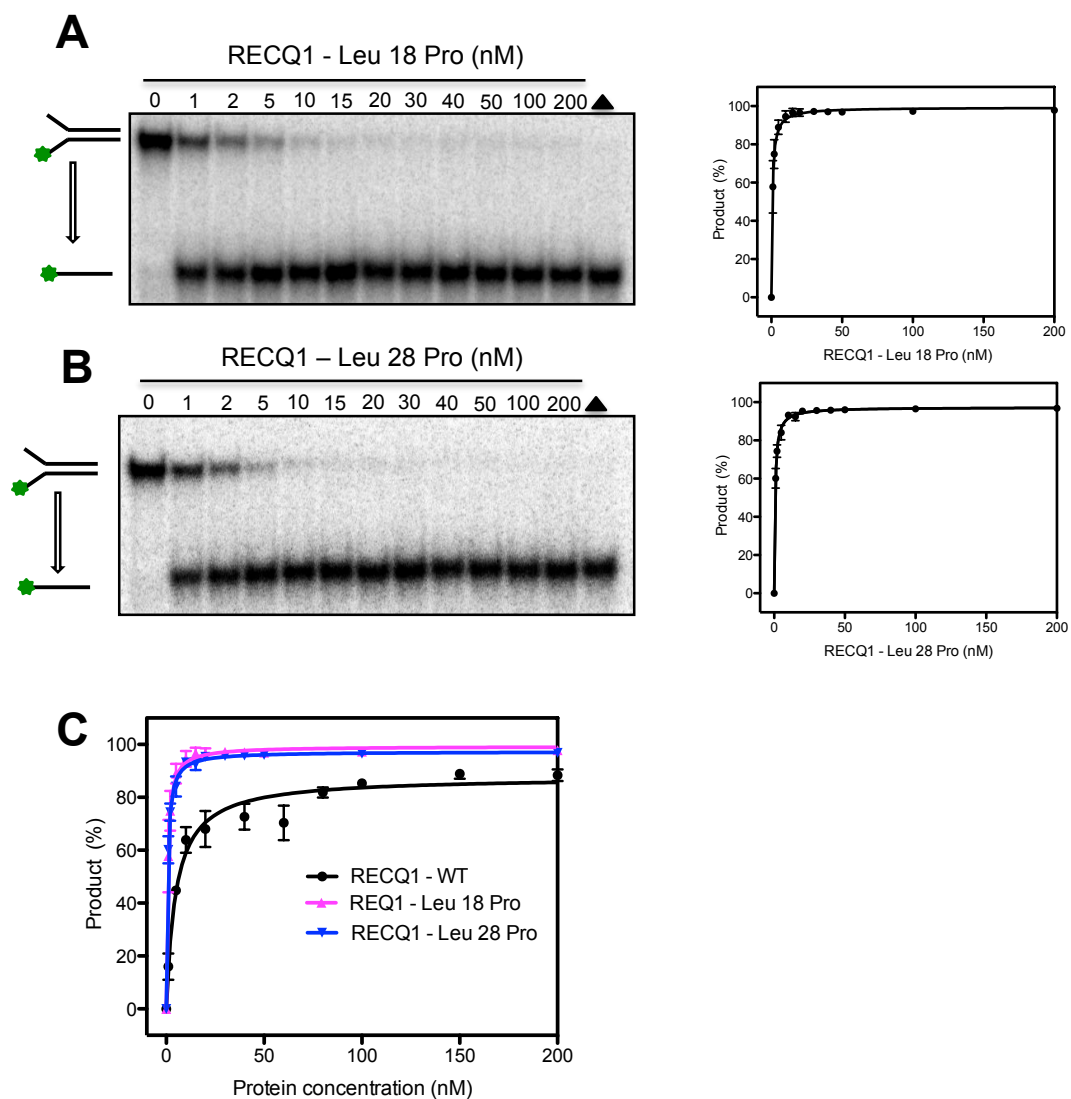
**Fig 3.28: Analysis of the unwinding activity of Leu18Pro and Leu28Pro RECQ1 using forked duplex DNA substrate on a 10% Native PAGE.** A) Unwinding assay using various concentrations of Leu18Pro RECQ1 (1 – 200 nM) and 0.5 nM of the forked duplex substrate. The reactions were incubated for 20 minutes at 37°C and stopped by the addition of quenching solution. Plot of the unwinding assay as a function of Leu18Pro RECQ1 concentration. The data points represent the mean of three independent experiments with the standard deviation indicated by error bars. B) Unwinding assay using various concentrations of Leu28Pro RECQ1 (1 – 200 nM) and 0.5 nM of the forked duplex substrate. The reactions were incubated for 20 minutes at 37°C and stopped by the addition of quenching solution. Plot of the unwinding assay as a function of Leu28Pro RECQ1 concentration. The data points represent the mean of three independent experiments with the standard deviation indicated by error bars. C) Plot comparing the helicase activities of the mutants Leu18Pro and Leu28Pro RECQ1 with the wild-type RECQ1. The data points represent the mean of three independent experiments with the standard deviation indicated by error bars.

## 3.45B Annealing activity of the Leu18Pro and Leu28Pro mutants:

Our previous studies suggested that RECQ1 tetramers are required for strand annealing. This conclusion was based on the observation that the truncated RECQ1$^{T1(49-616)}$, which cannot form tetramers in solution, is proficient in DNA unwinding, but lacks annealing activity [32]. My analysis of the strand annealing activity of the Leu18Pro and Leu28Pro mutants confirmed that these two mutants did not anneal complementary single strands even at the highest protein concentration tested (Figure 3.29). This is consistent with the notion that higher-order oligomers are required for single strand annealing.
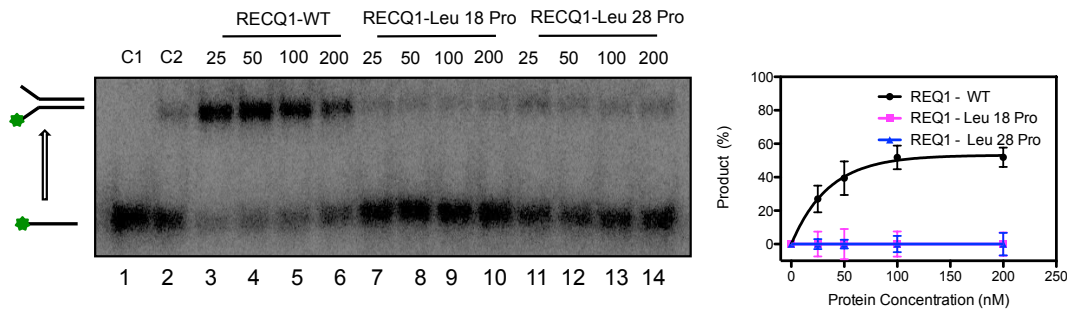


**Figure 3.29: Analysis of the annealing activity of the mutants and wild-type RECQ1.** Lane 1: Control reaction without the protein and cold strand. Lane 2: Control reaction with the cold strand and without the protein. Lane 3-6: Annealing assay using indicated concentration of wild-type RECQ1; Lane 7-10: Annealing assay using indicated concentration of Leu18Pro RECQ1; Lane 11-14: Annealing assay using the indicated concentration of Leu28Pro RECQ1. Right: Comparison of the annealing activity of the mutants with the wild-type RECQ1. The data points represent the mean of three independent experiments with the standard deviation indicated by error bars.

## 3.45C Branch migration activity of the Leu18Pro and Leu28Pro mutants:

Our mutagenesis studies with a truncated form of RECQ1 lacking the first 48 residues at the N-terminus show that this RECQ1 variant is unable to form tetramers and fails to catalyze HJ resolution, although it is still proficient in DNA unwinding [32]. Thus, I investigated whether the Leu18Pro and Leu28Pro mutant proteins can branch migrate Holliday junctions. In agreement with my observation that the two mutants cannot form tetramers, the results showed that they only retain a very limited branch migration activity that is only detectable at high protein concentrations (figure 3.30).
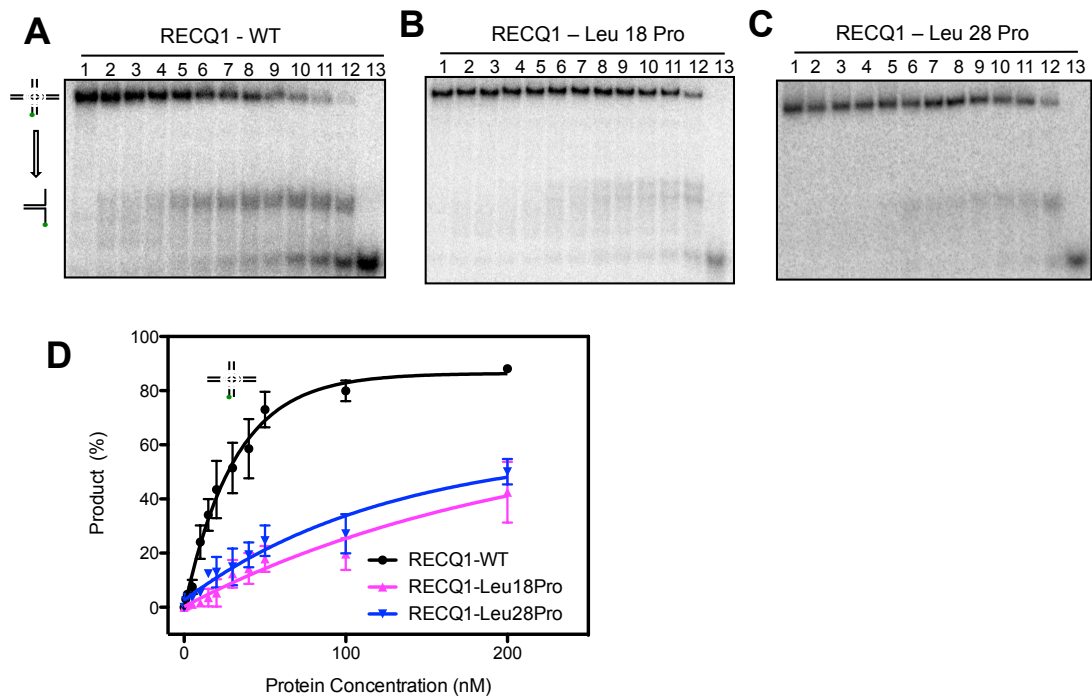
**Figure 3.30: Analysis of the branch migration activity of the mutants and wild-type RECQ1.** Holliday junction branch migration assay using different concentration of A) RECQ1 wild-type B) RECQ1 Leu18Pro mutant C) RECQ1 Leu28Pro mutant; Lane 1: control reaction without the protein; Lanes 2-12: branch migration assay with increasing protein concentrations (1, 2, 5, 10, 15, 20, 30, 40, 50 , 100, and 200 nM); Lane 13: Heat denatured substrate D) Plot of the HJ branch migration activity of the three proteins with respect to protein concentration. The data points represent the mean of three independent experiments with the standard deviation indicated by error bars.

# 4. DISCUSSION

RecQ helicases are a ubiquitous family of DNA unwinding enzymes that play an important role in DNA replication, repair and recombination [1, 23, 24] and hence they have been rightly called as multifunctional genome caretakers [118]. The interest around this highly conserved family of helicases increased significantly upon the discovery that three out of the five human RecQ helicase genes (*BLM*, *WRN* and *RECQ4*) are linked to specific genetic disorders characterized by premature aging, genomic instability and cancer predisposition [37, 73-75, 92]. The faithful replication of our genome is constantly threatened by endogenous or exogenous agents that can induce DNA damage and cause replication forks to stall or collapse [265]. Several proteins that are not part of the core replication machinery are required to mediate the efficient restart of these stalled replication forks to guarantee a faithful duplication of our genome [265].

RecQ helicases are among the key factors that assist replication forks in dealing with replication stress. For example, *E.coli* RecQ has at least two important roles at stalled replication forks. Along with RECJ, *E.coli* RecQ selectively promotes the degradation of the nascent lagging strand at blocked replication forks [266] and plays a role in suppressing illegitimate recombination [266-268]. Moreover, it has been reported that *E.coli* RecQ helps to eliminate structures that impede fork movement (e.g., G4 DNA structures) by binding to the ssDNA gap on the leading strand and unwinding the template dsDNA ahead of the fork. Subsequently, *E.coli* RecQ switches to the lagging strand and create an ssDNA region by unwinding the lagging strand, which may serve as an initiating signal for RecA-dependent SOS induction and recombination repair [269]. *S.cerevisiae* Sgs1 has also at least two roles during replication perturbation. At double strand breaks, Sgs1 unwinds the DNA to produce an intermediate that could be 5'-end resected by yeast Dna2. The resulting the 3' ssDNA overhang becomes the substrate for the DNA strand exchange protein RAD51 [270, 271]. Moreover, Sgs1 along with the ATM-related kinase Mec1 was shown to stabilize DNA polymerases $\alpha$ and $\varepsilon$ at the stalled forks following HU treatment [174].

In higher eukaryotes, the human BLM helicases was shown to be required for the efficient restart of the stalled replication forks [272] (figure 4.1). In particular, BLM is implicated in the transport of p53 to RAD51 sites at the stalled replication forks [208]. Moreover, BLM along with the topoisomerase IIIα and RMI1 proteins resolves converging replication forks [273] and double Holliday junctions without cross over product formation [64, 274]. Human Replication Protein A (RPA) specifically stimulates this activity of the BLM complex. In particular, RPA stimulates the unwinding activity of BLM and prevents BLM mediated re-annealing of the DNA strands [275].

WRN was also shown to assist fork restart by either preventing the accumulation of recombinogenic substrates or by suppressing of recombination itself [1, 210, 276-278]. Moreover, WRN was reported to be essential for fork progression following fork restart after HU stress [200]. WRN is recruited to stalled forks, where it interacts with the 9-1-1 complex to prevent DSB formation and recruitment of RAD51 [186, 279, 280].

RECQ4 has been implicated in replication fork restart after HU stress [192] and the C-terminus of RECQ4 was shown to play a role in replication elongation when the DNA template is damaged by ionizing radiation [194]. However, the mechanism by which RECQ4 performs this function is not known. Interestingly, a large body of evidence supports the notion that RECQ4 plays an additional and essential role during DNA replication initiation [98]. In agreement with these observations, our group showed that RECQ4 is recruited to origins of DNA replication during the late G1 phase of the cell cycle, after ORC and MCM complex assembly. Moreover, RECQ4 and RECQ1 are required for efficient PCNA loading that precedes and is required for polymerase loading onto the replication fork [191]. RECQ4 also facilitates the loading of the single-stranded-DNA binding protein RPA, as has already been shown for *Xenopus* [98, 189].
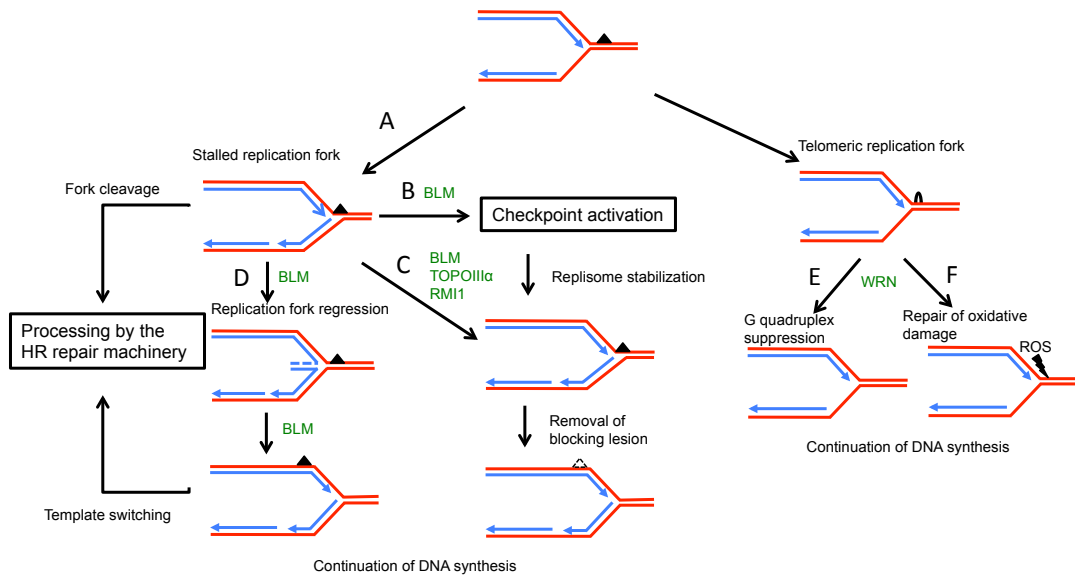
**Figure 4.1: Pathways of replication fork restart by BLM and WRN**. DNA lesion (black) on the leading strand is depicted A) Once the replication fork collides with this DNA lesion, leading and lagging strand synthesis becomes temporarily uncoupled, allowing lagging strand synthesis to continue for a short stretch beyond the site of the DNA lesion. BLM has been implicated in many roles at stalled replication forks, including B) activation of the cell cycle checkpoint C) BLM–TOPOIIIα–RMI1 complex facilitates the processing of HR intermediates when they arise, and D) the promotion of replication fork regression to create a "chicken-foot" structure in which the two nascent strands are paired. WRN also plays a role during replication fork stress E) WRN unwinds the G4 DNA at the telomere which would otherwise lead to replication fork stalling F) WRN also repairs oxidative damage to which the telomeric DNA is exquisitely sensitive.

An emerging model of how stalled or damaged forks are processed is that replication forks can reverse to aid repair of the damage [281, 282]. The idea that replication forks can reverse was initially proposed more than 30 years ago for replication across UV damage in mammalian cells [224]. While conceptually attractive, this model implies significant remodelling of replication fork structure into a four-way junction (reversed fork), reminiscent of Holliday junctions (HJs), i.e. a standard intermediate during homologous recombination. During fork regression, branch migration would help the replication fork to migrate away from the lesion (figure 4.2), thus allowing the repair of the lesion before replication can resume normally [283]. This model has been long discussed in the replication field and has found indirect experimental support in prokaryotic systems [283]. However, its existence and molecular determinants in eukaryotic cells are still debated.
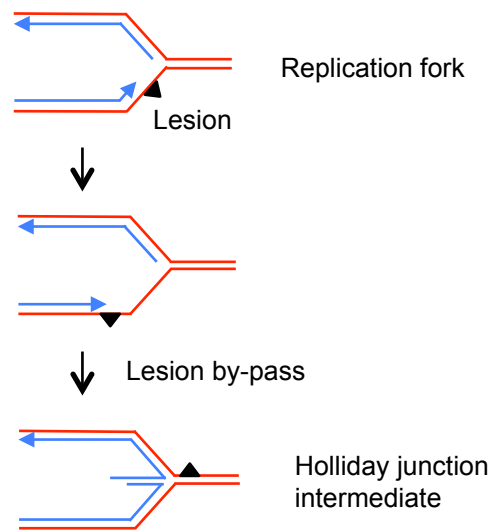
**Figure 4.2: Schematic of lesion bypass by branch migration.** A lesion in the leading strand template could result in the formation of a blocked fork with a gap. Branch migration would migrate the strands away from the lesion, preventing a fork collapse.

The first evidence that replication forks regress in human cells came from a recent study with topoisomerase I (TOP1) inhibitors, an important class of anticancer drugs currently in clinical use [245]. Their cytotoxicity, and thus their efficacy, has been generally linked to their ability to cause the accumulation of DNA nicks, which are later converted into double-stranded breaks (DSBs) by the collision of the DNA replication fork with the primary lesion [240, 284]. An alternative mechanism whereby DSBs originate from the Mus81 endonuclease-dependent cleavage of replication forks stalled by TOP1 inhibition has also been proposed [285]. The discovery that replication forks can regress upon TOP1 inhibition provided new insight into the molecular basis of TOP1 cytotoxicity by showing that clinically relevant, nanomolar doses of TOP1 poisons induce replication fork slowing and reversal in a process that can be uncoupled from DSB formation [245]. The same authors also showed that fork reversal requires poly(ADP-ribose) polymerase (PARP1) activity. However, the cellular factors required to restart replication forks after the lesion is repaired were not identified. Moreover, the role of PARP in promoting fork reversal remained unexplained.

RECQ helicases are likely candidates to be involved in fork reversal and restart because they possess a number of catalytic activities that might be relevant to restart reversed replication forks, such as their strong ATPase- and $Mg^{2+}$-dependent branch migration activity (BLM, WRN, RECQ1) [225, 232, 260], and their well-

characterized strand annealing activity (RECQ1, BLM, WRN, RECQ4 and RECQ5β) [34, 40, 101, 102].

My thesis sheds light on the role of the human RECQ1 helicase in replication fork restart. The notion that RECQ1 might be involved in replication stress response is supported by the previous observations that RECQ1 loads on DNA replication origins in a cell cycle dependent fashion and that the amount of RECQ1 loaded on replication origins increases upon DNA damage induction [191]. Moreover, RECQ1-deficient cells are sensitive to treatment with a range of replication inhibitors. In addition, RECQ1 also possesses a strong ATP-dependent branch migration activity similar to other proteins suggested to play a role in fork reversal and restart [286]. My experiments with purified RECQ1 on the substrates that mimic stalled fork or a regressed fork showed that RECQ1 is able to efficiently restore reversed replication forks in a concentration dependent fashion (figures 3.5 and 3.6). The human BLM and WRN helicases are able to catalyze the regression of model replication forks [230, 260] and can also convert reversed forks reminiscent of a HJ structure into functional replication forks [256]. On the other hand, my biochemical data show that RECQ1 differs from BLM and WRN beacause it can only promote fork restoration, but not the opposite reaction of fork reversal. This data is also supported *in vivo* by DNA fiber and electron microscopy experiments [199].

My results also provide a new understanding of the molecular role of PARP in fork reversal by showing that the PARylation activity of PARP is important to regulate the activity of RECQ1 on replication forks. Our lab has recently found that PARP1 interacts with RECQ1 *in vivo* and *in vitro* [199]. Following this finding, I tested the effect of PARP1 on RECQ1 activity and found that PARylated PARP1 inhibits the fork restoration activity of RECQ1 *in vitro*. I also demonstrated that the inhibitory effect of PARylated PARP1 on RECQ1 fork restoration activity is not due to a competition for DNA binding. The model that emerged from our studies (figure 4.3) proposes that PARP1 binds to the regressed replication forks and PARylates itself. RECQ1 is recruited and interacts with the PARylated PARP1 at the regressed forks. This interaction inhibits the fork restoration activity of RECQ1 until the lesion is repaired and thereby prevents the premature restart of the replication forks, which would otherwise lead to DSB accumulation. Studies performed by other members of our group validated this model in a cellular context [199]. An important next step

will be to identify factors that may trigger the RECQ1-catalyzed reaction of fork restart by regulating PARP activity. Poly(ADPribosyl) glycohydrolase (PARG), the enzyme responsible for PAR degradation, is one interesting candidate [287]. Once the lesion is repaired, PARG might cleave the PAR polymers thereby allowing RECQ1 to restart the regressed replication forks. Another important avenue for future studies will be to identify additional factors/pathways that mediate fork reversal and restart.
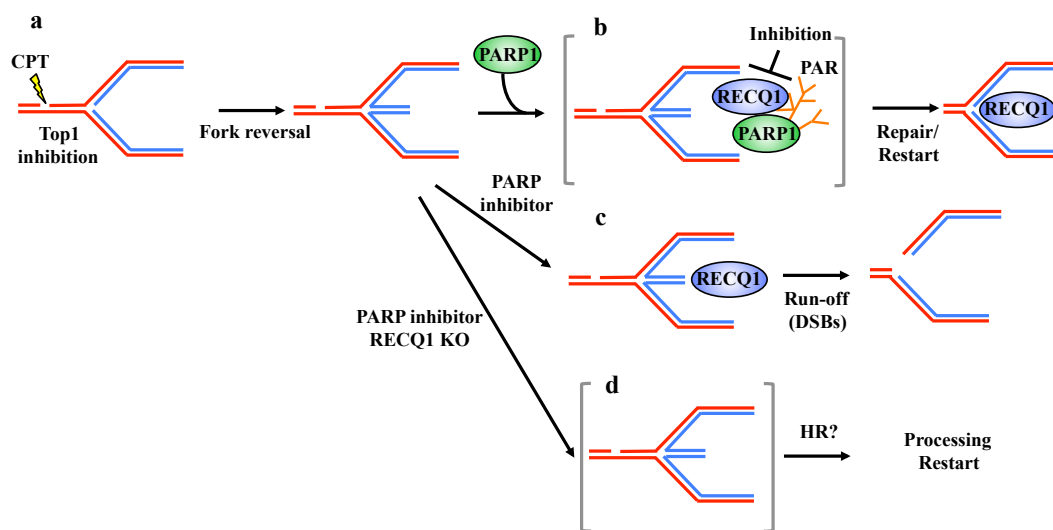


**Figure 4.3: Schematic model of the combined roles of PARP1 and RECQ1 in response to Top1 inhibition. (**a**), (**b**)** PARP poly(ADPribosyl)ation activity is not required to form reversed forks, but it promotes the accumulation of regressed forks by inhibiting RECQ1 fork restoration activity, thus preventing premature restart of the regressed forks (c) Inhibition of PARP activity leads to replication run-off and increased DSBs formation upon Top1 inhibition, as RECQ1 can cause untimely restart of reversed fork (d) PARP activity is no longer required in RECQ1-depleted cells were regressed forks accumulate because the cells lack the enzyme (RECQ1) necessary to promote fork restart. Homologous recombination (HR) might be required to promote fork restart in the absence of RECQ1 and PARP activity.

The identification of a specific and controlled biochemical activity that drives restart of reversed forks strongly supports the physiological relevance of this DNA transaction during replication stress in human cells. These data provide new mechanistic insight to predict the efficiency of combinatorial anticancer therapies with PARP and TOP1 inhibitors, which are currently in clinical trials. Our results also suggest that RECQ1 itself might represent a new therapeutic target, selective for cancer cells, to be used in conjunction with TOP1 inhibitors. Inducing fork reversal (TOP1 inhibitors) and inhibiting reversed fork reactivation (RECQ1 depletion) should in principle synergize, thus increasing the TOP1 inhibitor-sensitivity of

RECQ1-depleted cells. A cancer specific role of RECQ1 is supported by our recent results showing that RECQ1 is highly expressed in various types of solid tumors [288]. Moreover, RECQ1 depletion in cancer cells results in mitotic catastrophe and local and systemic administration of RECQ1-siRNA prevents tumor growth in murine models [289-291]. Our long-term goal is to find novel inhibitors selective for cancer cells that could be used together with TOP1 inhibitors or other DNA damaging agents to sensitize targeted cells (i.e. tumor cells) to lower doses of the selected chemotherapeutic agents that are not toxic to normal cells.

The second part of my thesis focuses on understanding the actual mechanism by which RECQ1 branch migrates HJs and promotes the restart of reversed replication forks. Understanding the mechanism of HJ branch migration is critical to explaining how cells resolve this universal HR intermediate. Many eukaryotic factors have been proposed to be involved in HJ branch migration [230, 256, 258-260]. However, our current knowledge of the actual mechanisms by which these factors branch migrate HJ structures is extremely limited. We recently discovered that RECQ1 plays a key role in the restart of reversed replication forks that regressed upon TOP1 inhibition [199]. However, the mechanism by which RECQ1 promotes the branch migration of reversed forks to restore a functional replication fork is unknown, and why other human RecQ helicases do not share the same function of RECQ1 in reversed fork restart is unclear.

My results on the analysis of the assembly state of RECQ1 bound to HJ provide essential information on the number of RECQ1 motors that load on four-way junction structures. Using a combination of analytical ultracentrifugation (AUC) and cryo electron microscopy (cryo-EM) approaches, we concluded that RECQ1 binds HJ as a homo-tetramer. My sedimentation velocity AUC experiments on RECQ1 showed an additional peak that sedimented at 13.8 S upon addition of the HJ substrate. The appearance of this peak is associated with the disappearance of the RECQ1 tetramer peak supporting the notion that RECQ1 binds to the HJ as a tetramer. Additional experiments at different ratio of HJ: RECQ1 confirmed the above result with the appearance of the peak at 13.8 S at all the ratios tested (data not shown). The results of cryo-EM experiments performed by the group of Dr. Alessandro Costa using the DNA-affinity grid method provide further support to the notion that RECQ1 binds to the HJ as a homo-tetramer (figure 3.19).

The bacterial RuvA helicase was also shown to bind to the HJ as a tetramer [292-294]. However, there are fundamental differences between RECQ1 and RuvA. First, RuvA binds to and branch migrates HJ in complex with RuvB, forming the so-called RuvAB complex. Second, the RuvAB complex contains two pairs of RuvA tetramers sandwiching the HJ [295]. Branch migration occurs as a result of translocation of a pair of RuvA tetramers and RuvB hexamers loaded on the opposite sides of the junction [293, 296, 297]. On the other hand, our results suggest that only one RECQ1 motor formed by four RECQ1 units is required for four-way junction branch migration, whereas RuvAB requires two motors poised head-to-head.

The HJ is an intermediate state for various genetic processes such as homologous recombination and replication fork regression/restoration, and it is targeted by a number of structure specific proteins [298]. The key aspect of the HJ is its dynamic structure, which can vary between a mobile "open-X" (extended) and an immobile "stacked-X" conformation, as shown in figure 4.4 [299].
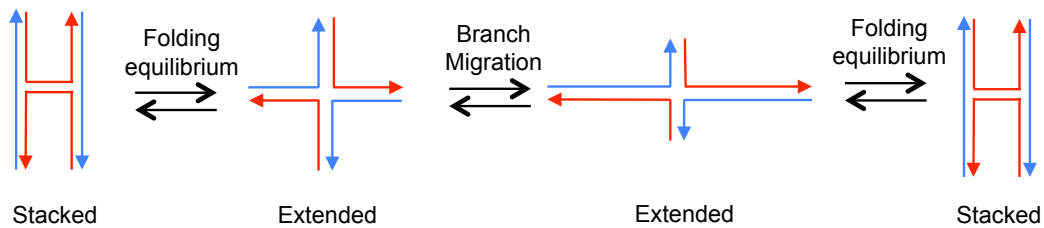


**Figure 4.4:** Schematics showing the extended and stacked conformations of the HJ and their folding equilibrium, which depends on the divalent cations [299].

The conformation adopted by the HJ is dependent on the type and concentration of divalent cations present in the solution [299]. Low salt favours the extended/open conformation because the negatively charged phosphates are largely unshielded and thus the arms extend away from each other due to repulsion. On the other hand, high salt favours stacked conformation due to condensation of cations around the phosphates allowing formation of a more compact structure in which the arms are stacked into double helices that are interrupted only by the crossing strand.
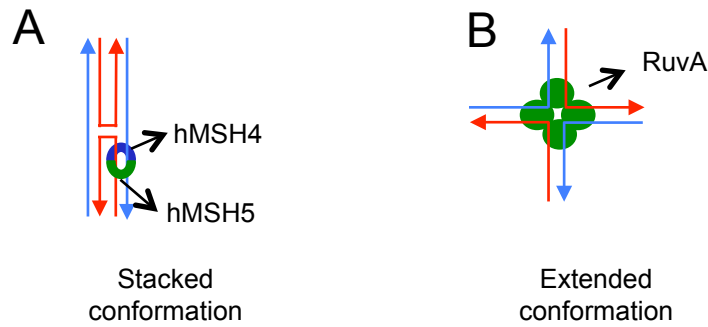
**Figure 4.5: Structure specific preference of HJ binding proteins.** A) The hMSH4-hMSH5 preferentially binds the stacked conformation of the HJ and embraces the arms of the HJ to form the meiosis-specific sliding camp [300]. B) The *E.coli* RuvA of the RuvAB complex binds to the extended conformation of HJ as a tetramer and stabilizes the HJ for subsequent branch migration by the RuvB protein [301].

Though there is no studies showing the conformation of the HJ structures *in vivo*, various *in vitro* studies have showed that the enzymes that bind to or branch migrate HJs are structure specific. Moreover, there are examples of proteins that prefer the open conformation *versus* the stacked conformation and *vice versa* (figure 4.5). The fact that these proteins exist is indirect evidence that these two different HJ conformations might indeed exist *in vivo*. For example, the *E.coli* RuvA protein binds to the extended/open conformation of HJ and promotes branch migration [301], whereas the hMSH4–hMSH5 complex prefers folded conformations of the HJ and acts as a clamp for branch migration and also cross-over during meiosis [300]. In cases where branch migration is required, keeping the junction in an unfolded conformation might be sufficient for providing a long-range spontaneous migration of the junction. At the same time, folding the junction is an effective brake that immediately blocks its movement. Therefore, various structural proteins competing for binding to the HJ can play roles as molecular switches turning on or off branch migration. Our cryo-EM data support the notion that RECQ1 binds the extended/open conformation of the HJ similar to the bacterial RuvA protein, although further biochemical studies at different salt concentrations will be needed to confirm this model.

I designed new RECQ1 mutants that cannot oligomerize to confirm that RECQ1 tetramers are indeed required for HJ branch migration. In particular, I identified a coiled-coil region in the N-terminus of RECQ1 that contains two Leucine residues well conserved among the RECQ1 homologs. Coiled-coil regions were

previously shown to promote protein oligomerization [263]. Previous studies performed in our laboratory have shown that the N-terminal region of human RECQ1 is involved in higher-order oligomer formation [231] and it is also essential for the annealing activity of the protein [32]. To gain more insight into the role of these Leucine residues in coiled-coil mediated oligomerization, I made two point mutants of RECQ1 - Leu18Pro RECQ1 and Leu28Pro RECQ1, and I biochemically characterized their assembly states and catalytic activities. First of all, I confirmed by analytical ultracentrifugation and size exclusion chromatography experiments that these two mutants do not form tetramers, even if ssDNA is added to the solution. However, they are still able to form RECQ1 dimers. The helicase assays with these two mutants confirmed that both mutants are still able to unwind DNA, in agreement with our previous observation that RECQ1 dimers are required for DNA unwinding. On the other hand, our previous studies suggest that RECQ1 tetramers are required for more specialized activities such as DNA strand annealing and HJ branch migration. In agreement with this conclusion, I found the Leu18Pro and Leu28Pro mutants were not able to anneal complementary single stranded DNA. Moreover, these mutants have a severely reduced branch migration activity (figure 3.30) suggesting that the active form of RECQ1 that branch migrates HJ is an indeed a tetramer [32]. Similar results were obtained using a truncated RECQ1 variant lacking the first 48 aa at the N-terminus and the last 33 aa in the C-terminus (hRECQ1 (49-616)) [32]. Collectively, these findings support the notion that RECQ1 tetramers are required for HJ branch migration.

All the five human RECQ helicases are known to promote the annealing of complementary single-stranded DNA fragments. In addition, several other DNA helicases such as human DNA2 [302], PIF1 [303] and TWINKLE [304] possess both DNA unwinding and annealing activities. The exact cellular function of the annealing activity of all these proteins has however yet to be determined. The Leu18Pro and Lue28Pro RECQ1 mutants represent two new "separation" of function mutants that retain the ability to unwind DNA, but lack annealing activity. These mutants might be useful to determine the biological pathways that require the strand annealing *versus* unwinding activity of RECQ1.

One possibility is that RecQ helicases might combine their unwinding and annealing activity to branch migrate HJ. The fact that the N-terminally deleted mutants of RECQ1 lack annealing activity and fail to branch migrate HJs would support this model. In agreement with this conclusion, the Leu18Pro and Leu28Pro mutants are also characterized by a weak branch migration activity that is detectable only at higher protein concentration.

Processing of HJs by various enzymes is a critical event for the maintenance of genome stability, and defects in HJ resolution are associated with many cancer related pathologies. Understanding how different proteins branch migrate HJ structures will provide the groundwork necessary to understand the link between deficiencies in these proteins, increased genomic instability and occurrence of well-characterized cancer-related pathologies. Moreover, the knowledge on the specific functions of these proteins in fork reversal and restart will offer new molecular perspectives for future chemotherapeutic regimens based on genotoxic agents that inhibit DNA replication and induce replication fork reversal.

# BIBLIOGRAPHY

1. Bachrati, C.Z. and I.D. Hickson, *RecQ helicases: guardian angels of the DNA replication fork.* Chromosoma, 2008. **117**(3): p. 219-33.

2. Ellis, N.A., *DNA helicases in inherited human disorders.* Current opinion in genetics & development, 1997. **7**(3): p. 354-63.

3. Matson, S.W., D.W. Bean, and J.W. George, *DNA helicases: enzymes with essential roles in all aspects of DNA metabolism.* BioEssays : news and reviews in molecular, cellular and developmental biology, 1994. **16**(1): p. 13-22.

4. von Hippel, P.H., *Helicases become mechanistically simpler and functionally more complex.* Nature structural & molecular biology, 2004. **11**(6): p. 494-6.

5. West, S.C., *DNA helicases: new breeds of translocating motors and molecular pumps.* Cell, 1996. **86**(2): p. 177-80.

6. Singleton, M.R., M.S. Dillingham, and D.B. Wigley, *Structure and mechanism of helicases and nucleic acid translocases.* Annual review of biochemistry, 2007. **76**: p. 23-50.

7. Velankar, S.S., et al., *Crystal structures of complexes of PcrA DNA helicase with a DNA substrate indicate an inchworm mechanism.* Cell, 1999. **97**(1): p. 75-84.

8. Maluf, N.K., C.J. Fischer, and T.M. Lohman, *A Dimer of Escherichia coli UvrD is the active form of the helicase in vitro.* J Mol Biol, 2003. **325**(5): p. 913-35.

9. Byrd, A.K. and K.D. Raney, *Protein displacement by an assembly of helicase molecules aligned along single-stranded DNA.* Nature structural & molecular biology, 2004. **11**(6): p. 531-8.

10. Byrd, A.K. and K.D. Raney, *Increasing the length of the single-stranded overhang enhances unwinding of duplex DNA by bacteriophage T4 Dda helicase.* Biochemistry, 2005. **44**(39): p. 12990-7.

11. Byrd, A.K. and K.D. Raney, *Protein displacement by an assembly of helicase molecules aligned along single-stranded DNA.* Nat Struct Mol Biol, 2004. **11**(6): p. 531-8.

12. Wong, I. and T.M. Lohman, *Allosteric effects of nucleotide cofactors on Escherichia coli Rep helicase-DNA binding.* Science, 1992. **256**(5055): p. 350-5.

13. Egelman, E.H., et al., *Bacteriophage T7 helicase/primase proteins form rings around single-stranded DNA that suggest a general structure for hexameric helicases.* Proc Natl Acad Sci U S A, 1995. **92**(9): p. 3869-73.

14. Patel, S.S. and M.M. Hingorani, *Oligomeric structure of bacteriophage T7 DNA primase/helicase proteins.* J Biol Chem, 1993. **268**(14): p. 10668-75.

15. Finger, L.R. and J.P. Richardson, *Stabilization of the hexameric form of Escherichia coli protein rho under ATP hydrolysis conditions.* J Mol Biol, 1982. **156**(1): p. 203-19.

16. Geiselmann, J., et al., *Physical properties of the Escherichia coli transcription termination factor rho. 1. Association states and geometry of the rho hexamer.* Biochemistry, 1992. **31**(1): p. 111-21.

17. Adachi, Y., J. Usukura, and M. Yanagida, *A globular complex formation by Nda1 and the other five members of the MCM protein family in fission yeast.* Genes Cells, 1997. **2**(7): p. 467-79.

18. Ishimi, Y., *A DNA helicase activity is associated with an MCM4, -6, and -7 protein complex.* J Biol Chem, 1997. **272**(39): p. 24508-13.

19. Lei, M., Y. Kawasaki, and B.K. Tye, *Physical interactions among Mcm proteins and effects of Mcm dosage on DNA replication in Saccharomyces cerevisiae.* Mol Cell Biol, 1996. **16**(9): p. 5081-90.

20. Nakayama, H., et al., *Isolation and genetic characterization of a thymineless death-resistant mutant of Escherichia coli K12: identification of a new mutation (recQ1) that blocks the RecF recombination pathway.* Molecular & general genetics : MGG, 1984. **195**(3): p. 474-80.

21. Cobb, J.A. and L. Bjergbaek, *RecQ helicases: lessons from model organisms.* Nucleic acids research, 2006. **34**(15): p. 4106-14.

22. Bachrati, C.Z. and I.D. Hickson, *RecQ helicases: suppressors of tumorigenesis and premature aging.* The Biochemical journal, 2003. **374**(Pt 3): p. 577-606.

23. Bohr, V.A., *Rising from the RecQ-age: the role of human RecQ helicases in genome maintenance.* Trends in biochemical sciences, 2008. **33**(12): p. 609-20.

24. Hickson, I.D., *RecQ helicases: caretakers of the genome.* Nature reviews. Cancer, 2003. **3**(3): p. 169-78.

25. Hanada, K. and I.D. Hickson, *Molecular genetics of RecQ helicase disorders.* Cellular and molecular life sciences : CMLS, 2007. **64**(17): p. 2306-22.

26. Mandell, J.G., et al., *Expression of a RecQ helicase homolog affects progression through crisis in fission yeast lacking telomerase.* The Journal of biological chemistry, 2005. **280**(7): p. 5249-57.

27. Hartung, F. and H. Puchta, *The RecQ gene family in plants.* Journal of plant physiology, 2006. **163**(3): p. 287-96.

28. Vindigni, A. and I.D. Hickson, *RecQ helicases: multiple structures for multiple functions?* HFSP journal, 2009. **3**(3): p. 153-64.

29. Lohman, T.M., E.J. Tomko, and C.G. Wu, *Non-hexameric DNA helicases and translocases: mechanisms and regulation.* Nature reviews. Molecular cell biology, 2008. **9**(5): p. 391-401.

30. Singleton, M.R. and D.B. Wigley, *Modularity and specialization in superfamily 1 and 2 helicases.* Journal of bacteriology, 2002. **184**(7): p. 1819-26.

31. Bernstein, D.A., M.C. Zittel, and J.L. Keck, *High-resolution structure of the E.coli RecQ helicase catalytic core.* The EMBO journal, 2003. **22**(19): p. 4910-21.

32. Pike, A.C., et al., *Structure of the human RECQ1 helicase reveals a putative strand-separation pin.* Proceedings of the National Academy of Sciences of the United States of America, 2009. **106**(4): p. 1039-44.

33. Bernstein, D.A. and J.L. Keck, *Domain mapping of Escherichia coli RecQ defines the roles of conserved N- and C-terminal regions in the RecQ family.* Nucleic acids research, 2003. **31**(11): p. 2778-85.

34. Garcia, P.L., et al., *Human RECQ5beta, a protein with DNA helicase and strand-annealing activities in a single polypeptide.* The EMBO journal, 2004. **23**(14): p. 2882-91.

35. Neff, N.F., et al., *The DNA helicase activity of BLM is necessary for the correction of the genomic instability of bloom syndrome cells.* Molecular biology of the cell, 1999. **10**(3): p. 665-76.

36. Bahr, A., et al., *Point mutations causing Bloom's syndrome abolish ATPase and DNA helicase activities of the BLM protein.* Oncogene, 1998. **17**(20): p. 2565-71.

37. Ellis, N.A., et al., *The Bloom's syndrome gene product is homologous to RecQ helicases.* Cell, 1995. **83**(4): p. 655-66.

38. Zittel, M.C. and J.L. Keck, *Coupling DNA-binding and ATP hydrolysis in Escherichia coli RecQ: role of a highly conserved aromatic-rich sequence.* Nucleic acids research, 2005. **33**(22): p. 6982-91.

39. Korolev, S., et al., *Major domain swiveling revealed by the crystal structures of complexes of E. coli Rep helicase bound to single-stranded DNA and ADP.* Cell, 1997. **90**(4): p. 635-47.

40. Sharma, S., et al., *Biochemical analysis of the DNA unwinding and strand annealing activities catalyzed by human RECQ1.* The Journal of biological chemistry, 2005. **280**(30): p. 28072-84.

41. Lu, J., et al., *Human homologues of yeast helicase.* Nature, 1996. **383**(6602): p. 678-9.

42. Bennett, R.J. and J.L. Keck, *Structure and function of RecQ DNA helicases.* Critical reviews in biochemistry and molecular biology, 2004. **39**(2): p. 79-97.

43. Marino, F., A. Vindigni, and S. Onesti, *Bioinformatic analysis of RecQ4 helicases reveals the presence of a RQC domain and a Zn knuckle.* Biophys Chem, 2013. **177-178**: p. 34-9.

44. Guo, R.B., et al., *Structural and functional characterizations reveal the importance of a zinc binding domain in Bloom's syndrome helicase.* Nucleic acids research, 2005. **33**(10): p. 3109-24.

45. Janscak, P., et al., *Characterization and mutational analysis of the RecQ core of the bloom syndrome protein.* Journal of molecular biology, 2003. **330**(1): p. 29-42.

46. Liu, J.L., et al., *The zinc finger motif of Escherichia coli RecQ is implicated in both DNA binding and protein folding.* The Journal of biological chemistry, 2004. **279**(41): p. 42794-802.

47. Berg, J.M. and Y. Shi, *The galvanization of biology: a growing appreciation for the roles of zinc.* Science, 1996. **271**(5252): p. 1081-5.

48. Onoda, F., et al., *Elevation of sister chromatid exchange in Saccharomyces cerevisiae sgs1 disruptants and the relevance of the disruptants as a system to evaluate mutations in Bloom's syndrome gene.* Mutation research, 2000. **459**(3): p. 203-9.

49. Daniels, D.S., et al., *DNA binding and nucleotide flipping by the human DNA repair protein AGT.* Nature structural & molecular biology, 2004. **11**(8): p. 714-20.

50. Gajiwala, K.S. and S.K. Burley, *Winged helix proteins.* Current opinion in structural biology, 2000. **10**(1): p. 110-6.

51. Gajiwala, K.S., et al., *Structure of the winged-helix protein hRFX1 reveals a new mode of DNA binding.* Nature, 2000. **403**(6772): p. 916-21.

52. Schultz, S.C., G.C. Shields, and T.A. Steitz, *Crystal structure of a CAP-DNA complex: the DNA is bent by 90 degrees.* Science, 1991. **253**(5023): p. 1001-7.

53. Huber, M.D., et al., *A conserved G4 DNA binding domain in RecQ family helicases.* Journal of molecular biology, 2006. **358**(4): p. 1071-80.

54.    von Kobbe, C., et al., *Werner syndrome protein contains three structure-specific DNA binding domains.* The Journal of biological chemistry, 2003. **278**(52): p. 52997-3006.

55.    Lee, J.W., et al., *Pathways and functions of the Werner syndrome protein.* Mechanisms of ageing and development, 2005. **126**(1): p. 79-86.

56.    Morozov, V., et al., *A putative nucleic acid-binding domain in Bloom's and Werner's syndrome helicases.* Trends in biochemical sciences, 1997. **22**(11): p. 417-8.

57.    Killoran, M.P. and J.L. Keck, *Three HRDC domains differentially modulate Deinococcus radiodurans RecQ DNA helicase biochemical activity.* The Journal of biological chemistry, 2006. **281**(18): p. 12849-57.

58.    Lillard-Wetherell, K., et al., *Association and regulation of the BLM helicase by the telomere proteins TRF1 and TRF2.* Human molecular genetics, 2004. **13**(17): p. 1919-32.

59.    Liu, Z., et al., *The three-dimensional structure of the HRDC domain and implications for the Werner and Bloom syndrome proteins.* Structure, 1999. **7**(12): p. 1557-66.

60.    Kitano, K., N. Yoshihara, and T. Hakoshima, *Crystal structure of the HRDC domain of human Werner syndrome protein, WRN.* The Journal of biological chemistry, 2007. **282**(4): p. 2717-28.

61.    Bernstein, D.A. and J.L. Keck, *Conferring substrate specificity to DNA helicases: role of the RecQ HRDC domain.* Structure, 2005. **13**(8): p. 1173-82.

62.    Bennett, R.J., J.A. Sharp, and J.C. Wang, *Purification and characterization of the Sgs1 DNA helicase activity of Saccharomyces cerevisiae.* The Journal of biological chemistry, 1998. **273**(16): p. 9644-50.

63.    Wu, L., et al., *The HRDC domain of BLM is required for the dissolution of double Holliday junctions.* The EMBO journal, 2005. **24**(14): p. 2679-87.

64.    Wu, L. and I.D. Hickson, *The Bloom's syndrome helicase suppresses crossing over during homologous recombination.* Nature, 2003. **426**(6968): p. 870-4.

65.    Huang, S., et al., *The premature ageing syndrome protein, WRN, is a 3'-->5' exonuclease.* Nature genetics, 1998. **20**(2): p. 114-6.

66.    Mushegian, A.R., et al., *Positionally cloned human disease genes: patterns of evolutionary conservation and functional motifs.* Proceedings of the National Academy of Sciences of the United States of America, 1997. **94**(11): p. 5831-6.

67.    Shen, J.C., et al., *Werner syndrome protein. I. DNA helicase and dna exonuclease reside on the same polypeptide.* The Journal of biological chemistry, 1998. **273**(51): p. 34139-44.

68.    Perry, J.J., et al., *WRN exonuclease structure and molecular mechanism imply an editing role in DNA end processing.* Nature structural & molecular biology, 2006. **13**(5): p. 414-22.

69.    Choudhary, S., J.A. Sommers, and R.M. Brosh, Jr., *Biochemical and kinetic characterization of the DNA helicase and exonuclease activities of werner syndrome protein.* The Journal of biological chemistry, 2004. **279**(33): p. 34603-13.

70.    Opresko, P.L., et al., *Coordinate action of the helicase and 3' to 5' exonuclease of Werner syndrome protein.* The Journal of biological chemistry, 2001. **276**(48): p. 44677-87.

71. Shimamoto, A., et al., *Human RecQ5beta, a large isomer of RecQ5 DNA helicase, localizes in the nucleoplasm and interacts with topoisomerases 3alpha and 3beta.* Nucleic acids research, 2000. **28**(7): p. 1647-55.

72. Kitao, S., et al., *Rothmund-thomson syndrome responsible gene, RECQL4: genomic structure and products.* Genomics, 1999. **61**(3): p. 268-76.

73. Siitonen, H.A., et al., *Molecular defect of RAPADILINO syndrome expands the phenotype spectrum of RECQL diseases.* Human molecular genetics, 2003. **12**(21): p. 2837-44.

74. Van Maldergem, L., et al., *Revisiting the craniosynostosis-radial ray hypoplasia association: Baller-Gerold syndrome caused by mutations in the RECQL4 gene.* Journal of medical genetics, 2006. **43**(2): p. 148-52.

75. Yu, C.E., et al., *Positional cloning of the Werner's syndrome gene.* Science, 1996. **272**(5259): p. 258-62.

76. Ellis, N.A. and J. German, *Molecular genetics of Bloom's syndrome.* Human molecular genetics, 1996. **5 Spec No**: p. 1457-63.

77. Chester, N., et al., *Stage-specific apoptosis, developmental delay, and embryonic lethality in mice homozygous for a targeted disruption in the murine Bloom's syndrome gene.* Genes & development, 1998. **12**(21): p. 3382-93.

78. Goss, K.H., et al., *Enhanced tumor formation in mice heterozygous for Blm mutation.* Science, 2002. **297**(5589): p. 2051-3.

79. Luo, G., et al., *Cancer predisposition caused by elevated mitotic recombination in Bloom mice.* Nature genetics, 2000. **26**(4): p. 424-9.

80. Frorath, B., et al., *Heterozygous carriers for Bloom syndrome exhibit a spontaneously increased micronucleus formation in cultured fibroblasts.* Human genetics, 1984. **67**(1): p. 52-5.

81. Rosin, M.P. and J. German, *Evidence for chromosome instability in vivo in Bloom syndrome: increased numbers of micronuclei in exfoliated cells.* Human genetics, 1985. **71**(3): p. 187-91.

82. Hand, R. and J. German, *A retarded rate of DNA chain growth in Bloom's syndrome.* Proceedings of the National Academy of Sciences of the United States of America, 1975. **72**(2): p. 758-62.

83. Ababou, M., et al., *Bloom's syndrome protein response to ultraviolet-C radiation and hydroxyurea-mediated DNA synthesis inhibition.* Oncogene, 2002. **21**(13): p. 2079-88.

84. Epstein, C.J., et al., *Werner's syndrome a review of its symptomatology, natural history, pathologic features, genetics and relationship to the natural aging process.* Medicine (Baltimore), 1966. **45**(3): p. 177-221.

85. Lauper, J.M., et al., *Spectrum and risk of neoplasia in Werner syndrome: a systematic review.* PLoS One, 2013. **8**(4): p. e59709.

86. Lebel, M. and P. Leder, *A deletion within the murine Werner syndrome helicase induces sensitivity to inhibitors of topoisomerase and loss of cellular proliferative capacity.* Proceedings of the National Academy of Sciences of the United States of America, 1998. **95**(22): p. 13097-102.

87. Lebel, M., R.D. Cardiff, and P. Leder, *Tumorigenic effect of nonfunctional p53 or p21 in mice mutant in the Werner syndrome helicase.* Cancer research, 2001. **61**(5): p. 1816-9.

88. Lombard, D.B., et al., *Mutations in the WRN gene in mice accelerate mortality in a p53-null background.* Molecular and cellular biology, 2000. **20**(9): p. 3286-91.

89.    Salk, D., et al., *Systematic growth studies, cocultivation, and cell hybridization studies of Werner syndrome cultured skin fibroblasts.* Human genetics, 1981. **58**(3): p. 310-6.

90.    Choi, D., et al., *Telomerase expression prevents replicative senescence but does not fully reset mRNA expression patterns in Werner syndrome cell strains.* FASEB journal : official publication of the Federation of American Societies for Experimental Biology, 2001. **15**(6): p. 1014-20.

91.    Balraj, P., et al., *An unusual mutation in RECQ4 gene leading to Rothmund-Thomson syndrome.* Mutation research, 2002. **508**(1-2): p. 99-105.

92.    Kitao, S., et al., *Mutations in RECQL4 cause a subset of cases of Rothmund-Thomson syndrome.* Nature genetics, 1999. **22**(1): p. 82-4.

93.    Lindor, N.M., et al., *Rothmund-Thomson syndrome due to RECQ4 helicase mutations: report and clinical and molecular comparisons with Bloom syndrome and Werner syndrome.* American journal of medical genetics, 2000. **90**(3): p. 223-8.

94.    Lype, M., et al., *Baller-Gerold syndrome: Further evidence for association with prenatal exposure to valproate.* Annals of Indian Academy of Neurology, 2008. **11**(1): p. 52-5.

95.    Ichikawa, K., T. Noda, and Y. Furuichi, *[Preparation of the gene targeted knockout mice for human premature aging diseases, Werner syndrome, and Rothmund-Thomson syndrome caused by the mutation of DNA helicases].* Nihon yakurigaku zasshi. Folia pharmacologica Japonica, 2002. **119**(4): p. 219-26.

96.    Hoki, Y., et al., *Growth retardation and skin abnormalities of the Recql4-deficient mouse.* Human molecular genetics, 2003. **12**(18): p. 2293-9.

97.    Mann, M.B., et al., *Defective sister-chromatid cohesion, aneuploidy and cancer predisposition in a mouse model of type II Rothmund-Thomson syndrome.* Human molecular genetics, 2005. **14**(6): p. 813-25.

98.    Sangrithi, M.N., et al., *Initiation of DNA replication requires the RECQL4 protein mutated in Rothmund-Thomson syndrome.* Cell, 2005. **121**(6): p. 887-98.

99.    Sharma, S., K.M. Doherty, and R.M. Brosh, Jr., *Mechanisms of RecQ helicases in pathways of DNA metabolism and maintenance of genomic stability.* The Biochemical journal, 2006. **398**(3): p. 319-37.

100.   Machwe, A., et al., *RecQ family members combine strand pairing and unwinding activities to catalyze strand exchange.* The Journal of biological chemistry, 2005. **280**(24): p. 23397-407.

101.   Cheok, C.F., et al., *The Bloom's syndrome helicase promotes the annealing of complementary single-stranded DNA.* Nucleic acids research, 2005. **33**(12): p. 3932-41.

102.   Macris, M.A., et al., *Biochemical characterization of the RECQ4 protein, mutated in Rothmund-Thomson syndrome.* DNA repair, 2006. **5**(2): p. 172-80.

103.   Sugiyama, T., J.H. New, and S.C. Kowalczykowski, *DNA annealing by RAD52 protein is stimulated by specific interaction with the complex of replication protein A and single-stranded DNA.* Proceedings of the National Academy of Sciences of the United States of America, 1998. **95**(11): p. 6049-54.

104. Lucic, B., et al., *A prominent beta-hairpin structure in the winged-helix domain of RECQ1 is required for DNA unwinding and oligomer formation.* Nucleic acids research, 2011. **39**(5): p. 1703-17.

105. Muzzolini, L., et al., *Different quaternary structures of human RECQ1 are associated with its dual enzymatic activity.* PLoS biology, 2007. **5**(2): p. e20.

106. Compton, S.A., et al., *The Werner syndrome protein binds replication fork and holliday junction DNAs as an oligomer.* The Journal of biological chemistry, 2008. **283**(36): p. 24478-83.

107. Muftuoglu, M., et al., *Acetylation regulates WRN catalytic activities and affects base excision DNA repair.* PloS one, 2008. **3**(4): p. e1918.

108. Ciccia, A. and S.J. Elledge, *The DNA damage response: making it safe to play with knives.* Molecular cell, 2010. **40**(2): p. 179-204.

109. Ward, I., et al., *The tandem BRCT domain of 53BP1 is not required for its repair function.* The Journal of biological chemistry, 2006. **281**(50): p. 38472-7.

110. Wang, M., et al., *PARP-1 and Ku compete for repair of DNA double strand breaks by distinct NHEJ pathways.* Nucleic acids research, 2006. **34**(21): p. 6170-82.

111. Lieber, M.R., *The mechanism of human nonhomologous DNA end joining.* The Journal of biological chemistry, 2008. **283**(1): p. 1-5.

112. Nimonkar, A.V., et al., *BLM-DNA2-RPA-MRN and EXO1-BLM-RPA-MRN constitute two DNA end resection machineries for human DNA break repair.* Genes Dev, 2011. **25**(4): p. 350-62.

113. San Filippo, J., P. Sung, and H. Klein, *Mechanism of eukaryotic homologous recombination.* Annual review of biochemistry, 2008. **77**: p. 229-57.

114. Nimonkar, A.V., R.A. Sica, and S.C. Kowalczykowski, *Rad52 promotes second-end DNA capture in double-stranded break repair to form complement-stabilized joint molecules.* Proceedings of the National Academy of Sciences of the United States of America, 2009. **106**(9): p. 3077-82.

115. Dobzhansky, T., *Genetics of Natural Populations. Xiii. Recombination and Variability in Populations of Drosophila Pseudoobscura.* Genetics, 1946. **31**(3): p. 269-90.

116. Lucchesi, J.C., *Synthetic lethality and semi-lethality among functionally related mutants of Drosophila melanfgaster.* Genetics, 1968. **59**(1): p. 37-44.

117. Stenner-Liewen, F., et al., *Definition of tumor-associated antigens in hepatocellular carcinoma.* Cancer Epidemiol Biomarkers Prev, 2000. **9**(3): p. 285-90.

118. Chu, W.K. and I.D. Hickson, *RecQ helicases: multifunctional genome caretakers.* Nat Rev Cancer, 2009. **9**(9): p. 644-54.

119. Branzei, D. and M. Foiani, *RecQ helicases queuing with Srs2 to disrupt Rad51 filaments and suppress recombination.* Genes Dev, 2007. **21**(23): p. 3019-26.

120. Raynard, S., W. Bussen, and P. Sung, *A double Holliday junction dissolvasome comprising BLM, topoisomerase IIIalpha, and BLAP75.* J Biol Chem, 2006. **281**(20): p. 13861-4.

121. Wu, L., et al., *BLAP75/RMI1 promotes the BLM-dependent dissolution of homologous recombination intermediates.* Proc Natl Acad Sci U S A, 2006. **103**(11): p. 4068-73.

122. Raynard, S., et al., *Functional role of BLAP75 in BLM-topoisomerase IIIalpha-dependent holliday junction processing.* J Biol Chem, 2008. **283**(23): p. 15701-8.

123. Chan, K.L., P.S. North, and I.D. Hickson, *BLM is required for faithful chromosome segregation and its localization defines a class of ultrafine anaphase bridges.* EMBO J, 2007. **26**(14): p. 3397-409.

124. Rao, V.A., et al., *Endogenous gamma-H2AX-ATM-Chk2 checkpoint activation in Bloom's syndrome helicase deficient cells is related to DNA replication arrested forks.* Molecular cancer research : MCR, 2007. **5**(7): p. 713-24.

125. Chabosseau, P., et al., *Pyrimidine pool imbalance induced by BLM helicase deficiency contributes to genetic instability in Bloom syndrome.* Nat Commun, 2011. **2**: p. 368.

126. Bhattacharyya, S., et al., *Telomerase-associated protein 1, HSP90, and topoisomerase IIalpha associate directly with the BLM helicase in immortalized cells using ALT and modulate its helicase activity using telomeric DNA substrates.* J Biol Chem, 2009. **284**(22): p. 14966-77.

127. Wyllie, F.S., et al., *Telomerase prevents the accelerated cell ageing of Werner syndrome fibroblasts.* Nat Genet, 2000. **24**(1): p. 16-7.

128. Opresko, P.L., et al., *Werner syndrome and the function of the Werner protein; what they can teach us about the molecular aging process.* Carcinogenesis, 2003. **24**(5): p. 791-802.

129. Crabbe, L., et al., *Defective telomere lagging strand synthesis in cells lacking WRN helicase activity.* Science, 2004. **306**(5703): p. 1951-3.

130. Arnoult, N., et al., *Human POT1 is required for efficient telomere C-rich strand replication in the absence of WRN.* Genes Dev, 2009. **23**(24): p. 2915-24.

131. Chang, S., et al., *Essential role of limiting telomeres in the pathogenesis of Werner syndrome.* Nat Genet, 2004. **36**(8): p. 877-82.

132. Crabbe, L., et al., *Telomere dysfunction as a cause of genomic instability in Werner syndrome.* Proc Natl Acad Sci U S A, 2007. **104**(7): p. 2205-10.

133. Dhillon, K.K., et al., *Functional role of the Werner syndrome RecQ helicase in human fibroblasts.* Aging Cell, 2007. **6**(1): p. 53-61.

134. Von Kobbe, C., et al., *Werner syndrome cells escape hydrogen peroxide-induced cell proliferation arrest.* FASEB J, 2004. **18**(15): p. 1970-2.

135. Szekely, A.M., et al., *Werner protein protects nonproliferating cells from oxidative DNA damage.* Mol Cell Biol, 2005. **25**(23): p. 10492-506.

136. Harrigan, J.A., et al., *The Werner syndrome protein operates in base excision repair and cooperates with DNA polymerase beta.* Nucleic Acids Res, 2006. **34**(2): p. 745-54.

137. Poot, M., K.A. Gollahon, and P.S. Rabinovitch, *Werner syndrome lymphoblastoid cells are sensitive to camptothecin-induced apoptosis in S-phase.* Hum Genet, 1999. **104**(1): p. 10-4.

138. Sallmyr, A., A.E. Tomkinson, and F.V. Rassool, *Up-regulation of WRN and DNA ligase IIIalpha in chronic myeloid leukemia: consequences for the repair of DNA double-strand breaks.* Blood, 2008. **112**(4): p. 1413-23.

139. Hu, Y., et al., *RECQL5/Recql5 helicase regulates homologous recombination and suppresses tumor formation via disruption of Rad51 presynaptic filaments.* Genes Dev, 2007. **21**(23): p. 3073-84.

140.  Aygun, O., et al., *Direct inhibition of RNA polymerase II transcription by RECQL5.* J Biol Chem, 2009. **284**(35): p. 23197-203.

141.  Aygun, O., J. Svejstrup, and Y. Liu, *A RECQ5-RNA polymerase II association identified by targeted proteomic analysis of human chromatin.* Proc Natl Acad Sci U S A, 2008. **105**(25): p. 8580-4.

142.  Islam, M.N., et al., *RecQL5 promotes genome stabilization through two parallel mechanisms--interacting with RNA polymerase II and acting as a helicase.* Mol Cell Biol, 2010. **30**(10): p. 2460-72.

143.  Zheng, L., et al., *MRE11 complex links RECQ5 helicase to sites of DNA damage.* Nucleic Acids Res, 2009. **37**(8): p. 2645-57.

144.  Schwendener, S., et al., *Physical interaction of RECQ5 helicase with RAD51 facilitates its anti-recombinase activity.* J Biol Chem, 2010. **285**(21): p. 15739-45.

145.  Petkovic, M., et al., *The human Rothmund-Thomson syndrome gene product, RECQL4, localizes to distinct nuclear foci that coincide with proteins involved in the maintenance of genome stability.* J Cell Sci, 2005. **118**(Pt 18): p. 4261-9.

146.  Jin, W., et al., *Sensitivity of RECQL4-deficient fibroblasts from Rothmund-Thomson syndrome patients to genotoxic agents.* Hum Genet, 2008. **123**(6): p. 643-53.

147.  Kumata, Y., et al., *Possible involvement of RecQL4 in the repair of double-strand DNA breaks in Xenopus egg extracts.* Biochim Biophys Acta, 2007. **1773**(4): p. 556-64.

148.  Park, S.J., et al., *A positive involvement of RecQL4 in UV-induced S-phase arrest.* DNA and cell biology, 2006. **25**(12): p. 696-703.

149.  Schurman, S.H., et al., *Direct and indirect roles of RECQL4 in modulating base excision repair capacity.* Hum Mol Genet, 2009. **18**(18): p. 3470-83.

150.  Woo, L.L., et al., *The Rothmund-Thomson gene product RECQL4 localizes to the nucleolus in response to oxidative stress.* Exp Cell Res, 2006. **312**(17): p. 3443-57.

151.  Fan, W. and J. Luo, *RecQ4 facilitates UV light-induced DNA damage repair through interaction with nucleotide excision repair factor xeroderma pigmentosum group A (XPA).* J Biol Chem, 2008. **283**(43): p. 29037-44.

152.  Ghosh, A.K., et al., *RECQL4, the protein mutated in Rothmund-Thomson syndrome, functions in telomere maintenance.* The Journal of biological chemistry, 2012. **287**(1): p. 196-209.

153.  Ferrarelli, L.K., et al., *The RECQL4 protein, deficient in Rothmund-Thomson syndrome is active on telomeric D-loops containing DNA metabolism blocking lesions.* DNA Repair (Amst), 2013.

154.  Sharma, S. and R.M. Brosh, Jr., *Human RECQ1 is a DNA damage responsive protein required for genotoxic stress resistance and suppression of sister chromatid exchanges.* PLoS One, 2007. **2**(12): p. e1297.

155.  Doherty, K.M., et al., *RECQ1 helicase interacts with human mismatch repair factors that regulate genetic recombination.* J Biol Chem, 2005. **280**(30): p. 28085-94.

156.  Evrin, C., et al., *A double-hexameric MCM2-7 complex is loaded onto origin DNA during licensing of eukaryotic DNA replication.* Proceedings of the National Academy of Sciences of the United States of America, 2009. **106**(48): p. 20240-5.

157. Brown, T.A., *Genomes*. 2nd ed. 2002, Oxford New York: Wiley-Liss. xxvii, 572 p.

158. Sclafani, R.A. and T.M. Holzen, *Cell cycle regulation of DNA replication.* Annual review of genetics, 2007. **41**: p. 237-80.

159. Branzei, D. and M. Foiani, *Maintaining genome stability at the replication fork.* Nat Rev Mol Cell Biol, 2010. **11**(3): p. 208-19.

160. Errico, A. and V. Costanzo, *Mechanisms of replication fork protection: a safeguard for genome stability.* Crit Rev Biochem Mol Biol, 2012. **47**(3): p. 222-35.

161. Burma, S., et al., *ATM phosphorylates histone H2AX in response to DNA double-strand breaks.* J Biol Chem, 2001. **276**(45): p. 42462-7.

162. Stracker, T.H. and J.H. Petrini, *The MRE11 complex: starting from the ends.* Nat Rev Mol Cell Biol, 2011. **12**(2): p. 90-103.

163. Difilippantonio, S., et al., *Distinct domains in Nbs1 regulate irradiation-induced checkpoints and apoptosis.* J Exp Med, 2007. **204**(5): p. 1003-11.

164. Difilippantonio, S. and A. Nussenzweig, *The NBS1-ATM connection revisited.* Cell Cycle, 2007. **6**(19): p. 2366-70.

165. Falck, J., J. Coates, and S.P. Jackson, *Conserved modes of recruitment of ATM, ATR and DNA-PKcs to sites of DNA damage.* Nature, 2005. **434**(7033): p. 605-11.

166. Lee, J.H. and T.T. Paull, *ATM activation by DNA double-strand breaks through the Mre11-Rad50-Nbs1 complex.* Science, 2005. **308**(5721): p. 551-4.

167. Stracker, T.H., et al., *The carboxy terminus of NBS1 is required for induction of apoptosis by the MRE11 complex.* Nature, 2007. **447**(7141): p. 218-21.

168. Smith, J., et al., *The ATM-Chk2 and ATR-Chk1 pathways in DNA damage signaling and cancer.* Adv Cancer Res, 2010. **108**: p. 73-112.

169. Di Virgilio, M., C.Y. Ying, and J. Gautier, *PIKK-dependent phosphorylation of Mre11 induces MRN complex inactivation by disassembly from chromatin.* DNA Repair (Amst), 2009. **8**(11): p. 1311-20.

170. Gatei, M., et al., *ATM protein-dependent phosphorylation of Rad50 protein regulates DNA repair and cell cycle control.* J Biol Chem, 2011. **286**(36): p. 31542-56.

171. Gatei, M., et al., *ATM-dependent phosphorylation of nibrin in response to radiation exposure.* Nat Genet, 2000. **25**(1): p. 115-9.

172. Lim, D.S., et al., *ATM phosphorylates p95/nbs1 in an S-phase checkpoint pathway.* Nature, 2000. **404**(6778): p. 613-7.

173. Zhao, S., et al., *Functional link between ataxia-telangiectasia and Nijmegen breakage syndrome gene products.* Nature, 2000. **405**(6785): p. 473-7.

174. Cobb, J.A., et al., *DNA polymerase stabilization at stalled replication forks requires Mec1 and the RecQ helicase Sgs1.* The EMBO journal, 2003. **22**(16): p. 4325-36.

175. Lucca, C., et al., *Checkpoint-mediated control of replisome-fork association and signalling in response to replication pausing.* Oncogene, 2004. **23**(6): p. 1206-13.

176. Lopes, M., et al., *The DNA replication checkpoint response stabilizes stalled replication forks.* Nature, 2001. **412**(6846): p. 557-61.

177. Sogo, J.M., M. Lopes, and M. Foiani, *Fork reversal and ssDNA accumulation at stalled replication forks owing to checkpoint defects.* Science, 2002. **297**(5581): p. 599-602.

178. Zou, L. and S.J. Elledge, *Sensing DNA damage through ATRIP recognition of RPA-ssDNA complexes.* Science, 2003. **300**(5625): p. 1542-8.

179. Lopez-Contreras, A.J. and O. Fernandez-Capetillo, *The ATR barrier to replication-born DNA damage.* DNA Repair (Amst), 2010. **9**(12): p. 1249-55.

180. Bartek, J. and J. Lukas, *DNA damage checkpoints: from initiation to recovery or adaptation.* Current opinion in cell biology, 2007. **19**(2): p. 238-45.

181. Branzei, D. and M. Foiani, *Regulation of DNA repair throughout the cell cycle.* Nature reviews. Molecular cell biology, 2008. **9**(4): p. 297-308.

182. Shiloh, Y., *The ATM-mediated DNA-damage response: taking shape.* Trends Biochem Sci, 2006. **31**(7): p. 402-10.

183. Davies, S.L., et al., *Phosphorylation of the Bloom's syndrome helicase and its role in recovery from S-phase arrest.* Molecular and cellular biology, 2004. **24**(3): p. 1279-91.

184. Pichierri, P., F. Rosselli, and A. Franchitto, *Werner's syndrome protein is phosphorylated in an ATR/ATM-dependent manner following replication arrest and DNA damage induced during the S phase of the cell cycle.* Oncogene, 2003. **22**(10): p. 1491-500.

185. Pirzio, L.M., et al., *Werner syndrome helicase activity is essential in maintaining fragile site stability.* J Cell Biol, 2008. **180**(2): p. 305-14.

186. Ammazzalorso, F., et al., *ATR and ATM differently regulate WRN to prevent DSBs at stalled replication forks and promote replication fork recovery.* EMBO J, 2010. **29**(18): p. 3156-69.

187. Masumoto, H., et al., *S-Cdk-dependent phosphorylation of Sld2 essential for chromosomal DNA replication in budding yeast.* Nature, 2002. **415**(6872): p. 651-5.

188. Xu, X. and Y. Liu, *Dual DNA unwinding activities of the Rothmund-Thomson syndrome protein, RECQ4.* The EMBO journal, 2009. **28**(5): p. 568-77.

189. Matsuno, K., et al., *The N-terminal noncatalytic region of Xenopus RecQ4 is required for chromatin binding of DNA polymerase alpha in the initiation of DNA replication.* Mol Cell Biol, 2006. **26**(13): p. 4843-52.

190. Rossi, M.L., et al., *Conserved helicase domain of human RecQ4 is required for strand annealing-independent DNA unwinding.* DNA Repair (Amst), 2010. **9**(7): p. 796-804.

191. Thangavel, S., et al., *Human RECQ1 and RECQ4 helicases play distinct roles in DNA replication initiation.* Molecular and cellular biology, 2010. **30**(6): p. 1382-96.

192. Xu, X., et al., *MCM10 mediates RECQ4 association with MCM2-7 helicase complex during DNA replication.* EMBO J, 2009. **28**(19): p. 3005-14.

193. Im, J.S., et al., *Assembly of the Cdc45-Mcm2-7-GINS complex in human cells requires the Ctf4/And-1, RecQL4, and Mcm10 proteins.* Proc Natl Acad Sci U S A, 2009. **106**(37): p. 15628-32.

194. Kohzaki, M., et al., *The helicase domain and C-terminus of human RecQL4 facilitate replication elongation on DNA templates damaged by ionizing radiation.* Carcinogenesis, 2012. **33**(6): p. 1203-10.

195. Ge, X.Q., D.A. Jackson, and J.J. Blow, *Dormant origins licensed by excess Mcm2-7 are required for human cells to survive replicative stress.* Genes Dev, 2007. **21**(24): p. 3331-41.

196. Davies, S.L., P.S. North, and I.D. Hickson, *Role for BLM in replication-fork restart and suppression of origin firing after replicative stress.* Nature structural & molecular biology, 2007. **14**(7): p. 677-9.

197. Wang, Y., et al., *Kaposi's sarcoma-associated herpesvirus ori-Lyt-dependent DNA replication: involvement of host cellular factors.* J Virol, 2008. **82**(6): p. 2867-82.

198. Wang, P., et al., *Topoisomerase I and RecQL1 function in Epstein-Barr virus lytic reactivation.* J Virol, 2009. **83**(16): p. 8090-8.

199. Berti, M., et al., *Human RECQ1 promotes restart of replication forks reversed by DNA topoisomerase I inhibition.* Nat Struct Mol Biol, 2013. **20**(3): p. 347-54.

200. Sidorova, J.M., et al., *Distinct functions of human RECQ helicases WRN and BLM in replication fork recovery and progression after hydroxyurea-induced stalling.* DNA Repair (Amst), 2013. **12**(2): p. 128-39.

201. Sidorova, J.M., et al., *The RecQ helicase WRN is required for normal replication fork progression after DNA damage or replication fork arrest.* Cell cycle, 2008. **7**(6): p. 796-807.

202. Lonn, U., et al., *An abnormal profile of DNA replication intermediates in Bloom's syndrome.* Cancer Res, 1990. **50**(11): p. 3141-5.

203. Rao, V.A., et al., *Phosphorylation of BLM, dissociation from topoisomerase IIIalpha, and colocalization with gamma-H2AX after topoisomerase I-induced replication damage.* Mol Cell Biol, 2005. **25**(20): p. 8925-37.

204. Pichierri, P., et al., *Werner's syndrome protein is required for correct recovery after replication arrest and DNA damage induced in S-phase of cell cycle.* Molecular biology of the cell, 2001. **12**(8): p. 2412-21.

205. Hu, Y., et al., *Recql5 plays an important role in DNA replication and cell survival after camptothecin treatment.* Mol Biol Cell, 2009. **20**(1): p. 114-23.

206. Popuri, V., et al., *RECQ1 is required for cellular resistance to replication stress and catalyzes strand exchange on stalled replication fork structures.* Cell Cycle, 2012. **11**(22): p. 4252-65.

207. Davalos, A.R., et al., *ATR and ATM-dependent movement of BLM helicase during replication stress ensures optimal ATM activation and 53BP1 focus formation.* Cell Cycle, 2004. **3**(12): p. 1579-86.

208. Sengupta, S., et al., *BLM helicase-dependent transport of p53 to sites of stalled DNA replication forks modulates homologous recombination.* EMBO J, 2003. **22**(5): p. 1210-22.

209. Chaudhury, I., et al., *FANCD2 regulates BLM complex functions independently of FANCI to promote replication fork recovery.* Nucleic Acids Res, 2013.

210. Pichierri, P., et al., *Werner's syndrome protein is required for correct recovery after replication arrest and DNA damage induced in S-phase of cell cycle.* Mol Biol Cell, 2001. **12**(8): p. 2412-21.

211. Poot, M., et al., *Werner syndrome diploid fibroblasts are sensitive to 4-nitroquinoline-N-oxide and 8-methoxypsoralen: implications for the disease phenotype.* FASEB J, 2002. **16**(7): p. 757-8.

212. Prince, P.R., et al., *Cell fusion corrects the 4-nitroquinoline 1-oxide sensitivity of Werner syndrome fibroblast cell lines.* Hum Genet, 1999. **105**(1-2): p. 132-8.

213. Saintigny, Y., et al., *Homologous recombination resolution defect in werner syndrome.* Mol Cell Biol, 2002. **22**(20): p. 6971-8.

214. Yannone, S.M., et al., *Werner syndrome protein is regulated and phosphorylated by DNA-dependent protein kinase.* J Biol Chem, 2001. **276**(41): p. 38242-8.

215. Robinson, K., et al., *c-Myc accelerates S-phase and requires WRN to avoid replication stress.* PLoS One, 2009. **4**(6): p. e5951.

216. Chakraverty, R.K. and I.D. Hickson, *Defending genome integrity during DNA replication: a proposed role for RecQ family helicases.* Bioessays, 1999. **21**(4): p. 286-94.

217. Huang, P., et al., *SGS1 is required for telomere elongation in the absence of telomerase.* Curr Biol, 2001. **11**(2): p. 125-9.

218. Cohen, H. and D.A. Sinclair, *Recombination-mediated lengthening of terminal telomeric repeats requires the Sgs1 DNA helicase.* Proc Natl Acad Sci U S A, 2001. **98**(6): p. 3174-9.

219. Johnson, F.B., et al., *The Saccharomyces cerevisiae WRN homolog Sgs1p participates in telomere maintenance in cells lacking telomerase.* EMBO J, 2001. **20**(4): p. 905-13.

220. Michel, B., et al., *Recombination proteins and rescue of arrested replication forks.* DNA repair, 2007. **6**(7): p. 967-80.

221. Wu, L. and I.D. Hickson, *DNA helicases required for homologous recombination and repair of damaged replication forks.* Annual review of genetics, 2006. **40**: p. 279-306.

222. Pages, V. and R.P. Fuchs, *Uncoupling of leading- and lagging-strand DNA replication during lesion bypass in vivo.* Science, 2003. **300**(5623): p. 1300-3.

223. Mazloum, N. and W.K. Holloman, *Brh2 promotes a template-switching reaction enabling recombinational bypass of lesions during DNA synthesis.* Molecular cell, 2009. **36**(4): p. 620-30.

224. Higgins, N.P., K. Kato, and B. Strauss, *A model for replication repair in mammalian cells.* Journal of molecular biology, 1976. **101**(3): p. 417-25.

225. Constantinou, A., et al., *Werner's syndrome protein (WRN) migrates Holliday junctions and co-localizes with RPA upon replication arrest.* EMBO reports, 2000. **1**(1): p. 80-4.

226. Karow, J.K., et al., *The Bloom's syndrome gene product promotes branch migration of holliday junctions.* Proceedings of the National Academy of Sciences of the United States of America, 2000. **97**(12): p. 6504-8.

227. Mohaghegh, P., et al., *The Bloom's and Werner's syndrome proteins are DNA structure-specific helicases.* Nucleic acids research, 2001. **29**(13): p. 2843-9.

228. Sharma, S., et al., *WRN helicase and FEN-1 form a complex upon replication arrest and together process branchmigrating DNA structures associated with the replication fork.* Molecular biology of the cell, 2004. **15**(2): p. 734-50.

229. Ralf, C., I.D. Hickson, and L. Wu, *The Bloom's syndrome helicase can promote the regression of a model replication fork.* J Biol Chem, 2006. **281**(32): p. 22839-46.

230. Machwe, A., et al., *The Werner and Bloom syndrome proteins catalyze regression of a model replication fork.* Biochemistry, 2006. **45**(47): p. 13939-46.

231. Popuri, V., et al., *The Human RecQ helicases, BLM and RECQ1, display distinct DNA substrate specificities.* J Biol Chem, 2008. **283**(26): p. 17766-76.

232. Karow, J.K., et al., *The Bloom's syndrome gene product promotes branch migration of holliday junctions.* Proc Natl Acad Sci U S A, 2000. **97**(12): p. 6504-8.

233. Boddy, M.N., et al., *Mus81-Eme1 are essential components of a Holliday junction resolvase.* Cell, 2001. **107**(4): p. 537-48.

234. Ip, S.C., et al., *Identification of Holliday junction resolvases from humans and yeast.* Nature, 2008. **456**(7220): p. 357-61.

235. Heller, R.C. and K.J. Marians, *Replisome assembly and the direct restart of stalled replication forks.* Nat Rev Mol Cell Biol, 2006. **7**(12): p. 932-43.

236. Wu, L., *Role of the BLM helicase in replication fork management.* DNA Repair (Amst), 2007. **6**(7): p. 936-44.

237. Wang, J.C., *Cellular roles of DNA topoisomerases: a molecular perspective.* Nature reviews. Molecular cell biology, 2002. **3**(6): p. 430-40.

238. Stewart, L., et al., *A model for the mechanism of human topoisomerase I.* Science, 1998. **279**(5356): p. 1534-41.

239. Koster, D.A., et al., *Friction and torque govern the relaxation of DNA supercoils by eukaryotic topoisomerase IB.* Nature, 2005. **434**(7033): p. 671-4.

240. Pommier, Y., *Topoisomerase I inhibitors: camptothecins and beyond.* Nature reviews. Cancer, 2006. **6**(10): p. 789-802.

241. Pommier, Y., et al., *DNA topoisomerases and their poisoning by anticancer and antibacterial drugs.* Chem Biol, 2010. **17**(5): p. 421-33.

242. Strumberg, D., et al., *Conversion of topoisomerase I cleavage complexes on the leading strand of ribosomal DNA into 5'-phosphorylated DNA double-strand breaks by replication runoff.* Molecular and cellular biology, 2000. **20**(11): p. 3977-87.

243. Koster, D.A., et al., *Antitumour drugs impede DNA uncoiling by topoisomerase I.* Nature, 2007. **448**(7150): p. 213-7.

244. Koster, D.A., et al., *Cellular strategies for regulating DNA supercoiling: a single-molecule perspective.* Cell, 2010. **142**(4): p. 519-30.

245. Ray Chaudhuri, A., et al., *Topoisomerase I poisoning results in PARP-mediated replication fork reversal.* Nature structural & molecular biology, 2012. **19**(4): p. 417-23.

246. Curtin, N.J., *PARP inhibitors for cancer therapy.* Expert Rev Mol Med, 2005. **7**(4): p. 1-20.

247. Kummar, S., et al., *Phase I study of PARP inhibitor ABT-888 in combination with topotecan in adults with refractory solid tumors and lymphomas.* Cancer Res, 2011. **71**(17): p. 5626-34.

248. Cui, S., et al., *Characterization of the DNA-unwinding activity of human RECQ1, a helicase specifically stimulated by human replication protein A.* The Journal of biological chemistry, 2003. **278**(3): p. 1424-32.

249. Sambrook, J. and D.W. Russell, *Isolation of DNA fragments from polyacrylamide gels by the crush and soak method.* CSH Protoc, 2006. **2006**(1).

250. Bugreev, D.V., M.J. Rossi, and A.V. Mazin, *Cooperation of RAD51 and RAD54 in regression of a model replication fork.* Nucleic acids research, 2011. **39**(6): p. 2153-64.

251. Karras, G.I., et al., *The macro domain is an ADP-ribose binding module.* EMBO J, 2005. **24**(11): p. 1911-20.

252. Cui, S., et al., *Analysis of the unwinding activity of the dimeric RECQ1 helicase in the presence of human replication protein A.* Nucleic acids research, 2004. **32**(7): p. 2158-70.

253. Pawelczak, K.S. and J.J. Turchi, *Purification and characterization of exonuclease-free Artemis: Implications for DNA-PK-dependent processing of DNA termini in NHEJ-catalyzed DSB repair.* DNA repair, 2010. **9**(6): p. 670-7.

254. Ying, S., F.C. Hamdy, and T. Helleday, *Mre11-dependent degradation of stalled DNA replication forks is prevented by BRCA2 and PARP1.* Cancer research, 2012. **72**(11): p. 2814-21.

255. Ferro, A.M. and B.M. Olivera, *Poly(ADP-ribosylation) in vitro. Reaction parameters and enzyme mechanism.* J Biol Chem, 1982. **257**(13): p. 7808-13.

256. Machwe, A., et al., *The Werner and Bloom syndrome proteins help resolve replication blockage by converting (regressed) holliday junctions to functional replication forks.* Biochemistry, 2011. **50**(32): p. 6774-88.

257. von Kobbe, C., et al., *Poly(ADP-ribose) polymerase 1 regulates both the exonuclease and helicase activities of the Werner syndrome protein.* Nucleic Acids Res, 2004. **32**(13): p. 4003-14.

258. Bugreev, D.V., O.M. Mazina, and A.V. Mazin, *Rad54 protein promotes branch migration of Holliday junctions.* Nature, 2006. **442**(7102): p. 590-3.

259. Gari, K., et al., *Remodeling of DNA replication structures by the branch point translocase FANCM.* Proc Natl Acad Sci U S A, 2008. **105**(42): p. 16107-12.

260. Mazina, O.M., et al., *Polarity and bypass of DNA heterology during branch migration of Holliday junctions by human RAD54, BLM, and RECQ1 proteins.* J Biol Chem, 2012. **287**(15): p. 11820-32.

261. Crucifix, C., M. Uhring, and P. Schultz, *Immobilization of biotinylated DNA on 2-D streptavidin crystals.* J Struct Biol, 2004. **146**(3): p. 441-51.

262. Rose, A. and I. Meier, *Scaffolds, levers, rods and springs: diverse cellular functions of long coiled-coil proteins.* Cell Mol Life Sci, 2004. **61**(16): p. 1996-2009.

263. Perry, J.J., et al., *Identification of a coiled coil in werner syndrome protein that facilitates multimerization and promotes exonuclease processivity.* J Biol Chem, 2010. **285**(33): p. 25699-707.

264. Woolfson, D.N., *The design of coiled-coil structures and assemblies.* Adv Protein Chem, 2005. **70**: p. 79-112.

265. Petermann, E. and T. Helleday, *Pathways of mammalian replication fork restart.* Nature reviews. Molecular cell biology, 2010. **11**(10): p. 683-7.

266. Courcelle, J. and P.C. Hanawalt, *RecQ and RecJ process blocked replication forks prior to the resumption of replication in UV-irradiated Escherichia coli.* Mol Gen Genet, 1999. **262**(3): p. 543-51.

267. Hanada, K., et al., *RecQ DNA helicase is a suppressor of illegitimate recombination in Escherichia coli.* Proc Natl Acad Sci U S A, 1997. **94**(8): p. 3860-5.

268. Karow, J.K., L. Wu, and I.D. Hickson, *RecQ family helicases: roles in cancer and aging.* Curr Opin Genet Dev, 2000. **10**(1): p. 32-8.

269. Hishida, T., et al., *Role of the Escherichia coli RecQ DNA helicase in SOS signaling and genome stabilization at stalled replication forks.* Genes Dev, 2004. **18**(15): p. 1886-97.

270. Cejka, P., et al., *DNA end resection by Dna2-Sgs1-RPA and its stimulation by Top3-Rmi1 and Mre11-Rad50-Xrs2.* Nature, 2010. **467**(7311): p. 112-6.

271. Zhu, Z., et al., *Sgs1 helicase and two nucleases Dna2 and Exo1 resect DNA double-strand break ends.* Cell, 2008. **134**(6): p. 981-94.

272. Davies, S.L., P.S. North, and I.D. Hickson, *Role for BLM in replication-fork restart and suppression of origin firing after replicative stress.* Nat Struct Mol Biol, 2007. **14**(7): p. 677-9.

273. Suski, C. and K.J. Marians, *Resolution of converging replication forks by RecQ and topoisomerase III.* Mol Cell, 2008. **30**(6): p. 779-89.

274. Plank, J.L., J. Wu, and T.S. Hsieh, *Topoisomerase IIIalpha and Bloom's helicase can resolve a mobile double Holliday junction substrate through convergent branch migration.* Proc Natl Acad Sci U S A, 2006. **103**(30): p. 11118-23.

275. Yang, J., et al., *BLM and RMI1 alleviate RPA inhibition of TopoIIIalpha decatenase activity.* PLoS One, 2012. **7**(7): p. e41208.

276. Cheng, R.Z., et al., *Homologous recombination is elevated in some Werner-like syndromes but not during normal in vitro or in vivo senescence of mammalian cells.* Mutat Res, 1990. **237**(5-6): p. 259-69.

277. Fukuchi, K., G.M. Martin, and R.J. Monnat, Jr., *Mutator phenotype of Werner syndrome is characterized by extensive deletions.* Proc Natl Acad Sci U S A, 1989. **86**(15): p. 5893-7.

278. Yamagata, K., et al., *Bloom's and Werner's syndrome genes suppress hyperrecombination in yeast sgs1 mutant: implication for genomic instability in human diseases.* Proc Natl Acad Sci U S A, 1998. **95**(15): p. 8733-8.

279. Franchitto, A., et al., *Replication fork stalling in WRN-deficient cells is overcome by prompt activation of a MUS81-dependent pathway.* J Cell Biol, 2008. **183**(2): p. 241-52.

280. Pichierri, P., et al., *The RAD9-RAD1-HUS1 (9.1.1) complex interacts with WRN and is crucial to regulate its response to replication fork stalling.* Oncogene, 2012. **31**(23): p. 2809-23.

281. Michel, B., et al., *Rescue of arrested replication forks by homologous recombination.* Proc Natl Acad Sci U S A, 2001. **98**(15): p. 8181-8.

282. Seigneur, M., et al., *RuvAB acts at arrested replication forks.* Cell, 1998. **95**(3): p. 419-30.

283. Atkinson, J. and P. McGlynn, *Replication fork reversal and the maintenance of genome stability.* Nucleic Acids Res, 2009. **37**(11): p. 3475-92.

284. Hsiang, Y.H., M.G. Lihou, and L.F. Liu, *Arrest of replication forks by drug-stabilized topoisomerase I-DNA cleavable complexes as a mechanism of cell killing by camptothecin.* Cancer Res, 1989. **49**(18): p. 5077-82.

285. Regairaz, M., et al., *Mus81-mediated DNA cleavage resolves replication forks stalled by topoisomerase I-DNA complexes.* J Cell Biol, 2011. **195**(5): p. 739-49.

286. Bugreev, D.V., R.M. Brosh, Jr., and A.V. Mazin, *RECQ1 possesses DNA branch migration activity.* J Biol Chem, 2008. **283**(29): p. 20231-42.

287. Bonicalzi, M.E., et al., *Regulation of poly(ADP-ribose) metabolism by poly(ADP-ribose) glycohydrolase: where and when?* Cell Mol Life Sci, 2005. **62**(7-8): p. 739-50.

288. Mendoza-Maldonado, R., et al., *The human RECQ1 helicase is highly expressed in glioblastoma and plays an important role in tumor cell proliferation.* Mol Cancer, 2011. **10**: p. 83.

289. Arai, A., et al., *RECQL1 and WRN proteins are potential therapeutic targets in head and neck squamous cell carcinoma.* Cancer Res, 2011. **71**(13): p. 4598-607.

290. Futami, K., et al., *Induction of mitotic cell death in cancer cells by small interference RNA suppressing the expression of RecQL1 helicase.* Cancer Sci, 2008. **99**(1): p. 71-80.

291. Futami, K., et al., *Anticancer activity of RecQL1 helicase siRNA in mouse xenograft models.* Cancer Sci, 2008. **99**(6): p. 1227-36.

292. Ariyoshi, M., et al., *Crystal structure of the holliday junction DNA in complex with a single RuvA tetramer.* Proc Natl Acad Sci U S A, 2000. **97**(15): p. 8257-62.

293. Hargreaves, D., et al., *Crystal structure of E.coli RuvA with bound DNA Holliday junction at 6 A resolution.* Nat Struct Biol, 1998. **5**(6): p. 441-6.

294. Roe, S.M., et al., *Crystal structure of an octameric RuvA-Holliday junction complex.* Mol Cell, 1998. **2**(3): p. 361-72.

295. West, S.C., *Processing of recombination intermediates by the RuvABC proteins.* Annu Rev Genet, 1997. **31**: p. 213-44.

296. Hiom, K., I.R. Tsaneva, and S.C. West, *The directionality of RuvAB-mediated branch migration: in vitro studies with three-armed junctions.* Genes Cells, 1996. **1**(5): p. 443-51.

297. Yamada, K., et al., *Crystal structure of the RuvA-RuvB complex: a structural basis for the Holliday junction migrating motor machinery.* Mol Cell, 2002. **10**(3): p. 671-81.

298. Karymov, M., et al., *Holliday junction dynamics and branch migration: single-molecule analysis.* Proc Natl Acad Sci U S A, 2005. **102**(23): p. 8186-91.

299. Lilley, D.M., *Structures of helical junctions in nucleic acids.* Q Rev Biophys, 2000. **33**(2): p. 109-59.

300. Snowden, T., et al., *hMSH4-hMSH5 recognizes Holliday Junctions and forms a meiosis-specific sliding clamp that embraces homologous chromosomes.* Mol Cell, 2004. **15**(3): p. 437-51.

301. McGlynn, P. and R.G. Lloyd, *Action of RuvAB at replication fork structures.* J Biol Chem, 2001. **276**(45): p. 41938-44.

302. Masuda-Sasa, T., P. Polaczek, and J.L. Campbell, *Single strand annealing and ATP-independent strand exchange activities of yeast and human DNA2: possible role in Okazaki fragment maturation.* J Biol Chem, 2006. **281**(50): p. 38555-64.

303. Gu, Y., Y. Masuda, and K. Kamiya, *Biochemical analysis of human PIF1 helicase and functions of its N-terminal domain.* Nucleic Acids Res, 2008. **36**(19): p. 6295-308.

304. Sen, D., et al., *Human mitochondrial DNA helicase TWINKLE is both an unwinding and annealing helicase.* J Biol Chem, 2012. **287**(18): p. 14545-56.